CRYSTALLIZATION OF CALCIUM OXALATE ON MOLECULARLY IMPRINTED POLYMER SURFACES

Tewolde Siele Tewolde

Submitted in fulfillment of the requirements for the degree of Master of Science at the University of Cape Town

Supervisors: Associate Professor T. J. Egan

Professor A. L. Rodgers

February 2004

Acknowledgement

I express my sincere thanks to my supervisors: Prof. Allen Rodgers and Assoc. Prof. Timothy Egan for their expert supervision, support and constructive criticism in every part of the study.

This study was facilitated by the capable assistance of my colleagues at the Kidney Stone Research Laboratory, especially Dr. Dawn Webber; Kanyile Ncokazi at the Malaria Studies Research Laboratory and Ms. Miranda Waldron at the Electron Microscope Unit.

I thank the Eritrean Human Resources Development of the University of Asmara for sponsoring my study. Finally, and most importantly, I wish to sincerely acknowledge the support and encouragement that I received from my family and friends.

Publication

Egan TJ, Rodgers AL and Siele T (2004). Nucleation of calcium oxalate crystals on an imprinted polymer surface from pure aqueous solution and urine. J Biol Inorg Chem, accepted for publication, in press. Preprint publication online at Springer Link Journal of Biological Inorganic Chemistry Online First.

Conferences

- Poster, 36th Convention of the South African Chemical Institute, Port Elizabeth, July 2002. "Crystallization of calcium oxalate crystals on molecularly imprinted polymer surfaces."

- Poster and oral summary, 10th International Symposium on Urolithiasis, Istanbul, June 2003. "Crystallization of calcium oxalate crystals on molecularly imprinted polymer surfaces."

TABLE OF CONTENTS

List of Abbrevations

AAS	atomic absorption spectroscopy
abchc	azo-bis-cyclohexacarbonitrile
ARAG	aragonite
BRU	brushite
CaOx	calcium oxalate
COD	calcium oxalate dihydrate
COM	calcium oxalate monohydrate
COT	calcium oxalate trihydrate
CS	chondrotin sulphate
dvb	divinyl benzene
ESCA	electron spectroscopy for chemical analysis
FP	formation product
fnb	4-fluoro-4-(p-nitrophenyl)butan-2-one
FTIR	fourier transform infrared spectroscopy
GAG	glycosaminoglycans
Gla	γ-carboxyglutamic acid
HA	hyaluronic acid
HAP	hydroxyapatite
HPLC	high pressure liquid chromatography
HS	heparan sulphate
HSA	human serum albumin
maaha	6-methacrylamidohexanoic acid
MSL	metastable limit
NaOx	sodium oxalate
NC	nephrocalcin
OP	osteopontin
RS	relative supersaturation
SEM	scanning electron microscopy
SP	solubility product
SS	supersaturation
THM	Tamm-Horsfall mucoprotein
TOF-SIMS	time-of-flight secondary ion mas spectrometry
UPTF1	urinary prothrombin fragment1
XRD	X-ray powder diffraction

Abstract

Calcium oxalate (CaOx) is the most common component of human kidney stones. Heterogeneous nucleation is regarded as the key mechanism in this process. As such, crystallization of this substance has been studied in several different model systems. However, molecular imprinting has not been previously used in this field. In the present study, template crystals of calcium oxalate mono- and di-hydrate (COM and COD respectively) were used to imprint a copolymer of 6-methacrylamidohexanoic acid and divinylbenzene. Thereafter, the imprinted polymer was immersed in three different test solutions in an attempt to nucleate CaOx crystal formation. The test solutions were different concentrations of aqueous solutions of calcium chloride and sodium oxalate an artificial urine with varying magnesium and citrate concentrations and a sample of real urine. The crystals formed were characterized by X-ray powder diffraction, Fourier transform infrared spectroscopy, atomic absorption spectroscopy and scanning electron microscopy. Results showed that in the aqueous solution, the COM imprinted polymer specifically induced the nucleation of COM only. However, the COD-imprinted polymer induced only trace amounts of COD and large amounts of COM. In artificial and real urines, calcium phosphate formed spontaneously (attributed to high pH) in cases where no polymer was added and in the presence of the unimprinted polymer (control). The COM imprinted polymer precipitated pure COM crystals in some cases and a mixture of COM and calcium phosphate in others. The COD imprinted polymer, however, precipitated calcium phosphate with trace amounts of all three hydrates of calcium oxalate. Trace amounts of COD and large amounts of calcium phosphate precipitated only in cases where the magnesium and citrate concentrations of the artificial urine were reduced. In the urine

samples from healthy white South African male subjects, calcium phosphate precipitated when no polymer was added and in the presence of control polymer. This study provides evidence that the imprinted polymers direct formation of their morphologically-matched crystals and that rapid hydrate transformation of COD to COM might have occurred. Further, the study supports the hypothesis that heterogeneous nucleation plays a key role in CaOx stone formation and that the imprinted polymer model may provide an additional and superior diagnostic tool for stone researchers to assess stone-risk in urine.

CHAPTER ONE – KIDNEY STONE DISEASE

1.1. What are renal calculi?

The urinary tract consists of kidneys, ureters, bladder and urethra. Renal calculus can occur anywhere within this tract. Kidney stones are the most common. The disease in which urinary calculi are formed is called urolithiasis. This is a process in which crystals are retained somewhere in the urinary tract to further grow and aggregate and cause disease. Crystalluria on the other hand, is a process in which small crystals are flushed out of the kidney without causing harm. Crystalluria is a common event for both stone-formers and non-stone-formers (Hess and Kok, 1996). Kidney stones are composed of CaOx, calcium phosphate, uric acid, cystine, magnesium phosphate (table 1) or other insoluble salts (Sutor and Scheidt, 1968; Daudon *et al.*, 1993; Ramello *et al.*, 2000). The biomineralization of CaOx is of considerable interest, as it is the most common constituent of kidney stones. There are three hydrates of CaOx: calcium oxalate monohydrate (COM), calcium oxalate dihydrate (COD) and calcium oxalate trihydtare (COT) (Brecevic *et al.*, 1986). Of these, the first is the most stable thermodynamically (Grases *et al.*, 1990). COT is very rare in urine as it is thermodynamically unstable (Grases *et al.*, 1998).

Table 1.1. Common types of kidney stones and their relative incidence (Bullock *et al.*, 1998).

Pure calcium oxalate	45%
Calcium oxalate + phosphate	25%
Magnesium phosphate	20%
Calcium phosphate	3%
Uric acid	5%
Cystine	3%

Although there has been much research on this disease, the mechanism of stone formation is not completely understood. Attempts to control the mechanism by which crystallization in urine proceeds and hence provide insights into how kidney stone disease might be managed have not been entirely successful. No one has formulated an efficient prevention and cure procedure. The complexity of urine and the environment of the kidney mean that kidney stone disease is multifactorial.

1.2. Epidemiological factors

Stone disease has been known to be common since Hippocrates' times. "Stone waves" were seen during world wars I and II in the involved European countries. This was probably related to dietary deficiency (Prien, 1971). Diet, race, sex and age, climate, profession, geographic location and fluid intake are some of the factors that affect the epidemiology of nephrolithiasis (Rose and Westbury, 1979; Scott, 1985; Sakhaee *et al.*, 1987; Beukes *et al.*, 1987; Rodgers, 1991; Ramello *et al.*, 2000).

1.2.1. Geography

Some countries have "stone belts", for example, there is one in the United States that stretches through the south east of the country. People who live in this belt (Florida, Georgia, South Carolina and North Carolina) show a higher incidence of urolithiasis than those living in the rest of the United States (Boyce and Strawcutter, 1956).

1.2.2. Race

Several studies have shown that irrespective of the geographical area concerned, prevalence of kidney stone disease is higher in whites than in blacks (Reaser, 1935; Modlin, 1967; Robertson and Peacock, 1981). In South Africa, 10-15% of the white population form stones whereas in blacks the prevalence is <1% (Modlin, 1967; Whalley *et al.*, 1998). The chemical composition of urine from non stone-forming blacks and whites is different (Goodman *et al.*, 1995). Compared to whites, South African blacks have lower urinary calcium levels resulting from less calcium intake. In USA and Brazil, the ratio of white to black stone-formers is four-to-one (Ramello *et al.*, 2000). African blacks are reported to have higher urinary citrate excretion due to poor metabolic rate of circulating estrogens because of nutritional liver damage (Soucie *et al.*, 1994). As the African Americans changed their dietary habits to that of the Caucasians, an increased incidence of urolithiasis was observed (Robertson and Peacock, 1981). This loss of immunity was not originally observed in the black South Africans, possibly because they clung to their tribal dietary habits even when they moved to industrial areas (Modlin, 1967). However, more recent reports have suggested that the loss of immunity is beginning to be observed in urban blacks in South Africa where stone incidence has started to occur, but at a very low level (Whalley *et al.*, 1999).

1.2.3. Age and sex

The male-to-female ratios reported from all white population studies are greater than one (*i.e.* 1:3). Sex hormones are suggested to play a role in this difference (Iguchi *et al.*, 1999). Also, men generally have larger body mass and hence larger amount of material to excrete (Blacklock, 1982; Hess and Kok, 1996). The peak age of occurrence in men is 35 years while in women, a double distribution peak appears at 30 and 55 years; the latter peak is suggested to be due to menopausal bone reabsorption (Blacklock, 1982; Fan *et al.*, 1999). In industrialized countries, 5.9 to 12.5 percent of men and 3.7 to 5 percent of women suffer from urolithiasis during their lifetime (Ramello *et al.*, 2000).

1.2.4.Climate

CaOx urolithiasis is generally common in areas with a hot climate (Bateson, 1973; Robertson *et al.*, 1974; Hallson and Rose, 1975; Robertson *et al.*, 1975). This is suggested to be due to high supersaturation of urine with respect to calcium and oxalate, lower urinary pH and smaller urinary volume resulting from enhanced loss of liquid by sweating (Schwille and Herrmann, 1992). Saudi Arabia for example is the country with the highest occurrence of urolithiasis ever reported (Robertson and Hughes, 1994). About 21% of Saudi Arabians suffer from urolithiasis at sometime in their life time. Seasonal changes bring about changes in urinary biochemistry (Robertson *et al.* 1975). It is reported that in some European countries and the United States, the occurrence of stones is higher during the warmer seasons (Schwille and Herrmann, 1992). Some studies reported an increase in the incidence of urinary calculi in American and German soldiers assigned to the desert (Blacklock, 1982).

1.2.5. Profession

Many studies have reported that a high risk of urolithiasis is associated with sedentary occupations. For example, airline pilots, accountants, clerks and bus drivers have high risk of kidney stone formation compared with people involved in jobs with more physical activity like farmers and forestry workers (Blacklock, 1982; Robertson and Peacock, 1983; Rodgers, 1991). Compared to ground service (eg. drivers), pilots are reported to be more susceptible to stone disease probably due to the more sedentary nature of their work and lower intake of water before and during their flight (Garilevich, 1995; Ramello, 2000). Other studies have also reported a high prevalence of urolithiasis in workers exposed to a hot environment and massive sweating (pin *et al.*, 1992; Ramello *et al.*, 2000). Thus, chronic dehydration is an important risk factor of stone disease.

1.3. Physicochemical aspects of calcium oxalate stone formation

1.3.1. Calcium

As a constituent of CaOx, calcium is an important risk factor because it directly affects the supersaturation of urine with respect to CaOx (Massey *et al.*, 1993). A high stone occurrence is usually associated with a raised calcium excretion (Giannini *et al.*, 1999). Hypercalciuria is the term used for abnormally high calcium excretion in the urine but since the upper normal limit of calcium is different for different geographical locations, the cause for calcium stone disease is most often called as idiopathic hypercalciuria (Ryall, 1989; Hess and Kok, 1996). There is a significantly higher incidence of idiopathic hypercalciuria in stone-formers compared to the normal subjects of matched age and sex (Pak, 1998).

1.3.2. Oxalate

Oxalate, a dicarboxylate anion which forms insoluble CaOx salt with calcium in urine, is more influential than calcium in determining the risk of kidney stone formation (Robertson and Peacock, 1983; Ryall, 1989). This is because urinary oxalate brings about a more significant change in the supersaturation of urine with respect to CaOx than calcium, making oxalate play a more determining role (Robertson, 1999; Rodgers and Lewandowski, 2002). Studies have shown that compared to healthy controls, stone-formers have higher urinary oxalate levels (Wilson *et al.*, 1989).

1.3.3. Uric acid

Uric acid if present in excess can promote CaOx crystallization by epitaxy and possibly by interfering with the inhibitors in the urine (Robertson *et al.*, 1978). For example, colloidal particles of urate can bind glycosaminoglycans (GAG) and reduce their inhibitory potency and consequently enhance nucleation, growth and aggregation of CaOx crystals (Grover and Ryall, 1995)

1.3.4. pH

pH is an important risk factor because it changes the ionization of urinary inhibitors and the solubility of CaOx crystals (Tiselius, 1981). Urinary pH for healthy persons varies over the entire physiological range (4.5 to 8.4) whereas stone-formers do have relatively narrow pH ranges (Tietz, 1976). It is interesting that the physicochemical system of urine from stone-formers shows buffer properties due to the precipitated calculi (Bilobrov *et al.*, 1990). Sodium pyrophosphate, chondroitin and citrate are commonly used to inhibit CaOx crystal growth by increasing urinary pH. Sodium pyrophosphate is the best because it raises the pH significantly. The effect of pH on

inhibition is strongly dependent on the contribution of different urinary inhibitors present in the urine (Tiselius, 1981).

1.3.5. Urinary volume

Urinary volume is the most influential of all the risk factors (Ryall, 1989). The advice to drink more liquid as a treatment for urinary stone disease has been appreciated since Hippocrates' times. Increasing urine volume by increased fluid intake lowers the likelihood of stone recurrence (Curhan *et al.*, 1996). Although it needs to be accompanied by dietary modification and drugs, high fluid intake alone can be taken as a treatment to inhibit stone recurrence in single stone-formers (Pak, 1999). High intake of fluid dilutes the urine, lowers the concentration of stone forming ions, and thereby reduces the probability of stone formation (Ryall, 1989). The higher the fluid intake, the more dilute the urine and the lower the incidence of stone disease.

1.3.6. Supersaturation

Supersaturation is a prerequisite for crystallization and is the thermodynamic driving force for stone formation (Lingeman et al, 1999). Supersaturation is a concentration product or activity product above the solubility product or equilibrium activity product (Hess and Kok, 1996). The free energy of CaOx stone formation is given by

$$\Delta G = RT \ln A_i/A_o \quad - - - - - - - - - - - - - - - - \quad (1)$$

where R is the gas constant, T is the temperature, and A_i and A_o are activities of the unionized salt species at any given condition and at equilibrium respectively (Finlayson, 1978). It must be noted that the presence of a salt mixture and co-precipitation have significant effect on the thermodynamic solubility constant (Lingeman *et al.*, 1999). The state of urinary saturation with respect to CaOx can also

be computed using the computer program, EQUIL, formulated by Finlayson (1977). This program can be used to calculate relative supersaturation of urine based on the pH and total concentrations of sodium, potassium, calcium, magnesium, uric acid, chloride, ammonium, citrate, phosphate, sulphate, oxalate, pyrophosphate and carbon dioxide (Werness *et al.*, 1985).

The ratio of the actual concentration product or activity product to the solubility product or equilibrium activity product (A_i/A_o) is also referred to as relative supersaturation (RS) (Hess and Kok, 1996). At RS values <1, urine is said to be undersaturated, a condition under which no precipitation nor crystallization can occur and any stones in the solution can dissolve. Urine is saturated at RS value equal to 1, where existing stones will not dissolve or grow and no new stones will be formed; however existing stones can aggregate. The solubility product (SP) is the concentration at which the RS is exactly equal to 1 (figure 1). Urine is supersaturated at RS values >1. Under this condition, existing stones may grow but no precipitation occurs unless the upper limit of metastable limit (also called formation product, FP) is exceeded. (Robertson *et al.*, 1968; Nancollas and Gardner, 1974; Finlayson, 1978; Hess and Kok, 1996). Supersaturation has two stages; the metastable and unstable stages. The metastable stage, a level between SP and FP (figure 1), is one in which crystallization does not take place unless seed crystals or other foreign surfaces are added to disturb the stability or lower the level of formation product (FP* and FP', figure 1). Secondary nucleation refers to the process where crystals nucleate on the surface of crystals of their own species whereas in epitaxy, crystals are precipitated on the surface of other crystals with identical lattice dimensions (Hess and Kok, 1996). In the case of the

unstable stage, a level beyond FP (figure 1), there occurs spontaneous crystallization (or homogeneous nucleation) (Kavanagh, 1992).

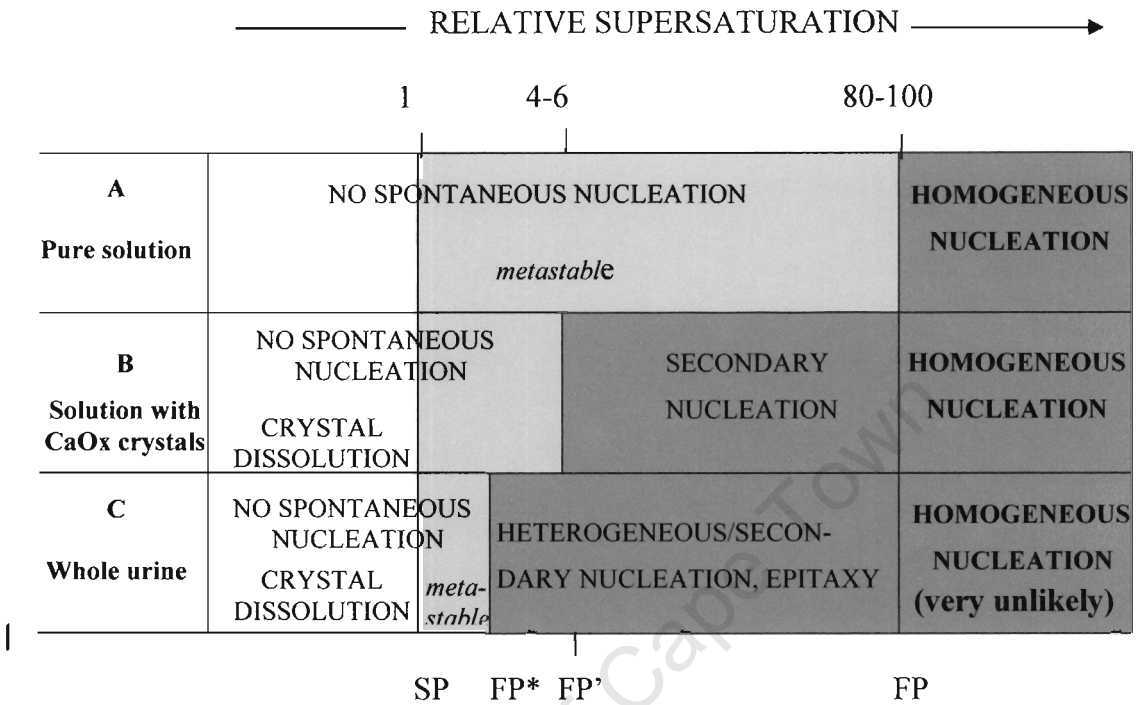

Figure 1. Relative supersaturation and CaOx crystal nucleation. A: perfectly clear aqueous solution of CaOx. B: Perfectly clear aqueous solution containing CaOx crystals. C: Whole urine containing foreign surfaces and crystals [Hess and Kok, 1996].

1.4. Dietary factors

Diet is an important urolithiasis risk factor because it influences urinary composition. Thus, any diet which affects the key urinary risk factors – calcium, oxalate, uric acid, citrate, pH and volume – is of significance (Vahlensieck, 1986; Hesse *et al.*, 1993; Hess, 1996; Hess *et al.*, 1998; Giannini *et al.*, 1999; Lewandowski *et al*, 2001).

1.4.1. Calcium

Diet containing dairy products, meat, fish and poultry are rich in calcium (Massey *et al.*, 1993). In normal individuals, only 6% of the dietary calcium appears in the urine (Goldfarb, 1994). Patients with hypercalciuric urolithiasis have increased gastrointestinal calcium absorption. Dietary calcium has been regarded as a risk factor for stones because it raises the urinary excretion of calcium (Curhan *et al.*, 1993). As such in the past, doctors frequently advised people with a history of CaOx stones to reduce their calcium consumption. However, recent studies note that calcium restriction is not a good therapy for CaOx stone-formers and even potentially dangerous (Curhan, 1997; Moyad, 2003). Negative body (eg. bone) calcium balance and high oxalate excretion due to reduced intestinal binding of oxalate are the main consequences of low calcium intake especially if accompanied by high protein intake (Goldfarb, 1994; Hess, 1996; Hirvonen *et al.*, 1999). Therefore, diet containing moderate amounts of calcium and oxalate accompanied by a high fluid intake is now recommended for lowering the risk of urolithiasis (Hesse *et al.*, 1993).

1.4.2. Oxalate

Abnormally high levels of urinary oxalate (also called hyperoxaluria) can come from foodstuff as well as from metabolic pathways (Hesse *et al.*, 1993; Goldfarb, 1994). Earlier reports (Finch *et al.*, 1981) suggested that dietary oxalate makes 10–20% of urinary oxalate excretion while later reports (Holmes and Assimos, 1999) suggested the contribution of dietary oxalate to urinary oxalate excretion to be up to 40%. Oxalate-rich foodstuff include: rhubarb, spinach, beetroot, peanuts, chocolate and black tea (Massey *et al.*, 1993). Most of urinary oxalate excretion comes from metabolic activity (Massey *et al.*, 1993). *Oxalobacter formigenes* is one of the anaerobic microflora of the

human intestine responsible for degrading oxalate (Massey *et al.*, 1993). Lower quantity and activity of oxalate degrading bacteria may be the possible explanation for the relatively higher oxalate excretion in South African blacks compared to the white population but this has not yet been explored (Lewandowski *et al.*, 2001).

1.4.3. Protein

High animal protein intake can increase urinary excretion of CaOx and uric acid and hence it can increase the prevalence of urolithiasis (Robertson *et al.*, 1979a; Curhan, 1997; Hess *et al.*, 1999; Giannini *et al.*, 1999; Hess, 2002). Hypertension and obesity have been reported to be possible stone risk factors (Goldfarb, 1994). Both are related to a rich diet with high animal protein intake. The increase in calcium and oxalate excretion due to increased resorption and oxalate metabolism respectively are more significant in animal protein consuming individuals than the vegetable protein consumers (Robertson *et al.*, 1979b). In addition, flesh protein increases uric acid excretion due to additional purine nitrogen (Hesse *et al.*, 1993). Moreover, vegeterian food lowers the risk of urolithiasis by increasing urinary pH and citric acid excretion and decreasing urinary calcium excretion (Robertson *et al.*, 1979b; Hesse *et al.*, 1993). Goldfarb (1994) has reported that the occurrence of upper tract stone formation in northern and western India, where animal protein intake is higher, is four times greater than that in the southern and eastern regions of India

1.4.4. Salts

Salts containing sodium and magnesium affect CaOx stone formation (Sakhaee *et al.*, 1993). High sodium intake contributes to hypercalciuria in patients with CaOx stones (Timio *et al.*, 2003). An increase in urinary calcium and a decrease in urinary citrate are the lithogenic consequences of excessive intake of dietary sodium chloride (Sakhaee *et al.*, 1993; Hesse *et al.*, 1993; Hess *et al.*, 1999; Timio *et al.*, 2003). On the other hand mineral water containing calcium and magnesium reduces the risk of urolithiasis (Rodgers, 1997). The former acts by binding oxalate in the gut thereby reducing its availability for absorption and the latter acts in a similar way to form a more soluble salt with oxalate. Higher intake of dietary potassium reduces the risk of stone disease (Curhan *et al.*, 1996). Raised excretion of nonreadily resorbable inorganic sulphate is reported to escalate the disease (Giannini *et al.*, 1999).

1.4.5. Fluid intake

Greater fluid intake reduces the risk of kidney stones (Curhan *et al.*, 1996; Borghi *et al.*, 1999). However, choice of drinks is crucial as its mineral content plays an important role. For example, fluids like coffee, black tea, cola and too much alcohol increase the risk (Hesse *et al.*, 1993; Rodgers, 1999). Sufficient consumption of herbal tea, mineral water, beer, and wine decreases the risk of kidney stones, whereas high intake of apple and grape fruit juice increases the risk (Hesse *et al.*, 1993; Curhan *et al.*, 1996; Rodgers, 1999). Mineral water high in calcium and bicarbonate is the ideal beverage to dilute urine (Vahlensieck, 1986; Hesse *et al.*, 1993). Increased fluid intake reduces the risk of urolithiasis by decreasing the concentrations of calcium and oxalate in urine (Goldfarb, 1994). Sufficient intake of tap water is recommended by Vahlensieck (1986). Although urinary stone formation is not very much associated with

hardness of water, the high magnesium content of hard water makes it preferable to soft water because magnesium inhibits stone formation (Rodgers and Spector, 1981).

1.5. Mechanism of Stone Formation

The mechanism of stone formation involves three processes, i.e. nucleation, growth and aggregation (Hess and Kok, 1996).

1.5.1. Nucleation

Nucleation refers to the process in which crystals are precipitated from a supersaturated solution. Nucleation of CaOx can take place either in the presence or absence of a substrate. A perfectly clear aqueous solution of CaOx remains stable over a wide range of supersaturation, called the zone of metastable supersaturation which goes up to RS values of 80 to 100 (figure 1, page 9) without nucleation of any crystals (Hess and Kok, 1996). But urine does not usually reach the supersaturation necessary for nucleation without a substrate and this suggests that crystal nucleation *in vivo* requires such a substance (Kok, 1997). Foreign surfaces such as cell debris, epithelial membranes, some urinary macromoleculaes like self-polymesised Tamm-Horsfall glycoprotein and other crystal species present in the urine can induce nucleation of CaOx (Khan *et al.*, 1990; Khan *et al.*, 1993; Hess and Kok, 1996). Thus it would appear that many surfaces in the urinary tract (including urinary macromolecules and epithelial linings) could act as nucleators of CaOx nucleation.

Homogeneous and heterogeneous nucleations

Homogeneous nucleation is a process by which nucleation takes place spontaneously. As it is evident from figure 1 (page 9), this process takes place just beyond the upper limit of the interval of the metastability, a level where the solution becomes unstable, also called the level of formation product (FP) (Worcester, 1996). In the case of heterogeneous nucleation, crystals are precipitated on the surface of other substances: secondary nucleation (FP' in figure 1) or epitaxy (FP* in figure 1) (Worcester, 1996; Hess and Kok, 1996). Some urinary macromolecules are heterogeneous nucleators of stone formation: in their presence precipitation takes place at lower RS value (FP* in figure 1) (Sohnel and Grases, 1995).

CaOx stones generally incorporate very small amounts of other crystalline particles (Geider *et al.*, 1996). Sohnel and Grases (1995) suggested that these crystalline particles can serve as nucleators of CaOx crystallization. Hydroxyapatite, calcium carbonate, brushite and uric acid satisfy this condition and they enable the supersaturated urine to crystallize CaOx (Geider *et al.*, 1996). The typical nucleation in stone formation is therefore heterogeneous nucleation because urine usually is not concentrated enough for homogeneous nucleation to occur (Finlayson *et al.*, 1984).

1.5.2. Growth

The process by which new crystal components are incorporated into the nucleus of previously formed crystals is called crystal growth (Hess and Kok, 1996). CaOx crystals in human urine are mostly small enough to be flushed out harmlessly. The normal transit time through the kidney is not long enough for crystals to grow to the

size range of the tubule which would culminate in them being trapped. Growth is therefore not regarded as a key formation in urolithiasis (Kok and Khan, 1994).

1.5.3. Aggregation

Aggregation is a process by which several particles in solution adhere together to form a large particle (Hess and Kok, 1996). Electrostatic attraction, van der Waals forces, liquid bridge, capillarity, viscous binder, solid bridge and shear force are the basic mechanisms by which aggregation takes place. The roles of liquid bridge and capillarity are not significant for the particles are totally immersed in urine. Because of the zeta potential (the repulsive electrostatic surface charge) of the immersed particles, the electrostatic forces are repulsive and work against aggregation of crystalline particles (Finlayson, 1978; Hess and Kok, 1996). Adsorbed proteins can act as viscous binders to help aggregation or can establish surfaces with increased negative charges leading to disaggregation (Scurr and Robertson, 1986; Christmass *et al.*, 2002). Measurement of zeta potential helps the study of mechanism of urinary inhibitors. This measurement is especially helpful in assessment of inhibition of CaOx by inhibitors. Solid bridges can stabilize aggregation only after other adhesive forces enable the particles to be placed next to each other (Finlayson, 1978). When interparticle distances are very small, van der Waals forces exert their attractive force and help aggregation. The shear forces exerted by the turbulence in the crystal suspension or by solvent currents in tubular fluids may work in the favour of, or against aggregation.

Healthy subjects can be distinguished from stone-formers by smaller degrees of aggregation. It is well known that crystalluria is common for normal and stone forming

subjects. However, urine from stone-formers contains more aggregated particles (Kok and Khan, 1994).

1.6. Theories of stone formation

There are three theories governing stone formation: (i) the matrix theory, (ii) the fixed particle theory and (iii) the inhibition/promotion theory.

1.6.1. The matrix theory

The matrix theory of stone formation argues that precipitation of the stone-forming salts is promoted by crystallization-promoting macromolecules in urine by providing a specific ground substance (Robertson and Nordin, 1982; Ryall and Stapleton, 1995). These crystallization-promoting substances act as heterogeneous nucleators and enable precipitation to occur at lower urinary saturation (Ryall and Stapleton, 1995). According to this theory the heterogeneous nucleators, besides causing the crystals to nucleate and grow, act as a framework for the deposition of stone salts (Robertson and Nordin, 1982). Heterogeneous nucleating macromolecules remain trapped in the stone architecture and become part of the final stone structure. However, a molecule that has become part of the stone does not necessarily mean it had played a role of a nucleator or an inhibitor, as some may get trapped without affecting the crystallization process at all (Ryall and Stapleton, 1995).

1.6.2. The fixed particle theory

According to this theory, a stone is mainly formed under conditions where particles are retained by adhesion to cells or disturbed urinary flow (Finlayson *et al.*, 1984). This theory implies that urinary crystals are endocytosed by the cells of the tubular surfaces to which they have adhered. Subepithelial calcified lesion can then be produced by subsequent migration of the endocytosed crystals. Upon losing its epithelial covering and coming into contact with urine at the level of supersaturation (SS), this lesion may act as nidus for the stone to further grow (figure 2) (Hess *et al.*, 2001).

Particle retention

In this theory, particle retention is the determining process for stone formation because only retained crystals have a sufficiently long residence time to grow into full-size stones (Edyvane *et al.*, 1987; Hess and Kok, 1996). Evidence exists that in calcium stone forming patients, patches of subepithelial papillary calcification (Randall's plaques) occur in the kidney of stone-formers to a higher degree than in nonstone-formers (Randall, 1940; Bullock *et al.*, 1998; Hess *et al.*, 2001). Solutes are believed to crystallize on these nidi to form microcalculi that then slough off into urine collecting system to form the nuclei of large stones (figure 2). Formation of papillary calculi is believed to be a consequence of some alteration of the epithelium covering the renal papilla (ranging from a reduction in the protective GAGs to papillary necrosis). This facilitates an increase in calcium concentration of the tissue and depending on duration and levels of crystallization effectors, the initial development of attached particles of insoluble calcium salts may take place. (Bullock *et al.*, 1998; Grases *et al.*, 1998).

Finlayson *et al.* (1984) reported that CaOx crystals become retained by adhering to the sticky glycocalyx of renal tubular cell membranes. Other reports from Riese *et al.* (1992) have also shown that CaOx crystals adhere to renal papillary collecting tubule cells from rats. It has been suggested that increased growth and aggregation of crystals retained as a result of the stickiness of tubular epithelia or as a consequence of epithelial injury are the main events that favour the process of particle retention (Finlayson *et al.*, 1984; Hess and Kok, 1996).

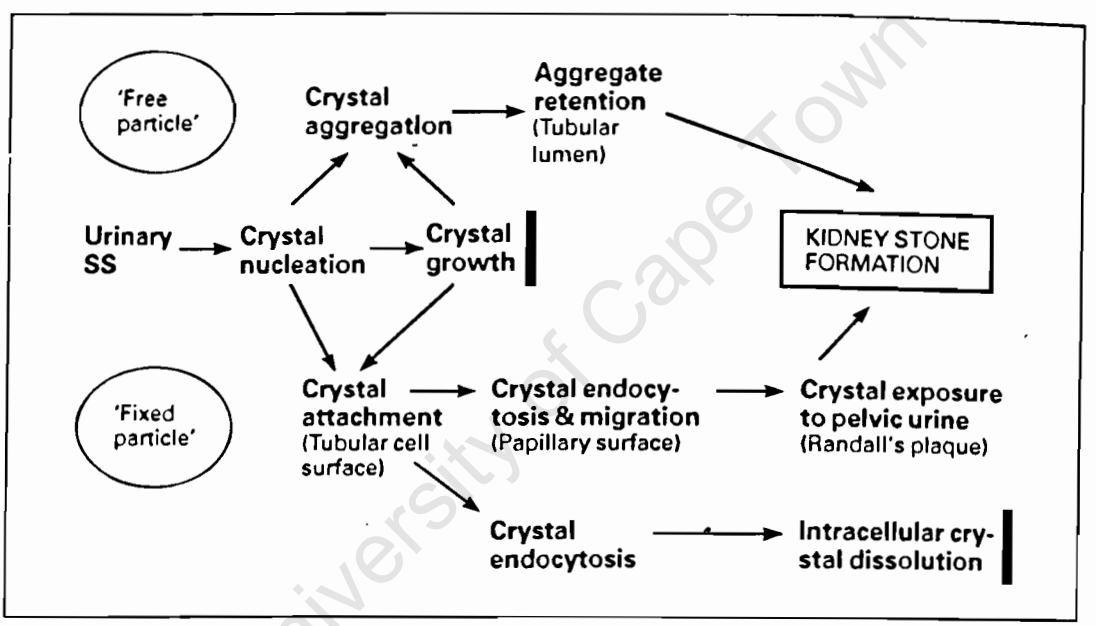

Figure 2. Process of particle retention [Hess *et al.*, 2001]

1.6.3. The inhibition/promotion theory

Inhibitors are urinary substances that retard one or more of the three processes of stone formation. Promotors are substances that enhance stone formation by either increasing the urinary supersaturation or by providing foreign surfaces for heterogeneous nucleation (Hess and Kok, 1996). According to this theory, stone-formers lack or are deficient in inhibitors of crystallization (Robertson and Nordin, 1982). Urinary

substances are either promoters or inhibitors of the formation of kidney stones. They affect stone formation by enhancing or retarding one or more of the three major processes of crystallization described in section 1.5. Some urinary components may have both effects. Examples of urinary promoters and inhibitors are described in the following paragraphs.

1.6.3.1. Promotors

Almost all urinary CaOx crystals contain proteins within them. This may be evidence that the proteins act as promoters of stone formation (Doyle *et al.*, 1995). Proteins like osteopontin (OP), Tamm-Horsfall mucoprotein (THM) and nephrocalcin (NC) may either promote or inhibit aggregation (Ryall and Stapleton, 1995). Both OP and NC promote aggregation at pH 5.7 (Christmas *et al.*, 2002) and at sufficiently low concentration (Ryall and Stapleton, 1995). Contradictory effects of THM are reported. Rose and Sulaiman (1982) reported THM to enhance CaOx precipitation in concentrated urine. On the other hand studies by Kitamura and Pak (1982) reported THM to be an inhibitor of CaOx nucleation and growth. Recent reports (Baumann, 1998; Dussol and Berland; Craig *et al.*, 2001) Suggest that under normal conditions, THM inhibits CaOx nucleation and growth but it promotes aggregation by presenting a preformed surface for crystallization when polymerized. Polymerization of THM is favoured by high concentration of THM itself, high urinary calcium and low pH conditions (Baumann, 1998; Dussol and Berland, 1998). Some studies have shown that OP can stimulate deposition of CaOx crystals on Madin-Darby canine kidney cells (Yamate *et al.* 1998, Yamate *et al.* 1999). It has recently been reported by Konya *et al.* (2003) that OP attached to collagen granule surfaces, may promote CaOx crystal deposition.

1.6.3.2. Inhibitors

There are three mechanisms by which inhibition takes place: binding of calcium and oxalate ions by chelating agents, steric hindrance and blocking of growth sites (Ryall, 1997; Christmas *et al.*, 2002). Some inhibitors retard nucleation by binding either calcium or oxalate (Ryall, 1997). This results in lowering the supersaturation of CaOx and hence the probability of precipitation is reduced (Grases *et al.*, 1989a). Other inhibitors retard both growth and aggregation by binding to the crystal surface. Few other inhibitors retard growth and aggregation by steric hindrance (Christmas *et al.*, 2002). Inhibitors can be classified as micromolecular (i.e., low molecular weight) or macromolecular (i.e., high molecular weight) inhibitors.

Micromolecular inhibitors

Low molecular weight or micromolecular inhibitors include magnesium, citrate and pyrophosphate.

Magnesiun

Magnesium is shown by many studies to be effective in reducing CaOx crystallization both *in vivo* and *in vitro* (Li *et al.*, 1985; Kohri *et al.*, 1988). It reduces the risk of stone formation by complexing oxalate to form magnesium oxalate, a salt more soluble than CaOx (Hallson *et al.*, 1982). Thus, magnesium acts as an inhibitor of CaOx crystallization in its capacity as a binder of oxalate (Ryall, 1997). The work of Li *et al.* (1985) concludes that though they may have some gastrointestinal side effects, magnesium compounds are recommended treatments for idiopathic stone patients. Berg *et al.* (1986) reported lower urinary magnesium excretion in stone-formers compared with the normal subjects. A recent study by Siener and Hesse (1995) reported the

influence of magnesium-rich ovo-lacto-vegeterian diet on urinary magnesium excretion and urinary concentration to be less than expected.

Citrate

Citrate inhibits nucleation, growth and aggregation by either complexing calcium or binding the crystal surface (Hallson *et al.*, 1982; Ryall *et al.*, 1985; Allie and Rodgers, 2003). It complexes calcium thereby reducing the supersaturation of urine with respect to CaOx and consequently inhibits nucleation of CaOx crystals. It also inhibits both crystal growth and aggregation by binding the crystal surface (Ryall, 1997). Citrate can also counteract the heterogeneous growth of CaOx crystals on the surface of calcium phosphate crystals (Tiselius *et al.*, 1993). CaOx stone-formers have lower urinary citrate excretion (hypocitraturia) compared to normal subjects (Grases *et al.*, 1989b; Tiselius *et al.*, 1993). The inhibitory effect of citrate is reported to be less effective in hypercalciuric patients than those individuals with lower urinary calcium excretion (Grases *et al.*, 1989b). As a consequence of the crucial role that citrate plays on CaOx crystallization, citrate supplementation has been a good therapy for CaOx stone disease (Tiselius *et al.*, 1993; Ryall, 1997). Among the common citrate supplements that have been used for stone disease treatment and found to be efficient are: potassium citrate (Pak and Fuller, 1986; Abdulhadi *et al.*, 1993), sodium potassium citrate (Schwille *et al.*, 1987; Berg *et al.*, 1990), calcium citrate (Levine *et al.*, 1994; Sakhaee *et al.*, 1994), calcium sodium citrate (Schwille *et al.*, 1997; Hermann *et al.*, 1999), potassium magnesium citrate (Sakhaee *et al.*, 1983; Pak *et al.*, 1992) and sodium citrate bicarbonate (Allie and Rodgers, 2003; Bosch *et al.*, 2003).

Pyrophosphate

Pyrophosphate inhibits nucleation, growth, and a combination of growth and aggregation from an inorganic solution (Ryall, 1997). The inhibitory activity of phyrophosphate is attributed to its capacity to irreversibly bind to CaOx crystal surfaces (Ryall, 1997). Shirane and Kagawa (1993) reported that pyrophosphate binds COM in preference to COD and that it binds calcium in the solid phase rather than in the solution phase. A study by Gardner (1978) reported that at physiological concentration of pyrophosphate, formation of COM can be retarded or prevented while the growth of COD and COT are not affected. It also reduces the deposition of CaOx from undiluted urine (Ryall, 1997). But its contribution to the inhibitory activity of diluted urine is small (Ryall *et al.*, 1981). Conte *et al.* (1989) reported reduced inhibitory effect of pyrophosphate from stone-formers to be due to lower transformation of orthophosphate into pyrophosphate.

Macromolecular Inhibitors

Macromolecules, collectively called organic matrix, comprise only a small portion (2-3%) of the stone's weight, but are found spread throughout the entire stone structure. Reports from Borghi *et al.* (1995) showed a significant increase in oxalate tolerance parameters when macromolecules are removed by ultrafiltration from urine of CaOx stone-formers. On the contrary, no significant change was observed when urine from controls was ultrafiltered. This shows that ultrafiltration removed the difference between stone-formers and controls. From this observation it can be suggested that urinary macromolecules play a determining role in CaOx stone formation. These comprise mainly two classes of compounds, namely GAGs and proteins (Doyle *et al.*, 1995; Ryall, 1997).

Glycosaminoglycans (GAG)

Urinary GAGs are polyanionic polysaccharides and are metabolic turnovers of those found in the tissues as proteoglycans (Shum and Gohel, 1993). Heparan sulphate (HS), chondrotin sulphate (CS) and hyaluronic acid (HA) are the most common urinary GAG molecules (Shum and Gohel, 1993). HS and HA are the only GAGs that have been shown to be present in kidney stones (Christmas *et al.*, 2002). CS, however, although it makes more than half of the GAGs in the urine it is not found in stones (Ryall, 1997). This may be due to the fact that CS has weak interaction with the surface of the CaOx crystals and therefore no inclusion.

HS inhibits aggregation in urine and the inhibitory activity of HS from normal controls is higher than that from stone-formers. It also has higher inhibitory activity than CS from both normal subjects and stone-formers (Shum and Gohel, 1993). The same group suggested that the presence of HS in some stones may prove its effect as heterogeneous nucleator. Iwata and co-workers (1994) also compared the inhibitory activities of the urinary and commercial GAGs (specifically HS and CS). They concluded that urinary and commercial GAGs have no significant differences and that HS is a stronger inhibitor compared to CS.

CS is reported to be a potent inhibitor of CaOx crystal growth and aggregation from inorganic media (Ryall *et al.*, 1981). CS is unique in promoting heterogeneous nucleation of COM on hydroxyapatite but inhibits growth (Beshensky *et al.*, 2000). In contrast to this, other works showed its contribution in CaOx crystallization *in vivo* to be insignificant (Ryall *et al.*, 1991; Ryall, 1997).

HA is suggested to promote crystallization in early stages in stone-formers (Gohel, *et al.*, 2000). Some genetic disorders like bladder cancer and Graves' disease bring about a change in the urinary excretion of HA (Gohel *et al.*, 2000). Its presence in urine in trace amounts and close structural similarity with CS makes the isolation and study of HA difficult (Zebrower *et al.*, 1986).

Proteins

Human urine contains many proteins but only a few of these proteins have thus far been identified as playing a role in CaOx stone formation (Ryall, 1996). Urinary prothrombin fragment 1 (UPTF1), Tamm-Horsfall mucoprotein (THM), osteopontin (OP), nephrocalcin (NC) and human serum albumin (HSA) will be discussed briefly in this section.

Urinary prothrombin fragment 1 (UPTF1)

UPTF1 is unique from other protein inhibitors in that it inhibits both growth and aggregation from both aqueous inorganic solution and human urine whereas most of the other inhibitors inhibit aggregation strongly and growth only weakly from both solutions (Doyle *et al.*, 1995). Compared to healthy controls, stone-formers have higher concentration of UPTF1 probably because its level rises in response to lithogenic conditions (Ryall, 1997). Reports from Grover *et al.*, (1998) showed that UPTF1 is a potent inhibitor of CaOx aggregation. Despite its low concentration in human urine, CaOx stones usually contain large quantities of UPTF1 probably due to the fact that UPTF1 has a better effect of binding to CaOx crystal surface. Recent studies by Webber *et al.* (2003) reported greater amount of UPTF1 in crystals from the urine of black South Africans compared to that from the white citizens. These workers have

speculated that this could be a contributory factor to explain the rarity of stones in the black population and serves to illustrate the role of this protein as a powerful inhibitor.

Tamm-Horsfall mucoprotein (THM)

Unlike most of the other macromolecular inhibitors, THM acts by steric hindrance rather than binding to the crystal surface (Ryall *et al.*, 1991; Doyle *et al.*, 1995). Its physical state in urine is affected by pH, ionic strength and its own concentration (Ryall *et al.*, 1991). Under normal conditions, its inhibitory effect on crystal nucleation and growth is not significant but under conditions like low pH and high ionic strength (Hess, 1994) it promotes nucleation. It is not found in CaOx crystals precipitated from urine and its urinary concentration does not differ between stone-formers and healthy subjects (Ryall, 1997). Self-polymerization of THM reduces its inhibitory effect on CaOx aggregation (Hess *et al.*, 1989). Although low pH and high ionic strength conditions reduce its activity, THM is a potent inhibitor of crystal aggregation (Hess *et al.*, 1989; Hess, 1994; Worcester, 1996). *In vitro* experiment on black versus white South Africans by Craig *et al.* (2001) suggests that THM inhibits CaOx nucleation and aggregation and that the inhibitory activity of the protein derived from blacks has greater inhibitory activity than that obtained from the white subjects.

Osteopontin (OP)

It was reported by Nishio *et al.* (1999) that OP is a strong inhibitor of growth of CaOx at physiological urinary concentrations but promotes CaOx formation at lower concentrations. It stereospecifically binds to the surface of the crystals thereby retarding growth (Ryall, 1997). OP at physiological concentrations can inhibit homogeneous nucleation, growth and aggregation of CaOx crystals in supersaturated solutions *in vitro*

(Worcester, 1996). The effect of OP in urine has not been studied but despite its lower concentration in urine compared to nephrocalcin, its presence in stones in quantities greater than nephrocalcin might suggest that it binds to CaOx crystals more strongly and may consequently be a more potent inhibitor (Ryall and Stapleton, 1995; Ryall, 1997; Grover *et al.*, 1998). Wesson *et al.* (2003) showed that OP inhibits crystal formation and retention *in vivo*. It inhibits stone formation by favouring COD at the expense of the crystal with high affinity to papillary cells, COM, and hence reduces retention. Recent evidence shows that OP is found in lower concentration in stone-formers than in healthy subjects (Nishio *et al.*, 2001).

Nephrocalcin (NC)

NC exists as a monomer, dimer, trimer or tetramer. The monomer has molecular weight approximately 14-15 kDa (Ryall and Stapleton, 1995). *In vitro* studies by Worcester (1996) suggest that at concentrations similar to those found in urine, NC can inhibit nucleation, growth and aggregation of CaOx crystals in supersaturated CaOx solutions. NC may also reduce cell-crystal adhesion (Worcester, 1996). NC is reported to contain between two and three γ-carboxyglutamic acids (Gla) per molecule. The inhibitory activity of NC is reduced when it is deficient in Gla (Grover *et al.*, 1998). NC from renal stones and urine of stone-formers lacks Gla (Hess *et al.*, 1989).

Human serum albumin (HSA)

Studies by Ryall *et al.* (1991) showed that HSA, although abundant in human urine is found in trace amounts (if any) in CaOx kidney stones. These workers suggest that HSA inhibits both growth and aggregation of CaOx crystals in aqueous inorganic medium but that its effect on CaOx crystallization in undilutued human urine is not

significant. The work of Cerini and associates (1999) suggested that HSA inhibits COM aggregation by favouring the formation of COD crystals. This is because COD crystals have lower affinity to renal papillary cell membranes (because they have lower negative charges compared to COM crystal). Mensah *et al.* (2003) demonstrated that HSA from black South Africans carries greater negative charges and shows greater inhibition of COM crystal aggregation than that derived from white subjects.

1.7. Conclusion

CaOx is the most common component of urinary calculi (Robertson and Peacock, 1980; Takasaki 1986; Edyvane *et al.*, 1987; Grases *et al.*, 1998). The conditions under which it crystallizes in the urine, either via the matrix theory (Ryall and Stapleton, 1995), or the fixed particle theory (Kok & Khan, 1994) or by invoking the activity of inhibitors and promoters (Ryall, 1997) continues to be the subject of research in many laboratories. Many attempts have been made to control the mechanisms of crystallization in urine (and hence provide insights into how kidney stone disease might be managed). Conservative methods like dietary intervention or alteration of urinary composition via administration of various preparations have had some measure of success. However, none of them have provided a complete understanding of the process. More basic research is required on controlling and directing crystallization processes in urine. One such area is molecular imprinting which has been used in some industrial and biological processes (Wulff, 1995) but has not been explored in the context of urolithiasis. Molecular imprinting presents an innovative approach to investigating CaOx crystallization processes. The next chapter provides background and motivation for pursuing the concept in the area of kidney stone formation.

CHAPTER TWO - MOLECULAR IMPRINTING

2.1. The concept of molecular imprinting

Molecular recognition is the basis for many biological processes that involve interactions between natural biomolecules such as enzymes, antibodies, nucleic acids and cellular receptors (Trotta *et al.*, 2002). Biological recognition elements have been interesting because of their extreme sensitivities and specificities. The discovery of the more stable recognition system obtained by molecular imprinting of polymers has made progress in solving the problem of durability and operational stability that the biological recognition elements lack (Kriz *et al.*, 1997). Molecular imprinting is a technique by which molecular recognition is produced by binding and crosslinking a polymerisable monomer around a template molecule (Spivac and Shea, 1999). A cavity with functional groups in a certain orientation and capable of chemical interaction is left in the polymer after removal of the template molecule (Rachkov and Minoura, 2001; Strikovsky *et al.*, 2003). For the imprinted polymer to be highly selective, the cavity is required to have a shape that exactly matches that of the template and the binding sites must have a definite spatial arrangement (Wulff, 1995). The molecular imprinting technology was first developed by Wulff and Mosbach in the 1970s for the purpose of synthesis of artificial enzyme mimics or chromatographic separations (Hirantani and Alvarez-Lorenzo, 2002). The synthesis is usually performed by copolymerization of functional and cross-linking monomers in the presence of a molecular template and additional solvents that induce porosity in the molecularly imprinted polymer (or porogens). A schematic representation of the process of molecular imprinting is shown in figure 3.

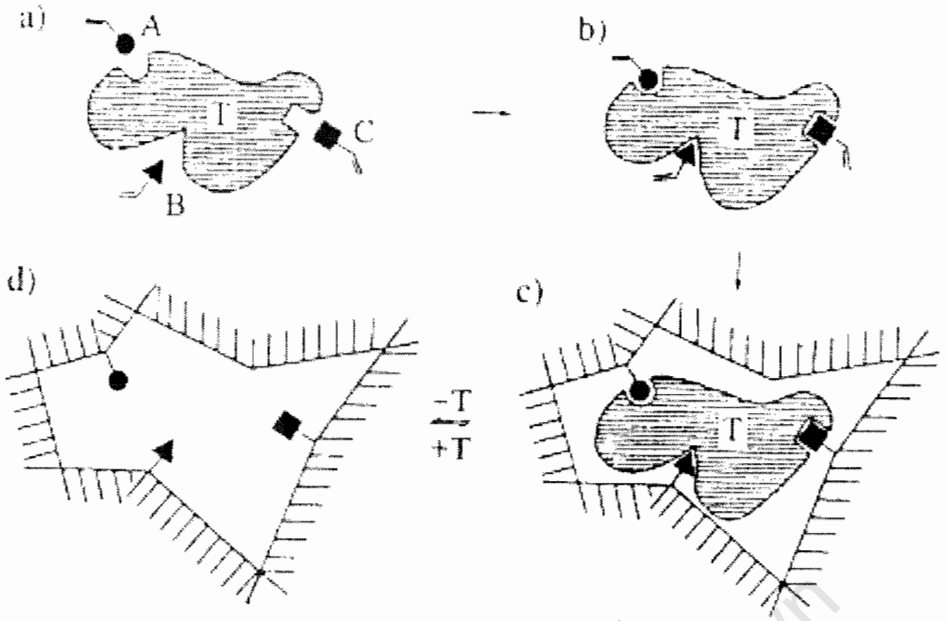

Figure 3. Schematic representation of the imprinting of specific cavities in a crosslinked polymer by a template (T) with three different binding groups showing (a) Pre-arrangement of functional groups of the monomer to appropriate sites in the template; (b) Pre-polymer complex; (c) Highly crosslinked polymer with well arranged chains; and (d) well-defined cavity left after template removal [Wulff, 1995].

The functional monomers have to interact with the template molecules by either covalent or noncovalent bonding, leading to two basic approaches to molecular imprinting: the covalent approach and the noncovalent approach (Ramstrom, 1996). Both approaches use a high percentage of crosslinking that helps in making the polymer rigid enough just to maintain its three-dimensional structure after template removal and to remain insoluble. Both approaches result in a common recognition mechanism. They only differ in their prepolymerization interactions.

In the covalent approach which was originally proposed by Wulff (figure 4), the template molecule and the monomer are linked by reversible covalent bonds prior to polymerization (Ramstrom, 1996). In this case derivatization of the template molecule

with the monomer is required before polymerization. The template is then removed by cleavage of the covalent bond and recognition sites complementary in shape and functionality to the template molecule are left in the polymer. The structure of the template molecule determines which interactions are most favourable in the specific case.

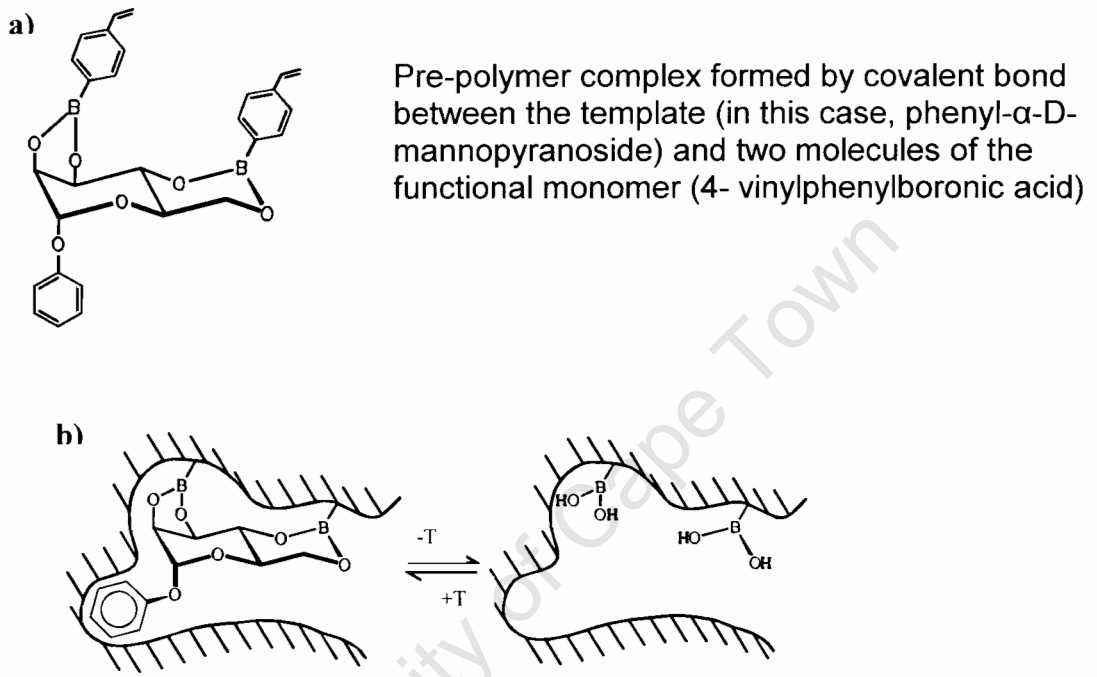

Figure 4. Schematic representation of a covalent bond interaction between the template and functional monomer [Wulff, 1995].

In the noncovalent approach which was initially proposed by Mosbach (figure 5), weak intermolecular interactions are involved in the prearrangement between the template molecule and the functional monomer (Ramstrom, 1996). Ionic or hydrophobic interactions, hydrogen bonding and metal coordination are the interactions commonly utilized in this approach. A self-assembled complex is spontaneously formed between the functional monomer and the template molecule. The polymerization reaction takes

place in the presence of a crosslinker, an initiator and a suitable solvent. A polymer matrix with specific recognition elements (cavities) then results after the washing out of the template molecule (Byrne *et al.*, 2002). Selectivity comes about because of the shape of the cavity and the arrangement of functional groups within it (Wulff, 1995).

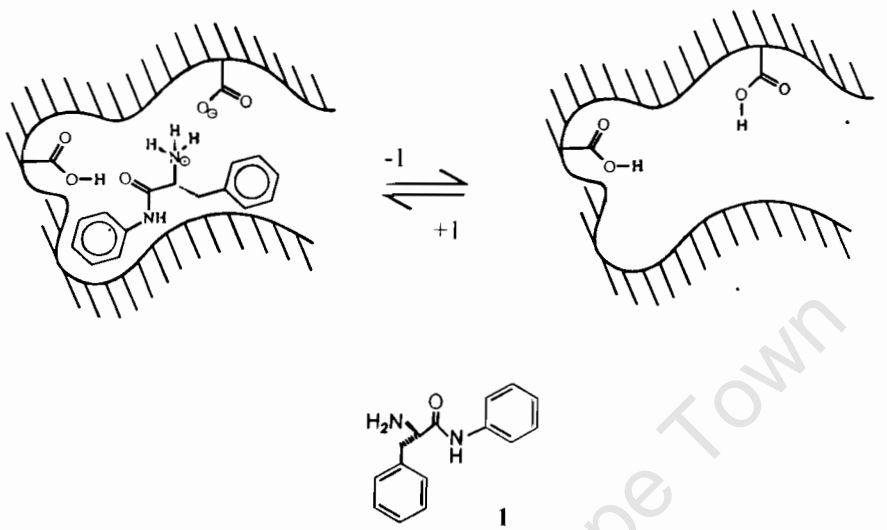

1

Figure 5. Schematic representation of noncovalent interaction. Hydrogen bonding and electrostatic interaction are involved here. Acrylic acid functional monomer (shown in figure 6, page 35) and L-phenylalanine anilide template (**1**) are used in this example [Wulff, 1995].

Sometimes polymers with better selectivities than both of the above mentioned strategies can be obtained by using the combination of covalent interactions and noncovalent interactions (Wulff, 1995).

2.2. Structure of the polymer matrix

The structure of the polymer matrix is very important in the imprinting process (Wulff, 1995). Systematic variation of parameters like the ratio of crosslinking agent, type and concentration of functional monomer, solvent and template molecules is usually required in order to optimize the polymer structure (Hentze and Antonietti, 2001). The following are some of the properties that the polymer needs to have.

a) *Flexibility.* High flexibility makes the equilibration with the substrate to be embedded rapidly and also helps the cavities to be accessible. But too high flexibility leads to a loss of structural definition and selectivity (Wulff, 1995; Hentze and Antonietti, 2001).

b) *Rigidity.* Since recognition requires three-dimensional orientation, control of the polymer chain relaxation is necessary. High ratio of crosslinking agent to functional monomers helps the polymer structure to be stiff and hence enables the cavities to retain their shape after removal of the template, resulting in high selectivity. Too rigid structure, however, leads to lower accessibility of the cavities (Byrne *et al.*, 2002; Wulff, 1995).

c) *Stability.* Mechanical, thermal and chemical stability of polymer enables it to be used for many applications. For example, mechanical stability is important if the imprinted polymer is meant for use in an HPLC column at high pressure or as a catalyst in a stirred reactor. Thermal stability enables it to tolerate high temperatures at which the kinetics are more favourable (Wulff, 1995). Chemical stability helps it to tolerate a wide range of pH and organic solvents.

From the first two properties discussed above, it can be concluded that a compromise must be found between a stiff structure to give high selectivity and flexibility which is necessary for good accessibility of the cavities (Wulff, 1995).

2.3. Function of the binding groups

2.3.1. Functional monomer

The choice of the functional monomer is a determining factor in preparing an imprinted polymer for a particular purpose. The functional monomer has to be one with a binding group that forms a strong bond with the template in order to have a definite orientation of the binding groups on the polymer chains when they are crosslinked (Sellergren, 2000). There must also be a complete removal of the template after polymerization is complete. Lastly, the interaction between the binding groups and the template molecule has to be as labile and reversible as possible. This property is especially useful when the purpose of the imprinting is for chromatographic separations or catalysis. Although the binding groups in the noncovalent approach are not fixed in space during polymerization as precisely as that of covalent interactions and a considerable excess of binding groups is required, noncovalent interactions have the advantages of easily removing the templates and rapidly reversible interactions with substrates (Wulff, 1995).

Depending on the type and spatial arrangement of the interacting groups, polymers vary in their effect on crystal morphology. For instance, carboxyl or phosphoryl side chains are more effective than sulphonyl side chains and neutral and amino acid side chains have no effect on CaOx crystallization (Wesson *et al.*, 2000). These workers have also

suggested that a morphology change within a crystal structure results from a face-specific inhibition of crystallization. The most commonly used functional monomers contain carboxylic acid, sulphonic acid, or heteroaromatic base functional groups. Methacrylic acid for example is very commonly used because the carboxylic acid group serves as a proton donor as well as acceptor in the hydrogen bonds formed (Sellergren, 2000). Some commonly used functional monomers are shown in figure 6.

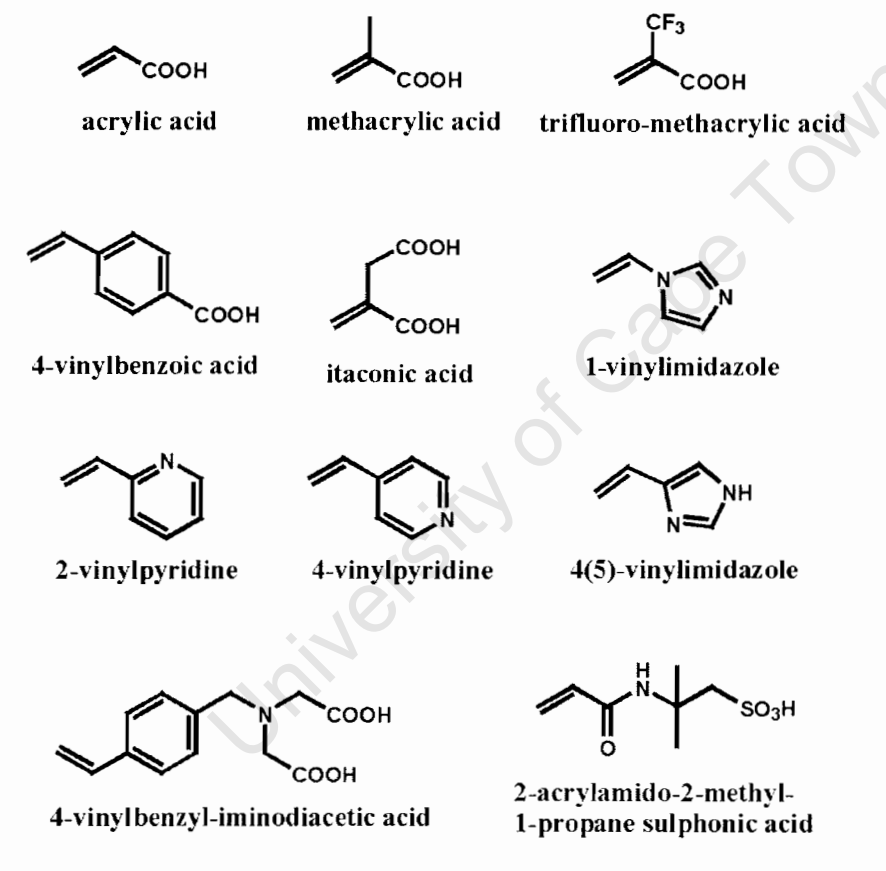

Figure 6. Some examples of functional monomers used in self-assembly imprinting [Ramstrom, 1996].

2.3.2. Templates and porogens

The pore size and morphology of the imprinted polymer can be controlled by making a good choice of porogens and templates. The porogens and templates have to be present until the end of the formation of the polymer matrix and removed after the reaction. Generally, the imprinted cavities embed the template molecules in preference to any other substance. The template, the selected target substance used in the imprinting process, needs to be soluble in the solvent to be used and stablity under the operational conditions is required (Sellergren, 2000). It has to be also one that does not react with the free radicals used to initiate the polymerization. If a solvent with too low polarity is used, the interactions with the functional monomer will not be specific enough, while a too high polarity also causes low solubility of the monomer solution (Hentze and Antonietti, 2001). High polarity also leads to poorer recognition because it weakens the interaction forces formed between template molecules and functional monomers (Ramstrom, 1996). The solvent should also not interfere or compete with any of the intended noncovalent interactions employed during template-monomer complex formation as otherwise a less effective recognition will result (Byrne *et al.*, 2002).

2.3.3. Crosslinking agent

The type and quantity of the cross-linking agent is crucial for high selectivity. Although it strongly influences the morphology of the polymer, the type of the porogen used has no significant effect on the selectivity of the cavities formed. Besides the cross-linking agent, the porosity and the inner surface area play an important role in determining the accessibility of the cavities (Wulff, 1995). The inner diffusion of imprinted molecules toward the reactive sites, which are deeply formed in the polymer matrix makes the reaction kinetics slow (Toorisaka *et al.*, 2003). As it is shown in figure 7, polymers

crosslinked by 1,4-divinylbenzene (dvb) are less efficient for molecular separations because of the stiffness of the structure. But it must be noted that imprinted polymers, especially those used for crystal imprinting (D'Souza *et al.*, 1999), need to be rigid. In this last case, dvb is preferred to ethylene dimethacrylate and tetramethylene dimethacrylate which are both more selective than dvb but are too flexible to be used for crystal nucleating polymers. Some examples of cross-linking agents are shown in figure 8.

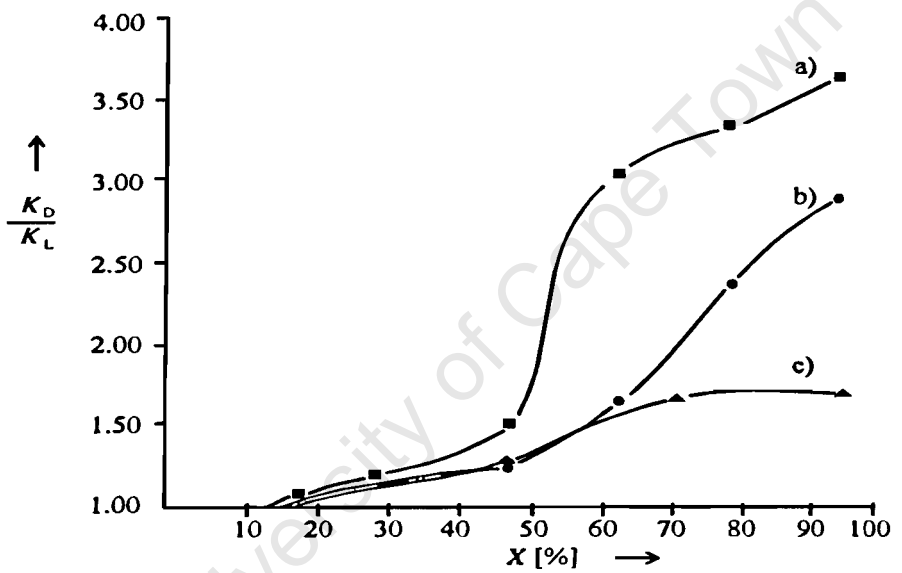

Figure 7. Selectivity of polymers as a function of the type and mole % (X) of crosslinking agent. Separation factor, $\alpha = K_D/K_L$ for the resolution of phenyl-D-L-mannopyranoside in a batch process after removal of the template (T) from the pre-polymer complex **'a'** (figure 4, page 31) polymerized with various proportions of the crosslinking agents a) ethylene dimethacrylate, b) tetramethylene dimethacrylate, and c) dvb [Wulff, 1995]

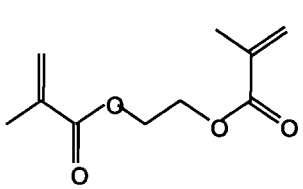

ethylene dimethacrylate

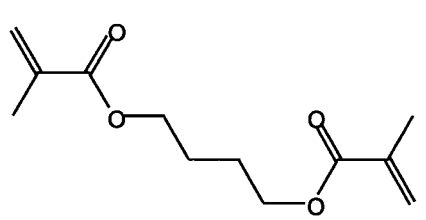

tetramethylene dimethacrylate

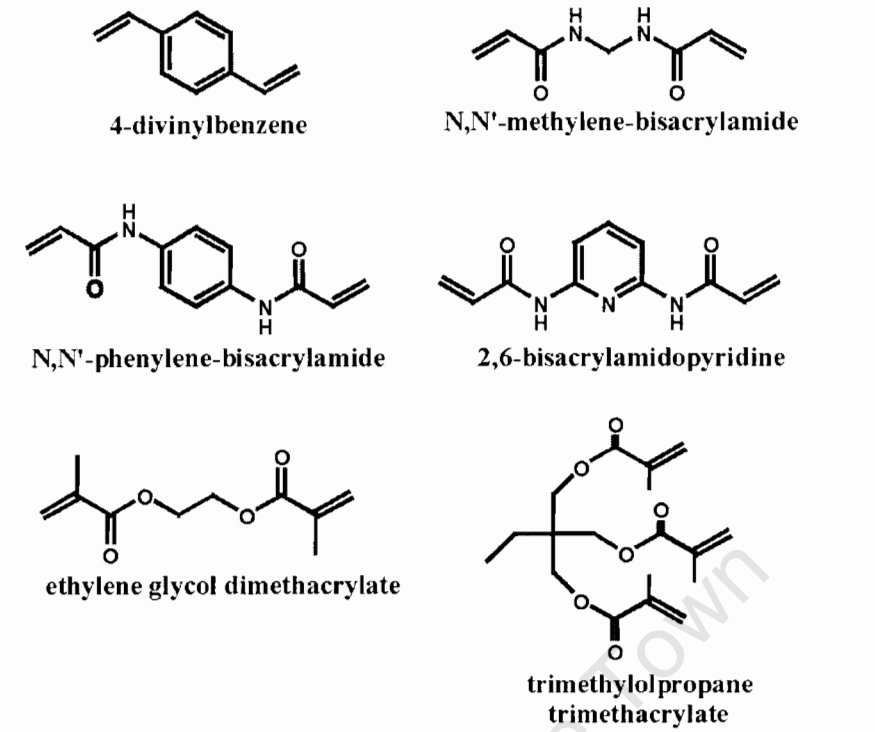

Figure 8. Some of the commonly used crosslinkers [Ramstrom, 1996].

2.3.4. Binding sites and substrate recognition

Unless otherwise cited, this section is composed of ideas taken from the review article by Wulff (1995). If the purpose of imprinting is for catalytic activity as in this work, a definite arrangement of the functional groups is very important (Hentze and Antonietti, 2001).

A specific embedding of the template molecule into a cavity that exactly fits to its size and that has functional groups that correspond to its interacting sites is required. Most template molecules have two binding groups which is the ideal number to optimize selectivity and kinetics. Most of the time these binding groups are identical but they can produce nonidentical binding sites in the imprinted cavities (figure 9). There can occur a productive (figure 9c) or unproductive (figure 9b) one-point binding. The productive one-point binding upon further reaction leads to the desired two-point binding

(figure 9a). However, no second bond is possible in case of the unproductive one-point binding. This bond has to be broken in order for one of the two productive one-point bonds to be formed. Although it is formed more slowly, the correct two-point bond has the highest association constant. Imprints with three or more binding sites are inefficient as the number of possible unproductive complexes is large and formation of the productive complex is correspondingly slower.

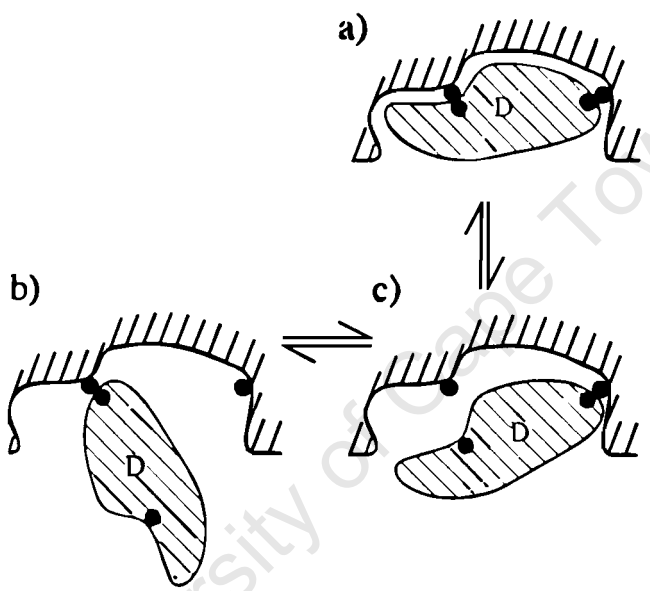

Figure 9. Schematic representation of two-point binding (a), unproductive one-point binding (b), and a productive one-point binding (c) [Wulff, 1995].

2.3.5. Effect of swelling

The volume of the polymers and especially of the cavities increases as a consequence of removal of the template. The extended cavities can then embed the template easily. Surprisingly, the cavities shrink to almost the original volume after the template is rebound. The higher the temperature the more selective is the imprinted polymer. This is partly due to the faster formation of the more selective two-point binding at raised temperatures. Besides, swelling makes the particularly highly selective cavities, those that are unaccessible at room temperature, accessible. On the other hand, sometimes,

relaxation of strain and swelling of the matrix after the removal of the template may cause the cavities to change their shape and make the embedding of the template impossible (Wulff, 1995). Swelling effects are more pronounced in aromatic solvents than in aliphatic organic solvents. The strong interaction between the imprinted polymer and the aromatic solvent causes swelling, and hence deformed cavities and consequently relatively low selectivity (Toorisaka *et al.*, 2003).

2.4. Applications of molecular imprinting

Molecularly imprinted polymers have been used in a wide range of applications that involve analysis and separation, as well as synthesis techniques. Antibody/antigen and receptor binding mimics (Shi *et al.*, 1999), selective catalysts (enzyme mimics) (Strikovski *et al.*, 2003; Mercier *et al.*, 2000; Lele *et al.*, 1999), chromatography (Rachkov *et al.*, 2000; Mathew-Kritz & Shea, 1996) and biosensors (Kriz *et al.*, 1997) are some of the promising areas where molecular imprinting is applied. This section will briefly discuss some of the above-mentioned applications and some other specific works reported on the application of molecularly imprinted polymers.

2.4.1. Molecularly imprinted polymers as artificial antibodies

Molecularly imprinted polymers have a number of advantages over their natural counterparts such as enzymes and antibodies. They are equally or more potent, they work at lower concentrations and are less expensive. Kriz *et al.*, (1997) have reported that molecularly imprinted polymers have recognition properties that tolerate acid, base, heat or organic phase treatment and this makes them suitable to be used as

chemical sensors. Molecular imprinting can be applied not only to low molecular weight targets but also to large molecules such as proteins (Sellergren, 2000).

Shi *et al.* (1999) imprinted three blood proteins; bovine albumin, serum immunoglobulin and fibrinogen to compare protein recognition by template-imprinted surfaces and non-template surfaces. A decrease in the nitrogen signal of electron spectroscopy for chemical analysis (ESCA) and the time-of-flight secondary ion mass spectrometry (TOF-SIMS) peaks which are indicative of protein fragments confirmed the removal of the imprinted proteins by a basic solution. They reported a better recognition of proteins by the protein imprints compared to the non-template polymers confirming the specificity of template recognition. Template recognition happens through a multistep adsorption, with the specificity resulting from shape selectivity and hydrogen bonding. Van der Waals forces also contribute to the specificity due to steric complementarity. From this it can be suggested that, like antibodies, molecularly imprinted polymers can be used in highly sensitive separation techniques like screening of proteins that are very similar to one another.

2.4.2. Molecularly imprinted polymers for chromatographic separations

Ye and Mosbach (2001) prepared molecularly imprinted polymers with binding sites made up of uniform polymer microspheres. They used phase controlled precipitation polymerization methods in a dilute solution of functional monomer and crosslinker to prepare the imprinted polymer.

The solvent used to prepare such microspheres by a noncovalent approach should not interfere with the driving force of the polymer matrix formation, but it has to be

miscible with the monomer and initiator used and it should not dissolve the polymer formed. These molecularly imprinted polymer microspheres have been used for chiral separation. Ye & Mosbach have cited an example in which (-)-ephedrine was used as a template and the racemates, ephedrine and salbutamol, were separated by capillary electrophoresis. Migration of the analyte towards the cathode and the molecularly imprinted polymer microspheres containing the bound enantiomer to the anode enabled the chiral separation.

2.4.3. Catalytically active molecularly imprinted polymers

Lele *et al.* (1999) synthesized a series of molecularly imprinted polymer mimics of chymotrypsin by grafting a Co(II) coordinated monomer-template assembly containing different functional groups like hydroxyl, carboxyl and imidazole groups on to the surface of a microporous support. They used the Michaelis-Menten kinetics model to evaluate the hydrolytic activity of the mimics. This activity was observed to increase with an increase in nucleophilicity of the monomer used and a decrease in surface area of the imprinted polymer produced. Kunitake and Okahata (1976) have also tried to synthesize the same series of mimics comprising imidazole and carboxyl functions, however, Lele *et al.* suggested that this study lacked a specific mechanism of bringing the two functional groups next to each other and a mechanism for template recognition.

Beach and Shea (1994) reported an effective catalytic acceleration by molecularly imprinted polymers using benzylmalonic acid template and N-(2-aminoethyl)-methacrylamide monomer. This imprinted polymer was observed to position the polymerizable amines in a definite arrangement in the cavity. Compared to the reaction in solution (figure 10) and in the presence of control polymer (figure 11), this template

imprinted polymer showed accelerated catalysis of the dehydroflourination of 4-fluoro-4-(*p*-nitrophenyl)butan-2-one (fnb, **2**)

Figure 10. Dehydroflourination of fnb [Beach and Shea, 1994]

As it is shown in figure 11, hydrogen bonding interaction between polymer and substrate is involved in this reaction. The polarity of the reaction solvent is, therefore, important. Beach and Shea proved that the use of more polar solvents such as acetonitrile and ethanol slowed down the rate of the dehalogenation reaction of the imprinted polymer.

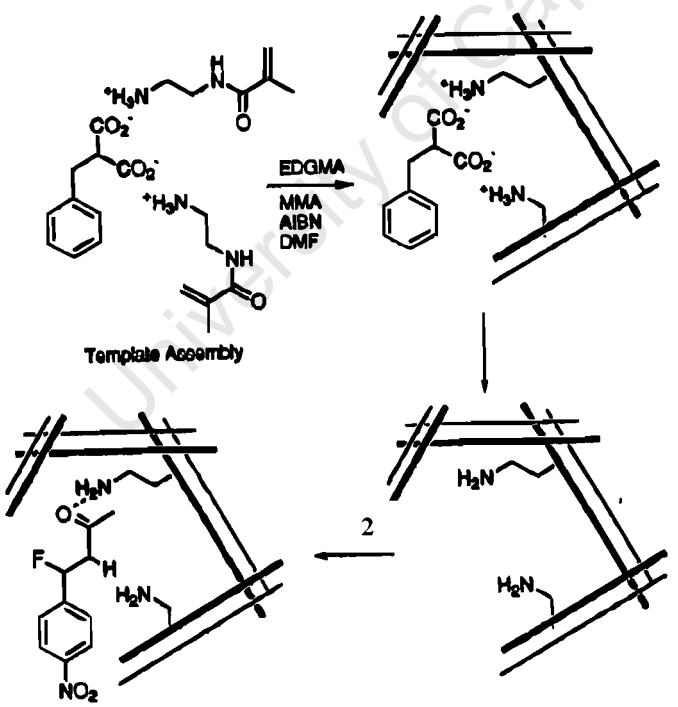

Figure 11. Catalyst design for the dehydroflourination of fnb [Beach and Shea, 1994)]

This template was also observed to exhibit effective turnover, Michaelis-Menten kinetics and competitive inhibition of the dehydrofluorination reaction of fnb.

2.4.4. Imprinting of crystals for structure-directed nucleation

Recently D'Souza *et al.* (1999) have reported the nucleation of calcite (calcium carbonate) crystals on the surface of a polymer imprinted with these crystals, demonstrating the utility of this approach in biomimetic mineralization. The polymer used was a co-polymer of 6-methacrylamidohexanoic acid (maaha) and dvb. After removal of calcite, this imprinted polymer was shown to be capable of nucleating calcite under conditions that would normally favor the growth of aragonite, another calcium carbonate polymorph, (figures 12 and 13). When they soaked 1.0 mg/ml of the calcite imprinted and washed polymer in an aqueous solution of (1.0 mM $CaCl_2$ and 0.8 mM $NaCO_3$), calcite crystals that are noticeably larger than those formed in the solution were observed. On the other hand, very few crystals were observed on the surface of the unimprinted (control) polymer soaked in the same solution (figure 12e).

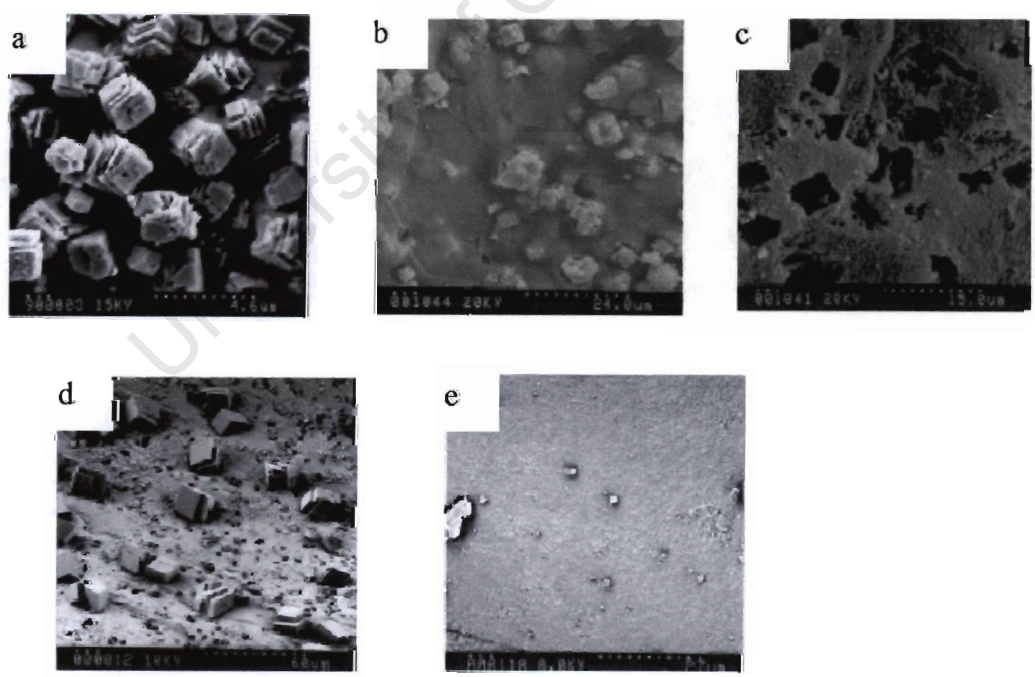

Figure 12. Nucleation of calcite at a polymer surface. Scanning electron micrographs showing: a) template calcite crystals, b) calcite imprinted polymer, c) calcite imprinted polymer after HCl/CH_3OH wash, d) nucleation of calcite crystals on the surface of imprinted and washed polymer, and e) unimprinted (control) polymer soaked in supersaturated $CaCO_3$(aq) [D'Souza *et al.*, 1999].

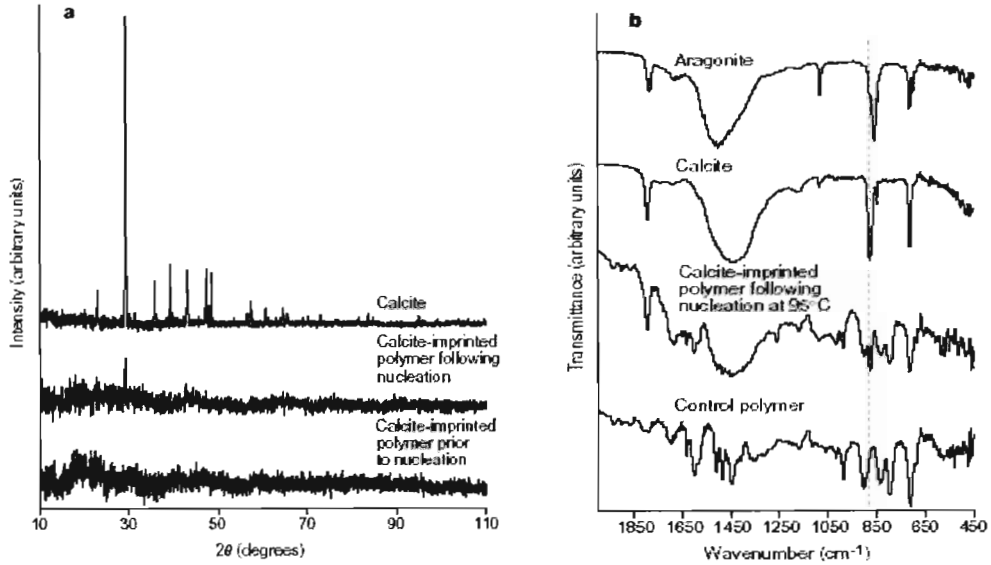

Figure 13. Characterization of $CaCO_3$ crystal polymorphs. a) XRD patterns recorded using Cu Kα radiation showing calcite nucleation on the imprinted polymer b) FT-IR spectra showing evidence of $CaCO_3$ nucleation on the polymer surface [D'Souza *et al.*, 1999].

The poor wettability of the polymer was modified by addition of 10% (v/v) acetonitrile which helped up to 50% of the sites to be occupied with crystals. They showed in a separate experiment that acetonitrile does not affect the crystallization of $CaCO_3$ crystals. The same monomer imprinted with aragonite, however, did not direct the nucleation of aragonite crystals. Why only the calcite imprinted polymer led to an efficient nucleation whereas the aragonite imprinted polymer did not is not clear. The number of crystals on the surface of the control polymer and imprinted polymers whose carbonyl groups were blocked before nucleation was negligible, demonstrating that nucleation was specifically bought about by the imprint sites.

2.5. Conclusion

It is well known that the concentration of calcium oxalate forming ions in urine is too small for spontaneous nucleation to occur. Nucleation of calcium oxalate crystals *in vivo* is thus believed to take place on the surface of a substrate (Nancollas *et al.*, 1991; Khan *et al.*, 1993). Urinary macromolecules which are mainly proteins and GAGs are the substances that are believed to act as substrates. Although several techniques have been used for studying the crystallization of calcium oxalate crystals *in vitro*, only a few have been able to crystallize CaOx below its metastable limit using some nucleation promoting surfaces (Khan *et al.*, 1990; Khan *et al.*, 1993). Moreover, the anionic functionality (e.g., carboxylate) present in anionic molecules or macromolecules determine the morphology of crystals and hence affect crystal aggregation and adhesion of crystals to cells (Sheng *et al.*, 2003).

The work of D'Souza and co-workers has opened the gate to molecular imprinting that can be used to direct crystal nucleation. Molecular imprinting provides a novel technique that may be used to mimic the *in vivo* crystallization of calcium oxalate crystals from solutions at concentrations that do not allow spontaneous precipitation of calcium oxalate to take place.

The work described in this thesis is aimed at utilizing molecular imprinting technology for crystallization of calcium oxalate crystals on the surface of a polymer imprinted with these crystals with a view to ultimately gaining a better insight into understanding the formation of human kidney stones.

CHAPTER THREE – OBJECTIVES

This study was aimed at investigating the crystallization of calcium oxalate crystals via a new method, molecular imprinting. The following objectives were defined

- To prepare calcium oxalate monohydrate (COM) and calcium oxalate dihydrate (COD) crystals
- To prepare unimprinted (control) polymer and to imprint samples thereof with both CaOx hydrates.
- To test formation of CaOx crystals of both hydrates from metastable CaOx solutions in the presence and absence of the imprinted and unimprinted polymers.
- To repeat the above experiments using synthetic urine with varying concentrations of magnesium and citrate.
- To investigate whether imprinted polymer of each hydrate is able to direct the formation of CaOx crystals under conditions which alternatively favour the formation of each hydrate itself.
- To measure metastable limit of human urine in the presence and absence of the control and imprinted polymers.
- To test human urine for the formation of CaOx crystals of both hydrates using the imprinted polymers.

CHAPTER FOUR - EXPERIMENTAL PROCEDURES

4.1. Preparation of calcium oxalate template crystals

4.1.1. Calcium oxalate monohydrate crystals

Calcium oxalate monohydrate (COM) crystals were prepared by the method of Pak *et al.*, (1975) by simultaneously mixing equal volumes of 0.010 M $CaCl_2$ and 0.010 M $Na_2C_2O_4$ at a rate of 1 ml per minute using a peristaltic pump to give a final total volume of 1000 ml. The reaction mixture was stirred at 6 °C in a cold room for one week. The precipitate was then filtered, washed with distilled water and methanol and then dried for 1 hour at 95 °C. A mass of 0.59 g of calcium oxalate was obtained, *i.e.* the percentage yield was 92 %.

4.1.2. Calcium oxalate dihydrate crystals

Calcium oxalate dihydrate (COD) was prepared according to the method of Brown *et al.*, (1989) with some modifications in the incubation temperature and final volume. A solution of volume 250 ml containing 1.398 g sodium citrate (0.01926 M), 1.423 g magnesium sulfate (0.0231 M) and 2.4025 g potassium chloride (0.1274 M) was prepared. To this was added 125 ml of 0.02508 M calcium chloride (prepared using $CaCl_2.2H_2O$) and the pH was adjusted to 6.5 by the addition of HCl. The solution was allowed to equilibrate at 26 °C for 15 minutes. Thereafter, 125 ml of 0.0064 M NaOx was added with continuous stirring. The solution was incubated for a further 15 minutes at 26 °C and then filtered through a 0.22 μm filter. Excess supernatant was poured off and the sample was suspended in methanol. The sample was centrifuged again and the excess methanol was removed. The crystals were dried at 37 °C for 2 – 4 hours.

Prior to using the above protocol, difficulties were experienced in obtaining pure COD crystals using the final volume of 5 litres recommended by Brown *et al.* (1989). The latter protocol yielded pure COD crystals for the first few batches only but thereafter yielded a mixture of COD and COM with trace amounts of COT. However the method yielded pure COD reproducibly when the final volume was reduced to 500 ml, the samples were filtered instead of centrifuged and the incubation temperature was raised from 22 °C to 26 °C, as described above.

Formation of pure COM and COD crystals was verified by X-ray powder diffraction (XRD), Fourier transform infrared spectroscopy (FTIR) and scanning electron microscopy (SEM). This will be discussed in detail in section 4.4.

4.2. Urine and urine like solutions

4.2.1. Saturated calcium oxalate solution

A series of three calcium oxalate solutions within the metastable region (table 4.1) were prepared by mixing calcium chloride and NaOx solutions as follows: (I) 0.006 M calcium chloride (10 ml) and 0.006 M NaOx (10 ml) to give 0.003 M CaOx solution, (II) 0.010 M calcium chloride (10 ml) and 0.010 M NaOx (10 ml) to give 0.005 M CaOx solution and (III) 0.012 M calcium chloride (10 ml) and 0.003 M NaOx solution (10 ml) to give a solution with a 4:1 calcium-to-oxalate ratio.

Table 4.1. CaOx solutions prepared for crystallization experiments

Solution I	Solution II	Solution III
0.003 M CaOx Prepared by mixing 0.006 M $CaCl_2$ with 0.006 M NaOx.	0.005 M CaOx Prepared by mixing 0.010 M $CaCl_2$ with 0.010 M NaOx.	4:1 Ca:Ox solution Prepared by mixing 0.012 M $CaCl_2$ with 0.003 M NaOx.

4.2.2. Artificial urine

Artificial urine was prepared by the method of Brown *et al.*, (1989) by sequentially dissolving the following components in water (final concentrations are given in brackets): 3.032 g NaCl (0.1055 M), 2.228 g $NaH_2PO_4.H_2O$ (0.323 M), 0.472 g $Na_3C_6H_5O_7.2H_2O$ (0.00321 M), 0.475 g $MgSO_4.7H_2O$ (0.00385 M), 1.204 g Na_2SO_4 (0.01695 M) and 2.375 g KCl (0.0637 M); to this solution was added 0.422 g $CaCl_2.2H_2O$ (0.00575 M) and 0.021 g $Na_2C_2O_4$ (0.000318 M). The pH was adjusted to 6.5 by first adding 0.740 g NH_4Cl (0.0276 M) followed by the required volume of concentrated NH_4OH. The solution was made up to 500 ml with distilled water in a volumetric flask and then filtered through a 0.22 μm filter before use.

For the experiments in which magnesium and citrate concentrations were varied, artificial urines were prepared as described above, but the latter components were decreased or omitted (see table 4.2).

Table 4.2. Artificial urine solutions prepared for crystallization experiments

Solution IV	Solution V	Solution VI	Solution VII
Artificial urine	Artificial urine from which magnesium is omitted	Artificial urine from which citrate is omitted	Artificial urine where magnesium and citrate concentrations are reduced to 0.001M and 0.0008M respectively.

4.2.3. Urine samples

Fifteen 24 h urine samples (solution VIII) were collected from healthy white male South African volunteers. THM and cellular debris were removed by filtering first with a pre-filter and then with a 0.45 µm filter paper. The pH and metastable limit of each sample were measured.

The CaOx metastable limit (corresponding to the concentrations of Ca^{+} and $C_2O_4^{2-}$ at which spontaneous nucleation and growth occur) was measured using the method of Ryall *et al.* (1985). 2.68 g of NaOx was dissolved in 100 ml water to prepare a 0.2 M solution. This stock solution was used to prepare a series of 13 dilutions with concentrations ranging from 0.015 to 0.195 M with incremental concentrations of 0.015 M. A series of vials each containing 20 ml filtered urine samples were incubated at 37 °C for 10 min. 100 µl of each dilution was added progressively to each vial at 3 min intervals and the particle number was recorded 30 min thereafter using a Coulter Counter (model 5.ST.II, England). The NaOx concentration at which the particle number increased abruptly was taken as a measure of the MSL.

Since polymer particles are large enough to block the aperture of the Coulter Counter, a HACH ratio turbidimeter (model 18900, USA), calibrated against the Courier Counter, was used to measure the metastable limits of urines to which the unimprinted and imprinted polymers had been added.

4.3. Preparation of functional monomer and imprinted polymers

4.3.1. Preparation of 6-methacrylamidohexanoic acid

The functional monomer, maaha, was prepared based on the Schotten-Baumann procedure (Mann and Saunders, 1967) from 6-aminohexanoic acid and methacrylic anhydride. The reaction (figure 14) involves nucleophilic attack by the lone pair of electrons on the 6-aminohexanoic acid nitrogen at the electron deficient carbonyl carbon atom of methacrylic anhydride, followed by deprotonation of the amine group. 3.67 g 6-aminohexanoic acid (**1**) was dissolved in a 10% (m/v) NaOH solution (25 ml). Methacrylic anhydride (**2**) (3.4 ml) was added and the reaction mixture was stirred for 24 hours. The solution was then acidified to pH 1 by adding concentrated HCl. Solid 6-methacrylamidohexanoic (**3**) acid was isolated and purified by silica gel column chromatography. The column was packed with a mixture of 80g silica gel in petroleum ether and a 3-4 cm layer of sand was packed on top of the column bed. The column was then eluted with a 20:80 (v/v) dichloromethane:ethyl acetate mixture which was added through separating funnel. Fractions (50 ml) were spotted on a thin layer chromatography plate and run with diethyl ether. The fractions containing only the desired product were retained, the solvent mixture was removed using a rotary evaporator and the product dried in vacuo. The dried product was characterized by ^{1}H NMR spectroscopy on a Varian VXR200 spectrometer (figure 22, *p.* 63).

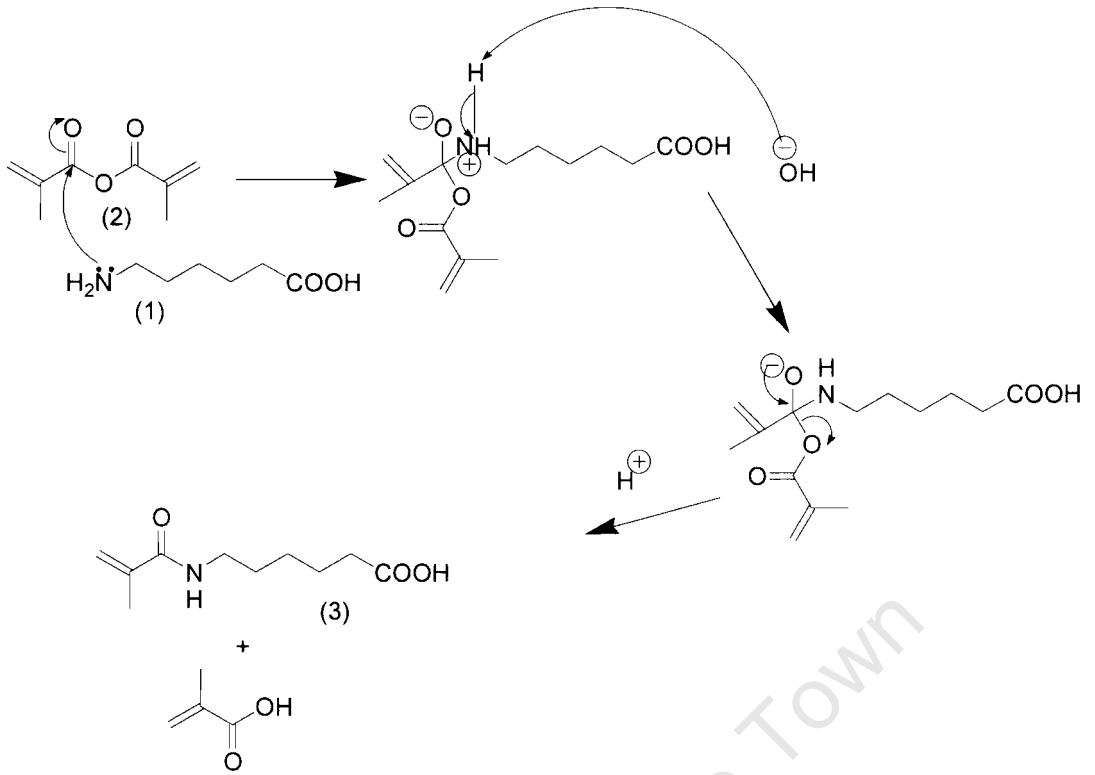

Figure 14. Mechanism of the preparation of maaha

4.3.2. Preparation of imprinted polymers

The strategy for the preparation of imprinted polymer and the subsequent nucleation of calcium oxalate on the polymer is illustrated in figure 15 (*p* 55) and is based on the approach of D'Souza *et al.* (1999). Briefly, template COM crystals (0.75 g) were stirred in a 5 ml solution of 0.020 M maaha in chloroform in a sealed tube for 24 hours. Thereafter, 1.41 ml of dvb (AR grade, 80%) was added with 0.039 g of azo-biscyclohexanecabonitrile (abchc) polymerization initiator. The sample mixture was degassed, sealed under reduced pressure and allowed to react for 6 hours at 4 °C following photochemical initiation of polymerization. After gelation, the polymer was heated at 65 °C for 15 hours to complete polymerization. The sample was then dried in vacuo and gently ground with mortar and pestle to produce particles with a diameter of about 100 μm.

Samples of COD imprinted polymer were produced using the same protocol, except COD crystals were used in place of COM. Unimprinted polymer was prepared in the absence of COM and COD.

XRD, FTIR and SEM techniques were used to confirm the incorporation of CaOx into the imprinted polymers.

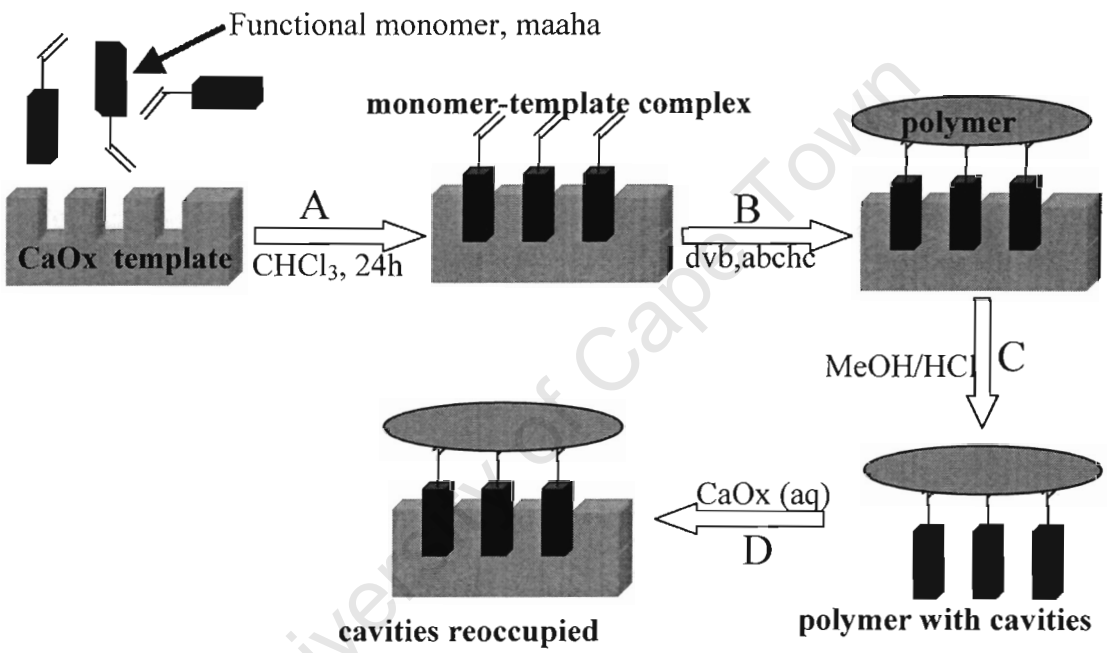

Figure 15. Schematic representation of molecular imprinting process.

A) Self-assembly of functional monomer on the surface of CaOx crystals by incubating in chloroform solution for 24 hours.

B) Co-polymerization of monomer with dvb in the presence of an initiator, abchc.

C) Template removal by dissolution and washing with acidified methanol (2M HCl, final concentration).

D) Specific nucleation of CaOx template crystals from a saturated solution of calcium oxalate, artificial urine, or real urine (solutions I to VIII).

4.3.3. Removal of template crystals by washing

Template crystals were then removed by soaking the polymer in 100 ml methanol acidified with HCl (2M final concentration with respect to HCl) for 2 days. The crystals were then washed four times with the acidified methanol solution. Finally the polymer was washed with acetonitrile (× 3) and water (× 1) and then dried in vacuo.

Complete removal of the template crystals from the imprinted polymers was confirmed by XRD, FTIR, SEM and atomic absorption spectroscopy (AAS) analyses.

4.3.4. Nucleation of calcium oxalate on imprinted and unimprinted polymer surfaces

Samples of imprinted and unimprinted polymers (0.1 g) were placed in a series of flasks. To each of these was added either 20 ml metastable CaOx solution (solutions I through III, table 4.1 *p* 50), 200 ml artificial urine (solutions IV though VII, table 4.2 *p* 50) or 200 ml real urine (solution VIII). The flasks were sealed and then agitated at 25 °C for 36 hours before filtration through 0.22 μm filter. The polymer was washed thoroughly with water to remove any weakly attached crystals.

Samples obtained using imprinted and unimprinted polymers were characterized by XRD, FTIR and SEM.

4.4. Characterization of samples

All of the prepared crystals, the unwashed and washed samples of the imprinted and unimprinted polymers, as well as nucleated polymers were characterized by XRD, FTIR, SEM and AAS analyses.

Powdered samples were packed into aluminium trays and x-ray powder diffraction patterns were measured using a Philips PW 1050/80 vertical goniometer in the 2θ range 12 – 40° with Cu Kα radiation of wavelength 1.5418Å produced at 40 kV and 25 mA.

In the XRD patterns, the peaks at 2θ values greater than 37° were removed since the aluminium sample holder diffracts at 38°. Thus, one of the characteristic peaks of COM (2θ = 38.4°) will not be shown in the XRD graphs. The d-spacings were compared with standard reference values (table 4.3) for COM, COD and COT (Sutor and Scheidt, 1968; Deganello *et al.*, 1981).

Infrared spectra were recorded between 2000 and 450 cm^{-1} on a Perkin-Elmer Paragon 1000 FTIR spectrophotometer using KBr pellets. 200mg KBr, previously dried in an oven and kept in a desiccator was thoroughly mixed with 2mg of the sample in a mortar and pestle. The mixture was then transferred to an appropriate dye, and pressed at 3000 kPa to form a pellet. The pellet was mounted in a holder and placed in the sample path of the spectrophotometer.

Table 4.3. Interplanar spacings and relative intensities of powder patterns of the three hydrates of calcium oxalate.

* Calcium oxalate monohydrate:		* Calcium oxalate dihydrate:		** Calcium oxalate trihydrate:	
d-spacing (Å)	*Relative intensity*	*d-spacing (Å)*	*Relative intensity*	*d-spacing (Å)*	*Relative intensity*
5.93	100	8.70	12	7.87	40
5.79	25	6.31	100	6.70	20
4.64	7	6.15		5.50	100
4.52	6	4.40	45	5.28	40
3.78		3.89	14	4.99	60
3.76	13	3.67	8	4.79	20
3.65	100	3.58	1	4.02	20
3.00	10	3.38	2	3.75	20
2.97	46	3.15	3	3.67	40
2.91	12	3.09	18	3.62	60
2.89	10	3.07		3.58	10
2.84	14	2.81	20	3.43	20
2.51	2	2.77	85	3.35	10
2.48	30	2.75		3.26	20
2.41	5	2.41	14	2.84	100
2.37	2	2.39	14	2.77	80
2.34	90	2.33	10	2.74	40
				2.69	40
				2.66	20
				2.64	40

** Sutor and Scheidt 1968; ** Deganello et al. 1981*

For SEM, the powdered sample was sprinkled onto an aluminum stub that had been coated in carbon glue. The stub was then sputter coated with gold palladium. The samples were examined on a Leica S440 scanning electron microscope (Leica Cambridge Ltd, Cambridge, England) operating at an accelerating voltage of 10 kV, a working distance of 10 – 15 mm and a probe current of 20 – 30 pA.

The SEM micrographs were also helpful for the examination of the cavities left after the removal of the template crystals and for the comparison of the surfaces of the imprinted, unimprinted and nucleated polymers.

CHAPTER FIVE – EXPERIMENTAL RESULTS AND DISCUSSION

5.1. Template crystals and functional monomer

5.1.1. Verification of COM crystals

The XRD pattern of the CaOx crystals prepared using the method described by Pak *et al.* (1975) with the d-spacings (labelled) is shown in figure 16. The diffraction peak assignments and the percentage composition of these crystals, based on the standard reference table (table 4.3, *p* 57) is summarized in table 5.1. The diffraction pattern exhibits all the peaks expected for COM and is devoid of peaks characteristic of COD or COT, indicating that the sample was 100% COM.

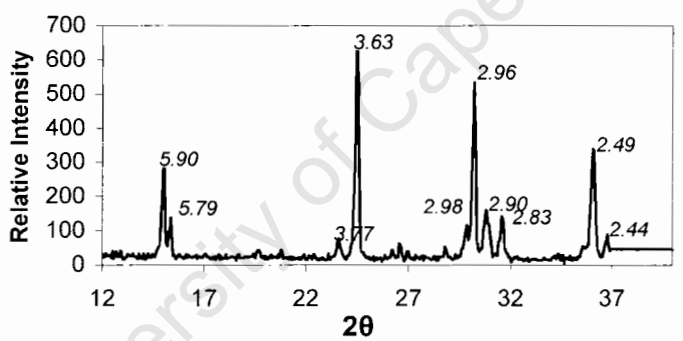

Figure 16. XRD pattern of COM crystals prepared according to Pak *et al.* (1975). d-spacings are expressed in Å and θ is the diffraction angle in degrees.

Table 5.1. X-ray powder diffraction peak assignments and percentage composition of CaOx crystals prepared according to Pak *et al.* (1975)

d-spacing (Å)	Assignment	
5.90	COM	100% COM
5.79	COM	
3.77	COM	
3.64	COM	
2.98	COM	
2.96	COM	
2.90	COM	
2.83	COM	
2.49	COM	
2.44	COM	

The infrared spectrum of the CaOx crystals grown according to the method of Pak *et al.* is shown in figure 17. Comparison with the characteristic bands previously reported (Bellanato *et al.*, 1973; Modlin and Davies, 1981) for COM (1590, 1370, 1320, 960, 890, 665, and 515 cm^{-1}) confirms that the crystals were indeed COM.

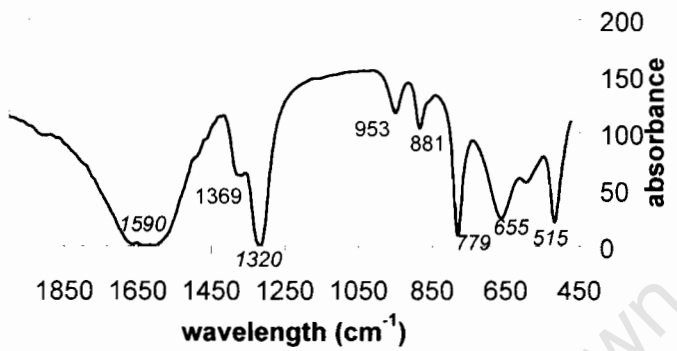

Figure 17. Infrared spectrum of the COM crystals grown according to the method of Pak *et al.*(1975)

Figure 18 shows the SEM micrographs of the CaOx crystals grown according to the method of Pak *et al.* at lower (a) and higher (b) magnifications. Although the morphology of these crystals is ill-defined, the coffin-like shape that has been previously reported for COM crystals (Khan, 1995) is evident, thereby providing further evidence in support of the formation of this particular hydrate. Furthermore, the bipyramidal morphology of COD crystals (Kim, 1982) and the layered morphology of COT crystals (Rodgers, 1999) are both absent indicating 100% purity of COM.

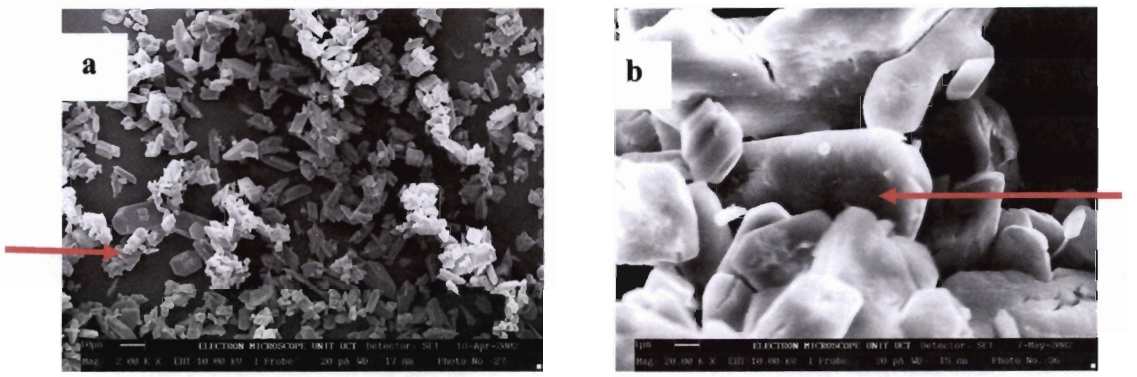

Figure 18. SEM micrographs of the COM crystals grown by the method of Pak *et al.* (1975) at low (×500, a) and higher (×2500, b) magnifications. The coffin-like morphology is indicated by arrows.

Thus, the XRD, FTIR, and SEM analyses support each other that the CaOx crystals grown by the method of Pak *et al.*, were pure COM crystals and contained no other hydrates of CaOx.

5.1.2. Verification of COD crystals

The XRD pattern of the CaOx crystals prepared according to the method of Brown *et al.* (1989) with the d-spacings expressed in Å (labelled) and the diffraction angle, θ in degrees is shown in figure 19. Table 5.2 summarizes the assignment of the prominent peaks and percentage composition of these crystals on the basis of the standard reference (table 4.3, *p* 57). The XRD pattern shows that the sample indeed consists of COD.

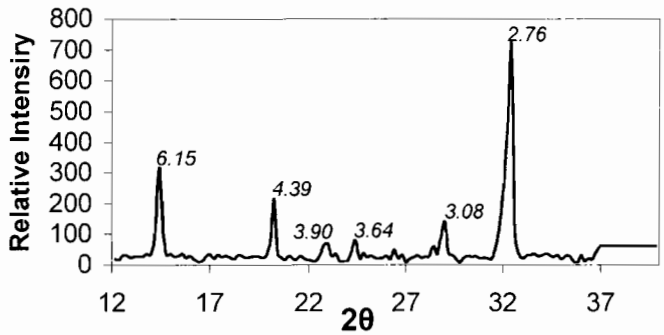

Figure 19. XRD pattern of COD crystals prepared according to Brown *et al.* (1989)

Table 5.2. X-ray powder diffraction peak assignments and percentage composition of CaOx crystals prepared according to Brown *et al.* (1989)

d-spacing (Å)	Assignment	
6.15	COD	100% COD
4.39	COD	
3.90	COD	
3.64	COD	
3.08	COD	
2.76	COD	

The FTIR spectrum for COD shows absorption at 1590, 1315, 780 and 520 and differs from that of COM in that it lacks the bands at 960, 890, and 665 and that the 520 bands are sharper for COM (Bellanato *et al.*, 1973; Modlin and Davies, 1981). Figure 20 shows the FTIR spectrum for the CaOx crystals grown in the present study according to Brown *et al.* (1989). This spectrum showed all of the characteristic bands of COD crystals. Bands characteristic of COM were absent. However, the presence of a weak (unassigned) band at 612 cm^{-1} is indicative of a trace amount of impurity.

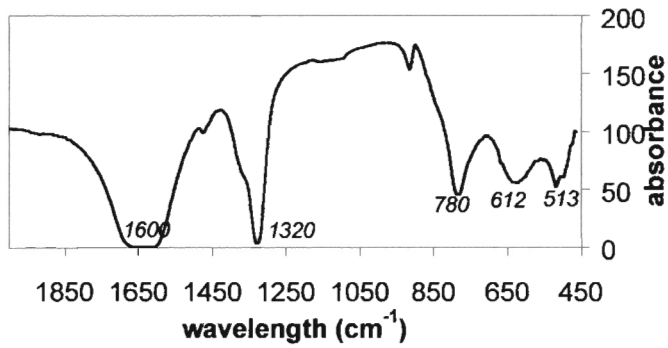

Figure 20. FTIR spectrum of COD crystals prepared according to the method of Brown *et al.* (1989)

SEM revealed the presence of single and aggregated COD crystals as well as sparse amounts of COT (figure 21). The failure of XRD to detect COT is indicative of the latter being present in very small quantities.

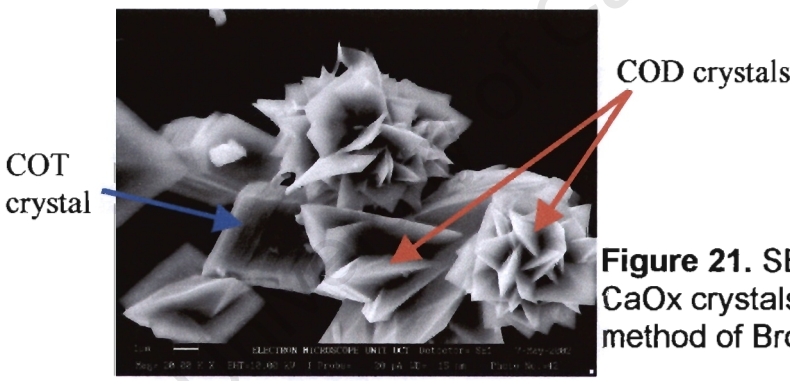

Figure 21. SEM micrograph of the CaOx crystals grown by the method of Brown *et al.* (1989).

Thus, with the exception of a single COT crystal revealed in SEM, the crystal grown was confirmed to be pure by XRD, FTIR and SEM analyses.

5.1.3. Characterization of the functional monomer

The prepared functional monomer used for this study was characterized by ^{1}H NMR spectroscopy (figure 22) on a Varian VXR200 spectrometer, ($CD_3CO_2C_2D_5$, 200 MHz) δ 1.53 (6H, m, CH_2), 1.92 (3H, s, CH_3), 2.32 (2H, t, J = 6.3 Hz, CH_2), 3.29 (2H, q, J = 5.8 Hz, CH_2), 5.28 (1H, d, J = 3.7 Hz, =CH), 5.65 (1H, s, =CH), 6.02 (1H, br s, NH). The peaks were compared with the estimated ^{1}H NMR peaks of the compound, 6-methacrylamidohexanoic acid, from the "Chemdraw" program. All of the peaks of the prepared product corresponded to the Chemdraw values, showing that the prepared functional monomer was 100 % pure 6-methacrylamidohexanoic acid.

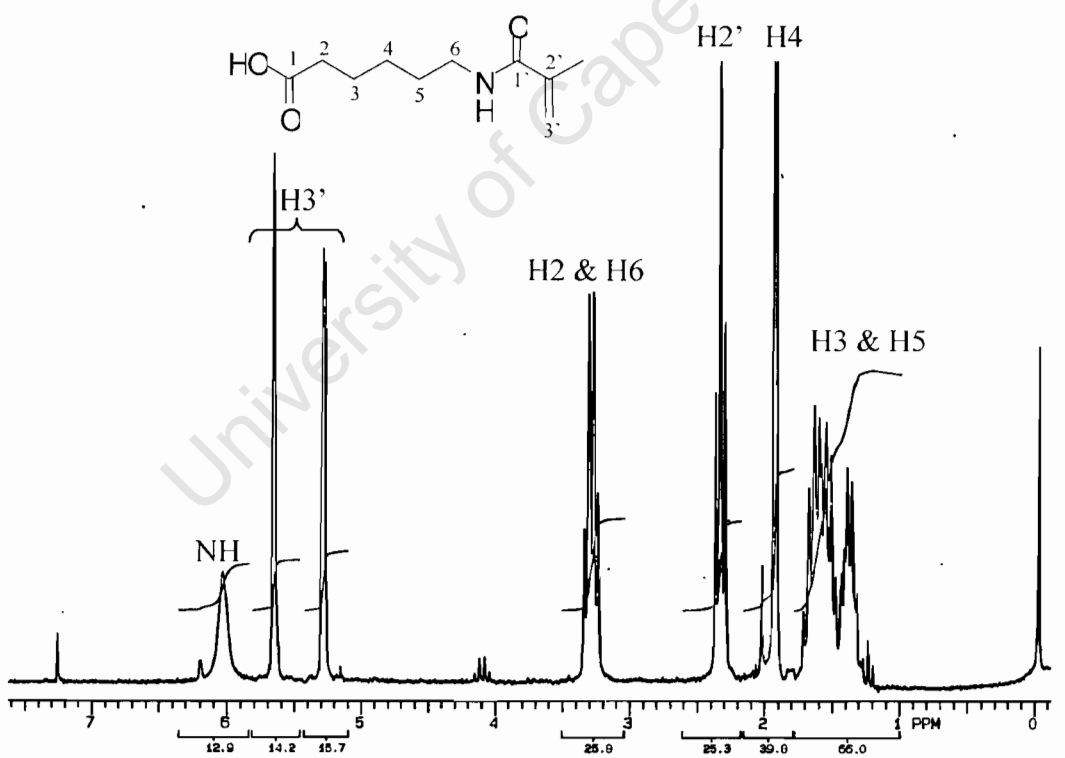

Figure 22. H[1] NMR spectrum of the prepared functional monomer

5.2. Imprinted and unimprinted polymers

5.2.1. COM imprinted polymer

The XRD pattern of unwashed COM imprinted polymer is shown in figure 23. The prominent peaks corresponded to the characteristic diffraction peaks of COM listed in table 5.1 (page 58).

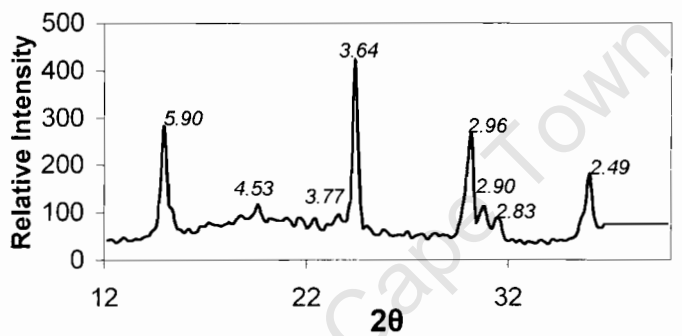

Figure 23. XRD pattern of unwashed polymer imprinted with COM

The FTIR spectrum of the unwashed COM imprinted polymer is shown in figure 24. The characteristic bands (cm^{-1}) of COM crystals (expected) at 1615 (1590), 1365 (1371), 1316 (1320), 985 (960), 894 (890), 779 (780), 511 (515) are evident.

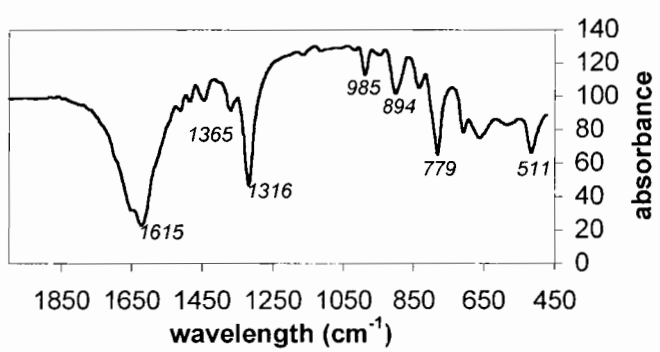

Figure 24. FTIR spectrum of unwashed polymer imprinted with COM

An SEM micrograph of unwashed COM imprinted polymer is shown in figure 25. The surface of the polymer is seen to be covered by numerous crystals. However, their morphological features are not obvious.

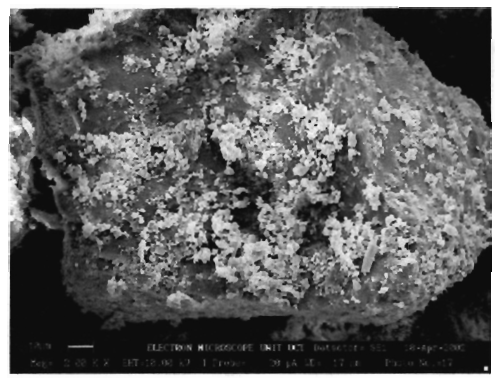

Figure 25. SEM micrograph of a particle of unwashed COM imprinted polymer

Thus, the data from XRD and FTIR experiments show that the COM template crystals have not been altered under the conditions in which the polymerisation reaction has been carried out.

5.2.2. COD imprinted polymer

The XRD pattern of unwashed COD imprinted polymer is shown in figure 26. Although the peaks are not well-defined, reflections characteristic of COD are indicated. Like in the COM imprinted polymer, the XRD pattern showed that the COD template crystals have not been altered under the conditions in which the polymerisation reaction has been carried out.

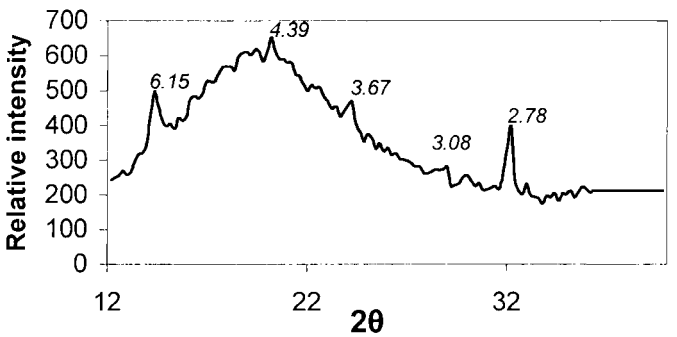

Figure 26. XRD pattern of unwashed COD imprinted polymer

Figure 27 shows the FTIR spectrum of the unwashed COD imprinted polymer. This spectrum shows the characteristic absorption bands (expected) for COD (cm^{-1}): 1620 (1590), 1323 (1315), 792 (780) and 512 (520).

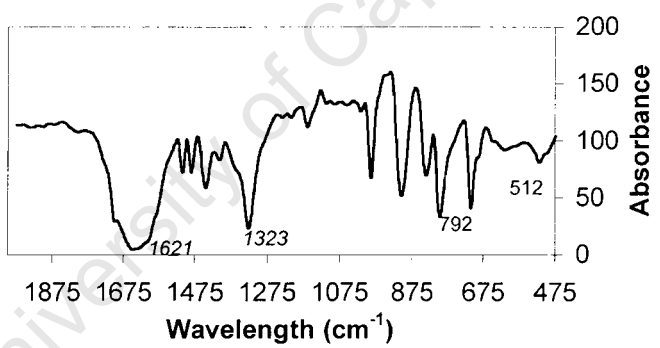

Figure 27. FTIR spectrum of unwashed COD imprinted polymer

The SEM micrograph of the unwashed COD imprinted polymer (figure 28) shows the presence of numerous particles. However, their morphological features are not obvious.

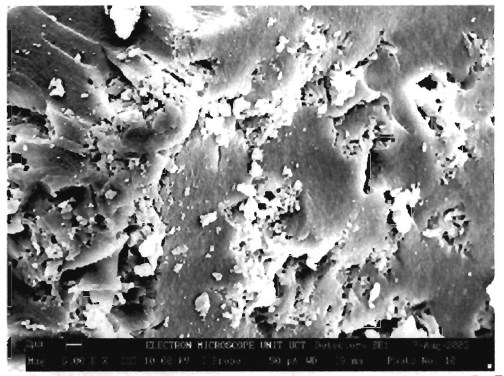

Figure 28. SEM micrograph of unwashed COD imprinted polymer

Thus, the XRD and FTIR analyses confirm that the COD template crystals have not been changed by the conditions of the polymerization process.

5.2.3. Unimprinted polymer

Since the polymer is an amorphous material, the XRD pattern of the unimprinted polymer has no peaks (figure 29). The unimprinted polymer is better characterized by infrared spectroscopy (figure 30). The FTIR spectrum shows distinct and sharp absorption at 1598, 1441, 986, 900, 831, 792 and 707 cm^{-1}. The SEM micrograph of this material is shown in figure 31. Unlike the imprinted surfaces, the unimprinted polymer has a relatively smooth surface and has no crystal deposits.

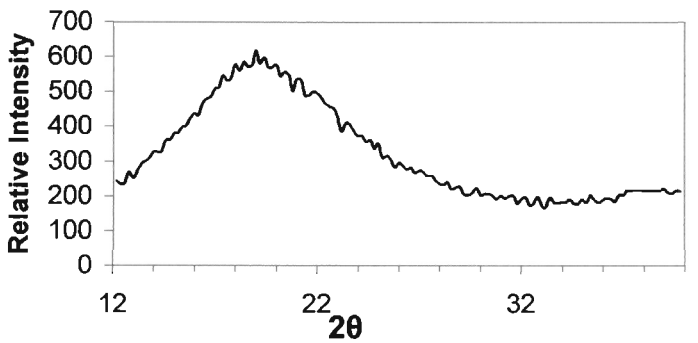

Figure 29. XRD pattern of unimprinted polymer

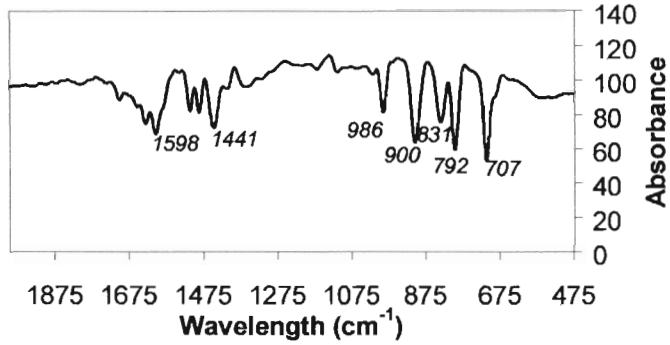

Figure 30. FTIR spectrum of unimprinted polymer

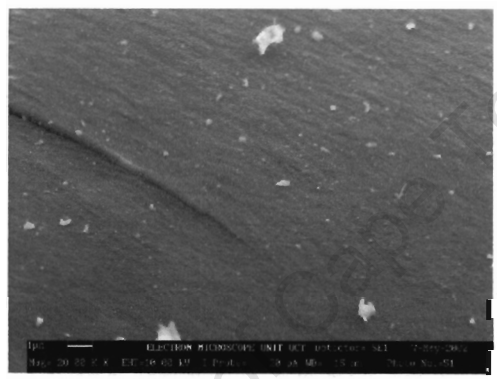

Figure 31. SEM micrograph of unimprinted polymer

5.3. Removal of template crystals from imprinted polymers

5.3.1. Washed COM imprinted polymer

The XRD pattern of the COM imprinted polymer after the acidified methanol wash shows no peaks, confirming that the imprinted template crystals have been completely removed (figure 32). The infrared spectrum (figure 33) also shows only the bands characteristic of the polymer, confirming complete removal of template COM crystals. The SEM micrographs of this material at low magnification (figure 34a) and higher magnification

(figure 34b) show that the washed polymer contains numerous vacant cavities that are casts of the original COM crystals.

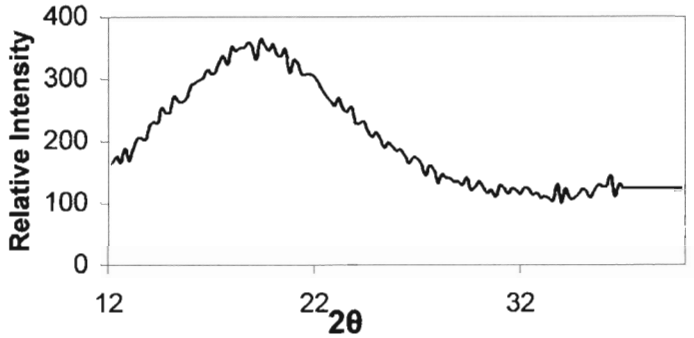

Figure 32. XRD pattern of washed COM imprinted polymer

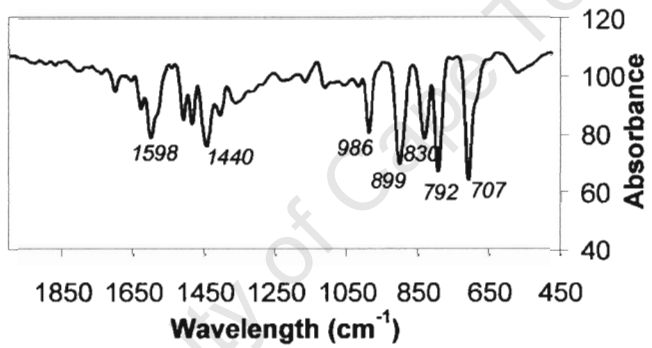

Figure 33. FTIR spectrum of washed COM imprinted polymer

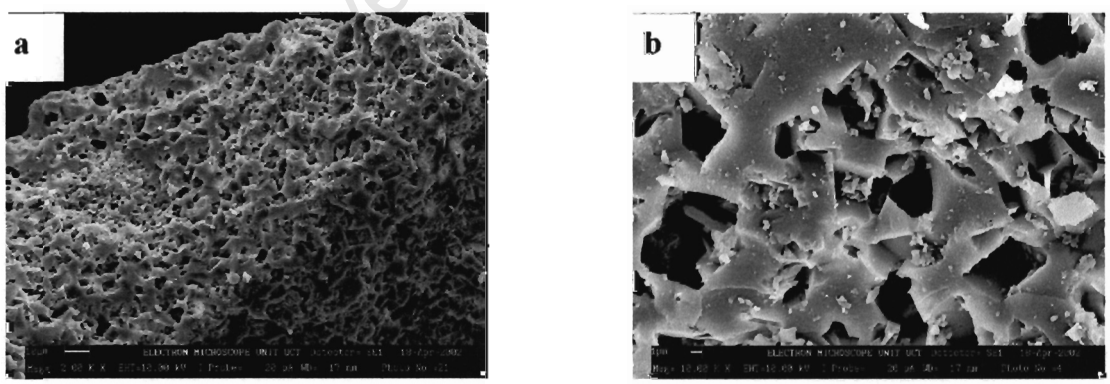

Figure 34. SEM micrograph of washed COM imprinted polymer at low magnification (× 500, a) and higher magnification (× 2500, b). Vacant cavities (casts of COM crystals) are clearly evident.

Atomic absorption (AA) analysis was conducted on the COM imprinted and washed polymers using a Technics AA5 Spectrophotometer to detect whether any COM crystals remained after washing i.e., to measure the extent of removal of the template COM crystals from the polymer. From these analyses, it was demonstrated that at least 99.8% of the imprinted COM crystals had been removed from the polymer (table 5.3).

Table 5.3 Calcium content of 0.200 g samples of unwashed and washed COM imprinted polymer

Ca in unwashed polymer (mg)	Ca in washed polymer (mg)	% Ca remaining after washing
46.48 ± 0.02	0.074 ± 0.004	0.16 ± 0.01

5.3.2. Washed COD imprinted polymer

Figure 35 shows the XRD pattern of the acid-washed COD imprinted polymer. No peaks were observed in this XRD pattern showing complete removal of the imprinted COD template crystals from the polymer. None but the polymer bands were observed in the FTIR spectrum of the washed COD imprinted polymer (figure 36). The SEM micrograph of the washed COD imprinted polymer is shown at low magnification in figure 37a and at greater magnification in figure 37b. Cavities (corresponding to COD crystals) are evident.

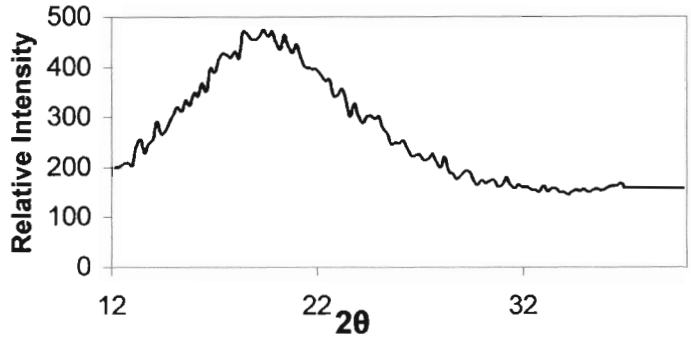

Figure 35. XRD pattern of washed COD imprinted polymer

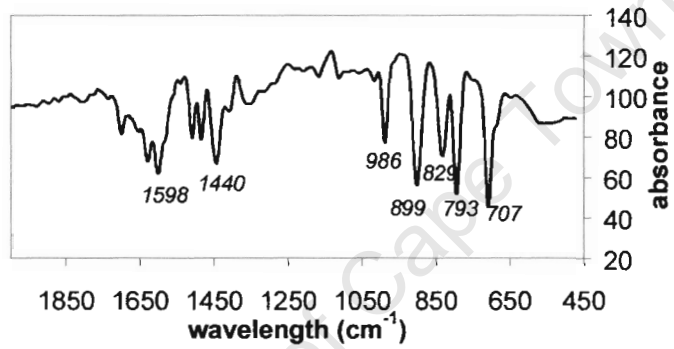

Figure 36. FTIR spectrum of washed COD imprinted polymer

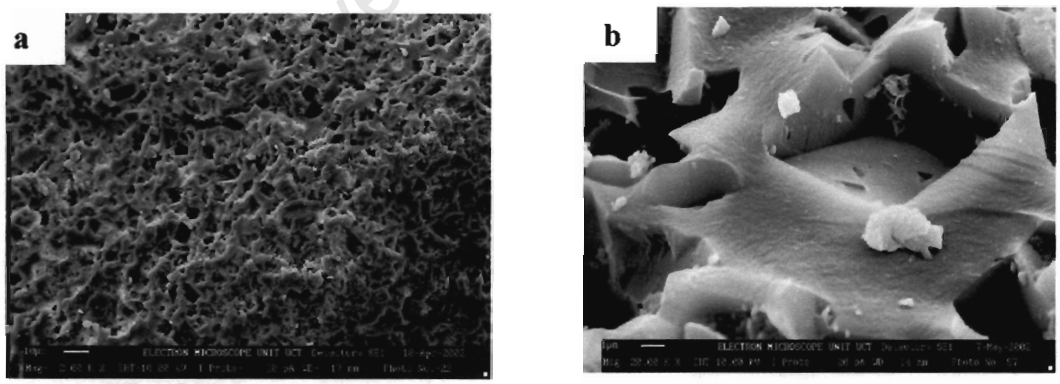

Figure 37. SEM micropgraphs of washed COD imprinted polymer at low magnification (×500, a) and higher magnification (× 5000, b)

The results of AA analysis, like those of the washed COM imprinted polymer, showed the removal of at least 99.8% of the CaOx present in the unwashed COD imprinted polymer (table 5.4).

Table 5.4. Calcium content of 0.200 g samples of unwashed and washed COD imprinted polymer

Ca in unwashed polymer (mg)	Ca in washed polymer (mg)	% Ca remaining after washing
41.49 ± 0.02	0.055 ± 0.004	0.13 ± 0.01

Thus, the XRD, FTIR and SEM experiments together with the AA analyses confirmed that the washed COD imprinted polymer was free of the template crystals.

5.4. Effect of imprinted polymers on CaOx precipitation

The effect of COM and COD imprinted polymers on CaOx precipitation will be discussed in this section. Unimprinted polymer is used as a control to compare the effect of the imprinted polymers. Control solutions are also used in the absence of any polymer for the same reason. Table 5.5 provides a summary of the results obtained from all of the experiments.

Table 5.5. Summary of the XRD patterns of crystallization experiments.

	Metastable CaOx Solutions			Solutions of Artificial urine				Real Urine
	I	II	III	IV	V	VI	VII	VIII
Control Solution	No detectable crystallization			**Fig. 48** BRU	**Fig. 49** HAP and traces of COD	**Fig. 50** BRU and traces of COM & COD	**Fig. 51** BRU and traces of COD	**Fig. 61** BRU
Unimprinted Polymer	**Fig. 38** No evident crystallization	**Fig. 39**	**Fig. 40**	**Fig. 52** BRU	**Fig. 53** HAP and COD (trace)	**Fig. 54** BRU and traces of COM and COD	**Fig. 55** BRU and COD (trace)	**Fig. 62** BRU
COM-Imprinted Polymer	**Fig. 41** COM	**Fig. 42** COM	**Fig. 43** COM	**Fig. 56** COM	**Fig. 57** COM	**Fig. 58** COM	**Fig. 59** COM	**Fig. 63** COM
				Fig. 60 COM and BRU				**Fig. 64** COM and BRU
COD-Imprinted Polymer	**Fig. 67** No crystals	**Fig. 68** COM and COD	**Fig. 69** COD	**Fig. 70** HAP and traces of COM, COD & COT	**Fig. 71** HAP and traces of COD and ARAG	**Fig. 72** BRU and traces of COM, COD and COT	**Fig. 73** BRU and COD	**Fig. 74** BRU

Solutions I to VII are discussed in tables 4.1 and 4.2 (*p* 50) and solution VIII is urine from healthy white South African volunteers.

5.4.1. Precipitation from CaOx solution on COM imprinted polymer surface

Table 5.5 shows that there was no spontaneous precipitation of any crystals in solutions I to III. There also occurred no evident crystallization when the unimprinted polymer was soaked in these three solutions (XRD pattern; figures 38 to 40). Figures 41 to 43 show XRD pattern of crystals which precipitated on COM imprinted polymer from solutions I to III respectively. Diffraction peaks due to COM are evident in all of them, including solution III in which the calcium-to-oxalate ration favours COD formation. The presence of precipitated COM on the washed imprinted polymer and its absence on the unimprinted polymer was also evident from FTIR (figures 44 and 45). In addition, SEM showed that the cavities on the surface of the washed imprinted polymer were reoccupied by a mass of small crystals (figure 46), but almost no deposition was observed on the surface of the unimprinted polymer (figure 47). Finally AAS (Table 5.6) data show that more than 50% of the calcium present in the solution precipitated on the surface of imprinted and washed polymer while negligible quantities were detected on the surface of the unimprinted polymer. Moreover, there was no precipitation in the absence of any polymer. It is therefore concluded that the imprinted polymer directs nucleation of calcium oxalate crystals from a metastable solution, a solution in which no spontaneous precipitation occurs.

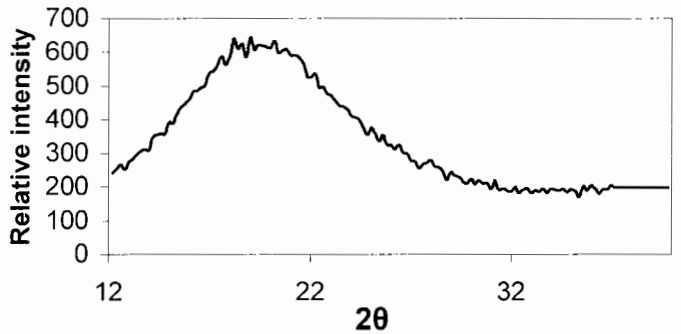

Figure 38. XRD pattern of unimprinted polymer soaked in 0.003 M CaOx solution

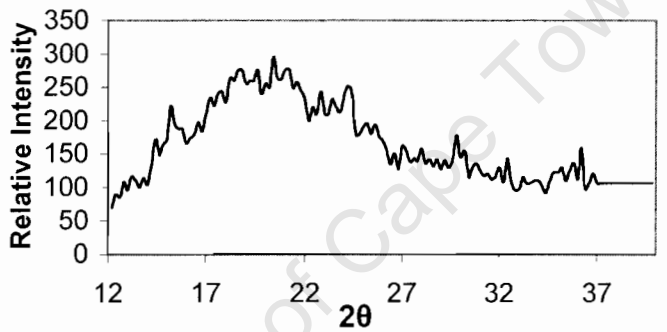

Figure 39. XRD pattern of unimprinted polymer soaked in 0.005 M CaOx solution

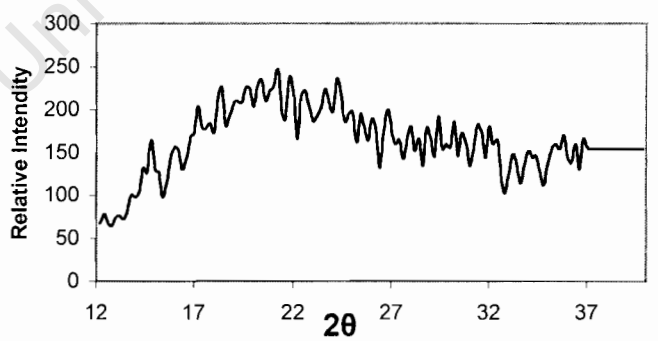

Figure 40. XRD pattern of unimprinted polymer soaked in CaOx solution with 4:1 calcium to oxalate ratio

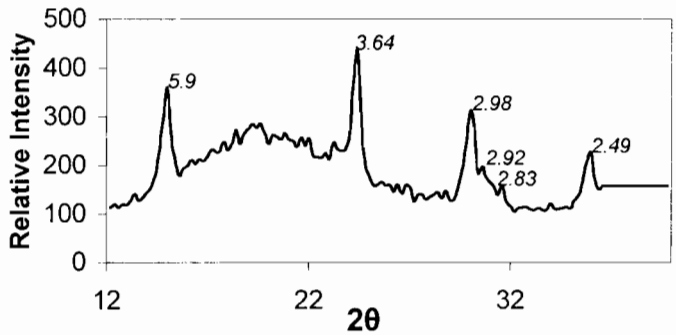

Figure 41. XRD pattern of COM precipitated on washed COM imprinted polymer after soaking in 0.003 M CaOx solution (i.e., Solution I)

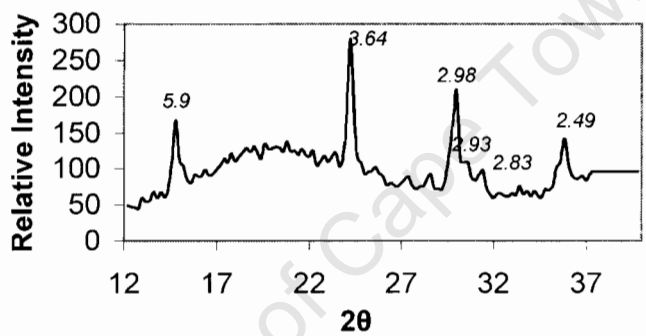

Figure 42. XRD pattern of COM precipitated on washed COM imprinted polymer after soaking in 0.005 M CaOx solution (i.e., Solution II)

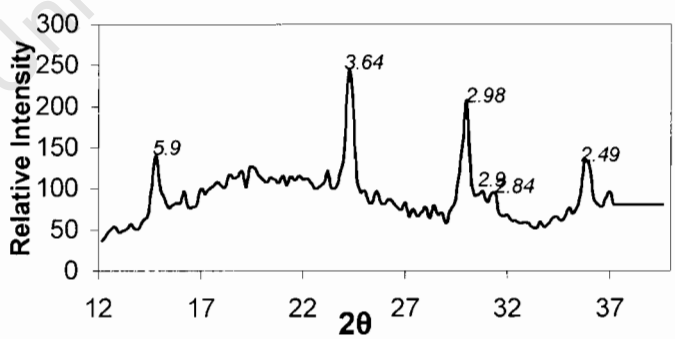

Figure 43. XRD pattern of COM precipitated on washed COM imprinted polymer after soaking in a solution with 4:1 calcium-to-oxalate ratio (i.e., Solution III)

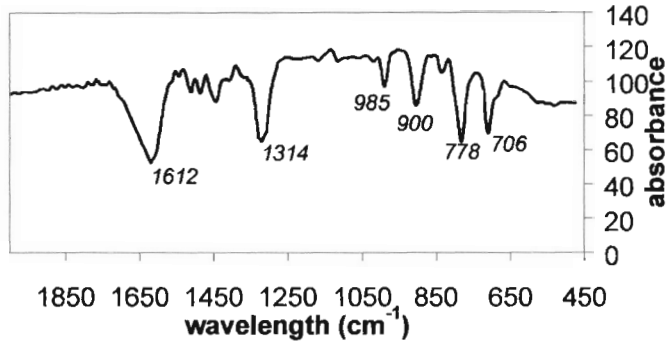

Figure 44. FTIR spectrum of washed COM imprinted polymer after soaking in 0.003 M CaOx solution (i.e., solution I) (Peak enlargement at 1314 and 1612 is due to COM)

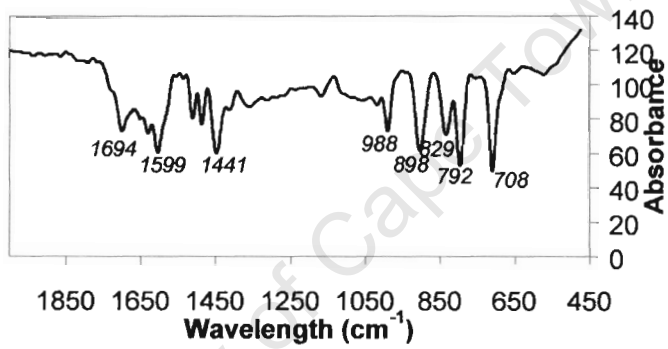

Figure 45. FTIR spectrum of unimprinted polymer soaked in 0.003 M CaOx solution (i.e., solution I) (The absence of peaks at 1314 and 1612 cm^{-1} indicates the absence of COM).

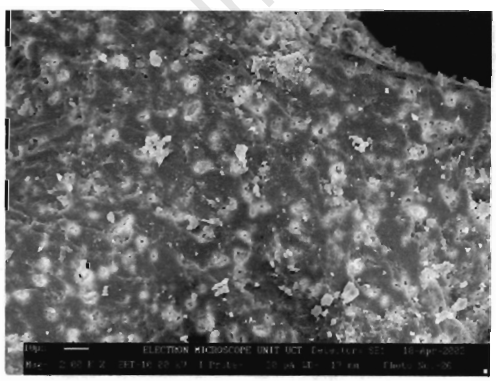

Figure 46. Washed COM imprinted polymer soaked in solution I. Heavy crystal deposits in the cavities are evident.

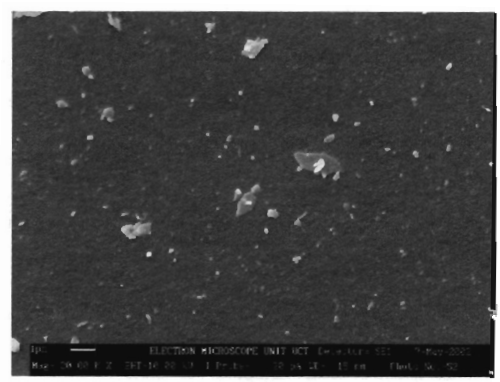

Figure 47. Unimprinted polymer soaked in solution I. Very little crystal deposition has occurred.

Table 5.6. Percentage of calcium precipitated from 0.020 l of 0.003 M CaOx solution on unimprinted and washed COM imprinted polymers.

% Ca precipitated on COM imprinted polymer	% Ca precipitated unimprinted polymer
55.8 ± 0.4	0.44 ± 0.05

5.4.2. Precipitation from artificial urine on COM imprinted polymer surface

When artificial urine (i.e., solution IV) was agitated at 25 °C for 36 hours in the absence of all polymers and in the presence of unimprinted polymer, brushite ($CaHPO_4.2H_2O$) precipitated spontaneously. This is shown by the XRD spectra, in figures 48 and 52 respectively. The characteristic peaks of brushite (BRU) were obtained from Sutor (1968). However, in the presence of the washed COM imprinted polymer, pure COM crystals were nucleated as demonstrated in the XRD spectrum shown in figures 56 to 59, but in some instances brushite precipitated simultaneously (XRD spectrum, figure 60). Neither COM alone nor the mixture of COM and brushite precipitated spontaneously.

When magnesium was omitted from the artificial urine (i.e., solution V) pure COM crystals precipitated on the surface of washed COM imprinted polymer, but there were cases in which hydroxyapatite (HAP), $Ca_{10}(PO_4)_6(OH)_2$, precipitated simultaneously. COD and hydroxyapatite (HAP) precipitated from this solution in the absence of any polymer and when unimprinted polymer was soaked in it. COM precipitated on the surface of washed COM imprinted polymer soaked in artificial urine prepared without citrate (i.e., solution VI). Under conditions where the concentrations of both magnesium and

citrate were reduced to 25% of those in solution IV, traces of COD and brushite precipitated in the absence of all polymers and when there is unimprinted polymer.

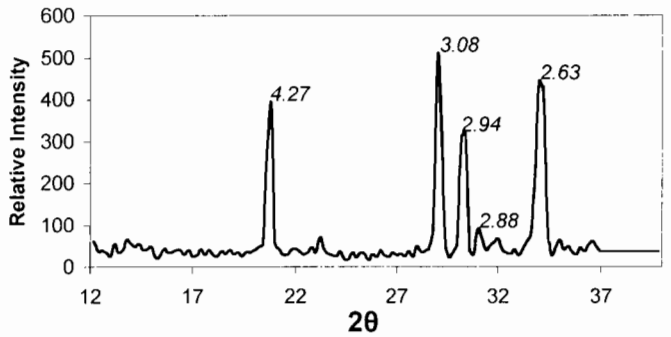

Figure 48. XRD pattern of brushite spontaneously precipitated from synthetic urine (i.e., solution IV)

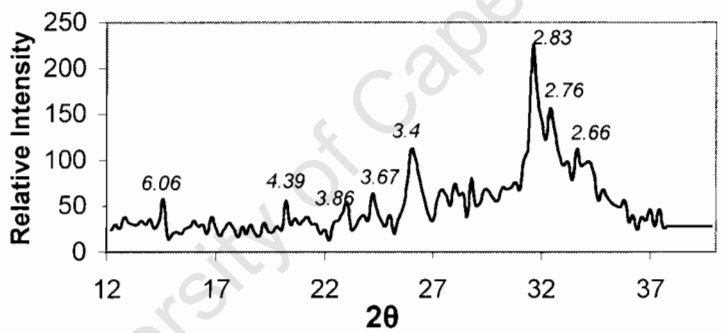

Figure 49. XRD pattern of HAP precipitated from artificial urine from which magnesium is omitted (i.e., solution V) (also contains traces of COD)

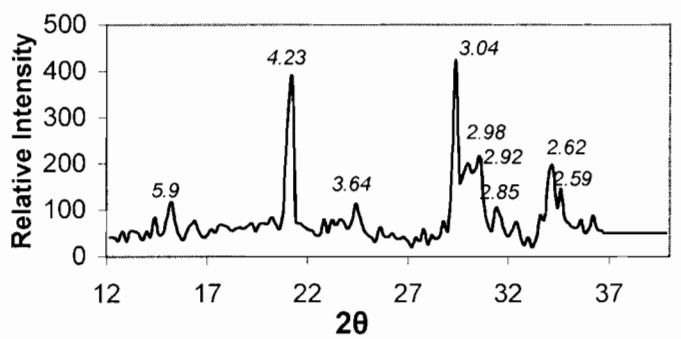

Figure 50. XRD pattern of BRU precipitated from artificial urine prepared without citrate (i.e., solution VI) (contains traces of COM and COD)

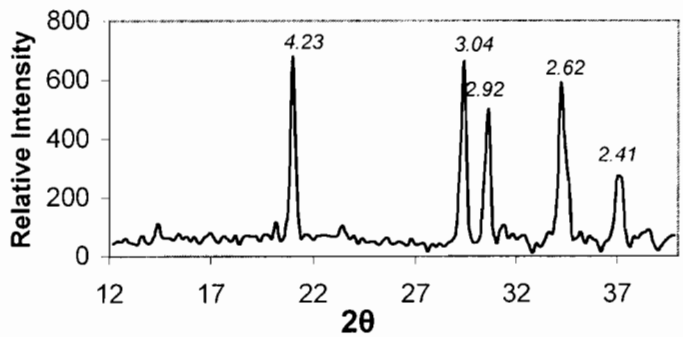

Figure 51. XRD pattern of BRU precipitated from artificial urine in which concentrations of magnesium and citrate were reduced to 25% of those in solution IV (i.e., solution VII)

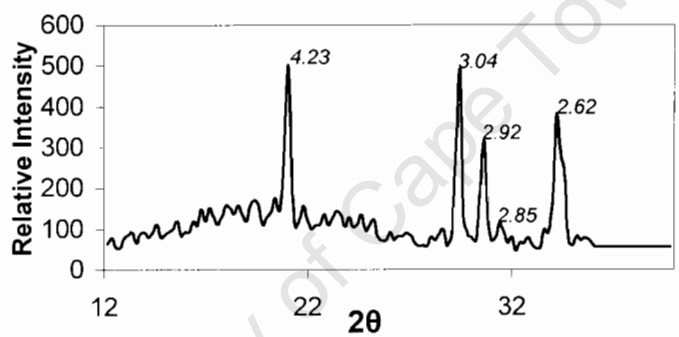

Figure 52. XRD pattern of brushite precipitated on unimprinted polymer after soaking in artificial urine (i.e., solution IV)

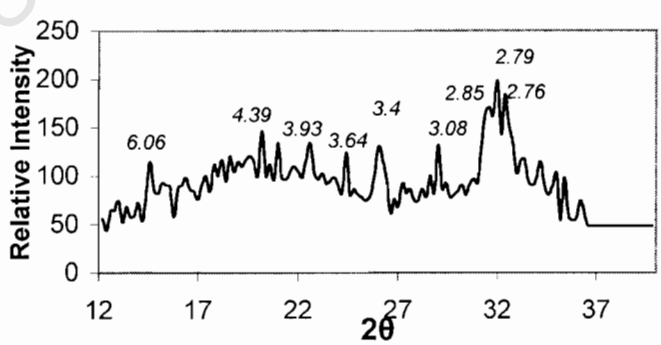

Figure 53. XRD pattern of HAP precipitated on unimprinted polymer after soaking in artificial urine without magnesium (i.e., solution V) (contains COD)

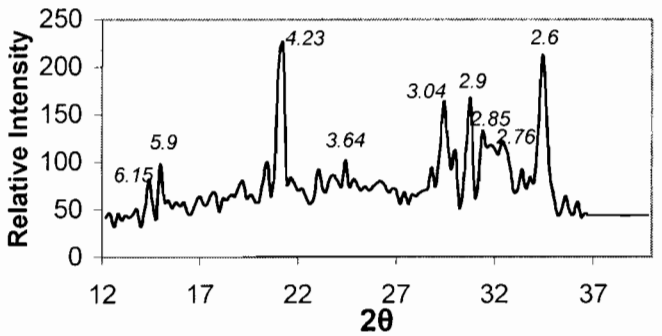

Figure 54. XRD pattern of BRU precipitated on unimprinted polymer after soaking in artificial urine without citrate (i.e., solution VI) (contains traces of COM and COD)

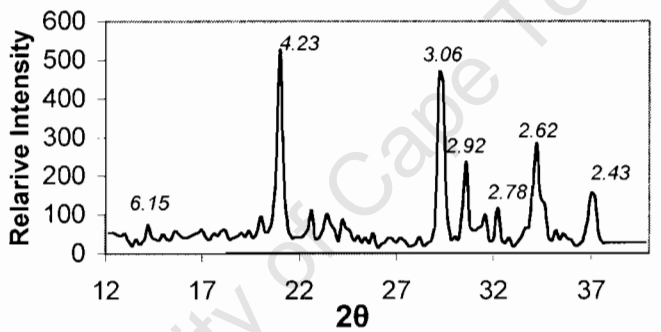

Figure 55. BRU precipitated on unimprinted polymer after soaking in artificial urine in which the concentrations of magnesium and citrate are quartered (i.e., solution VII) (contains traces of COD)

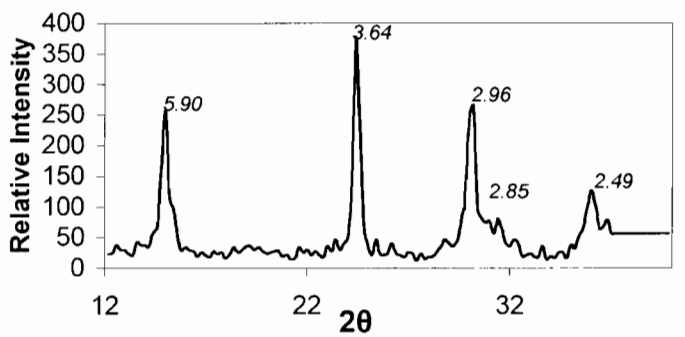

Figure 56. XRD pattern of COM precipitated on washed COM imprinted polymer after soaking in synthetic urine (i.e., solution IV)

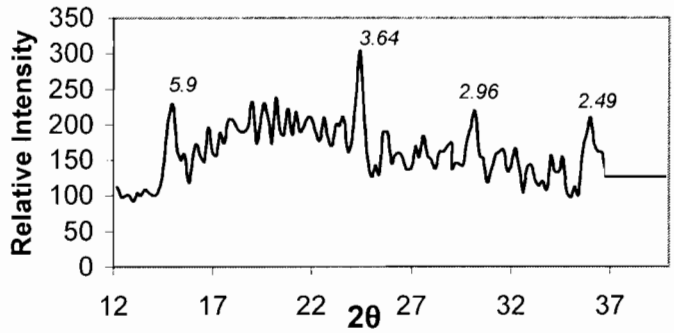

Figure 57. XRD pattern of COM precipitated on washed COM imprinted polymer after soaking in artificial urine in the absence of magnesium (i.e., solution V).

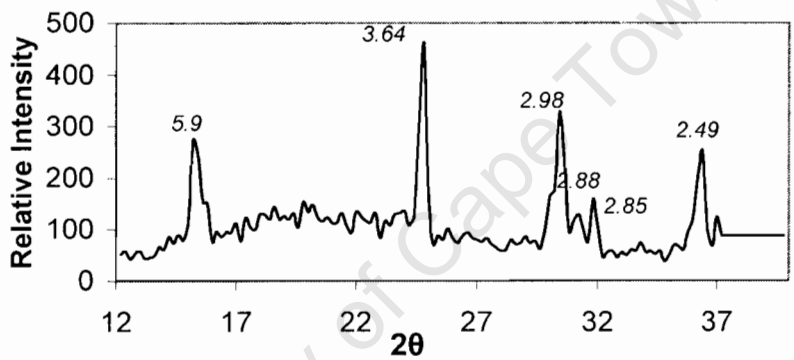

Figure 58. XRD pattern of COM precipitated on washed COM imprinted polymer after soaking in artificial urine without citrate (i.e., solution VI).

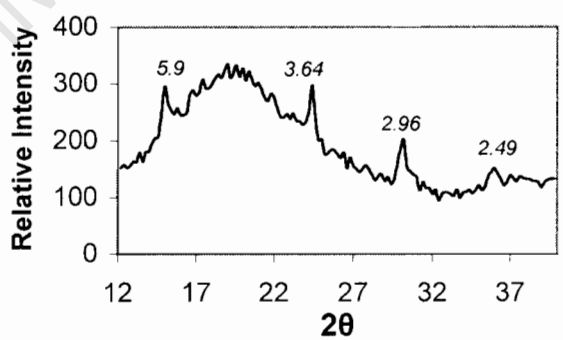

Figure 59. XRD pattern of COM precipitated on washed COM imprinted polymer after soaking in artificial urine in which the concentrations of magnesium and citrate were reduced to 25% of those in solution IV (i.e., solution VII).

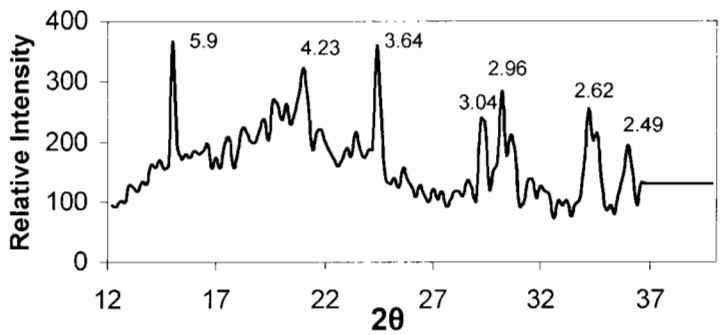

Figure 60. XRD pattern of a mixture of COM and brushite precipitated on washed COM imprinted polymer after soaking in synthetic urine (i.e., solution IV).

5.4.3. Precipitation from real urine on COM imprinted polymer surface

As with artificial urine, brushite usually precipitated spontaneously when real urine was agitated at 25 °C for 36 hours in the absence of all polymers (XRD spectrum: figure 61) and in the presence of unimprinted unimprinted polymer (XRD spectrum: figure 62). In most cases where the washed COM imprinted polymer was soaked in urine, both COM and brushite precipitated simultaneously (XRD spectrum: figure 64). In one case, COM precipitated exclusively from the urine with no brushite being formed (XRD spectrum: figure 63). Neither COM alone nor simultaneously precipitated spontaneously from urine unless the washed COM imprinted polymers is soaked in it.

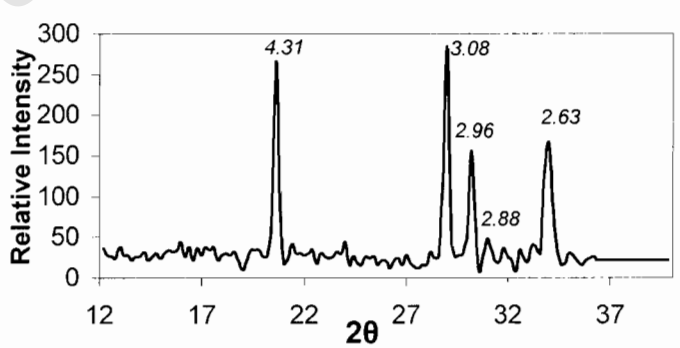

Figure 61. XRD pattern of brushite spontaneously precipitated from urine (i.e., solution VIII)

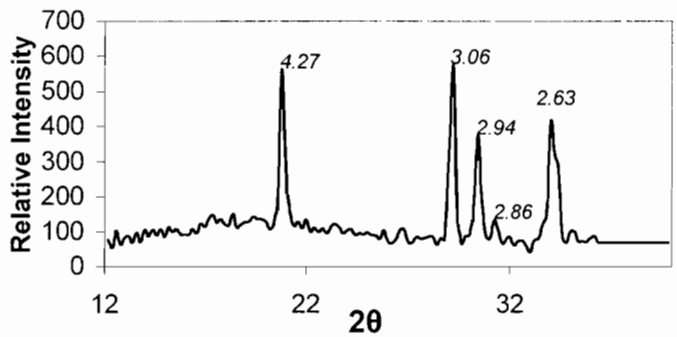

Figure 62. XRD pattern of brushite precipitated on unimprinted polymer after soaking in real urine (i.e., solution VIII)

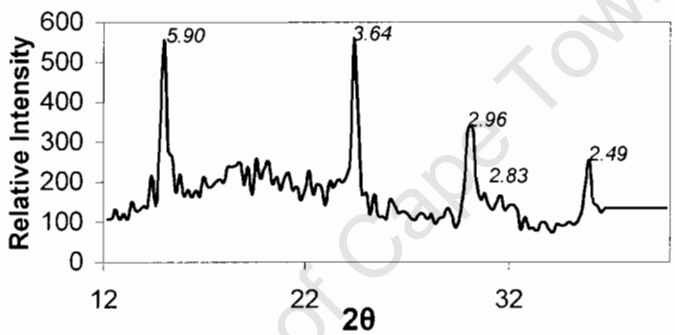

Figure 63. XRD pattern of COM precipitated on washed COM imprinted polymer after soaking in real urine (i.e., solution VIII)

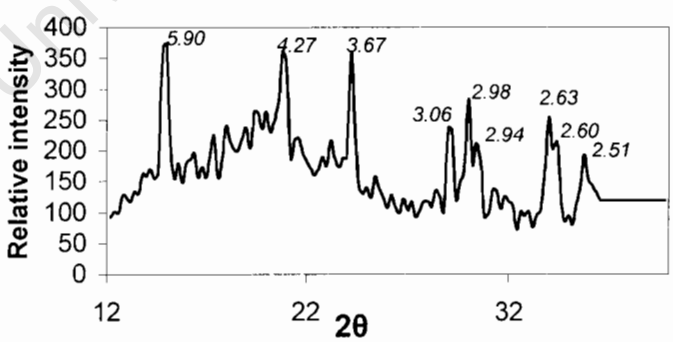

Figure 64. XRD pattern of a mixture of COM and brushite precipitated on washed COM imprinted polymer after soaking in real urine (i.e., solution VIII)

5.4.4. Effect of COM imprinted polymer on the CaOx metastable limit of urine

The MSLs of five urine samples from white healthy South African volunteers were measured by the method of Ryall *et al.* (1985) using the Coulter Counter. Four of these were found to be 0.045 M (figure 65).

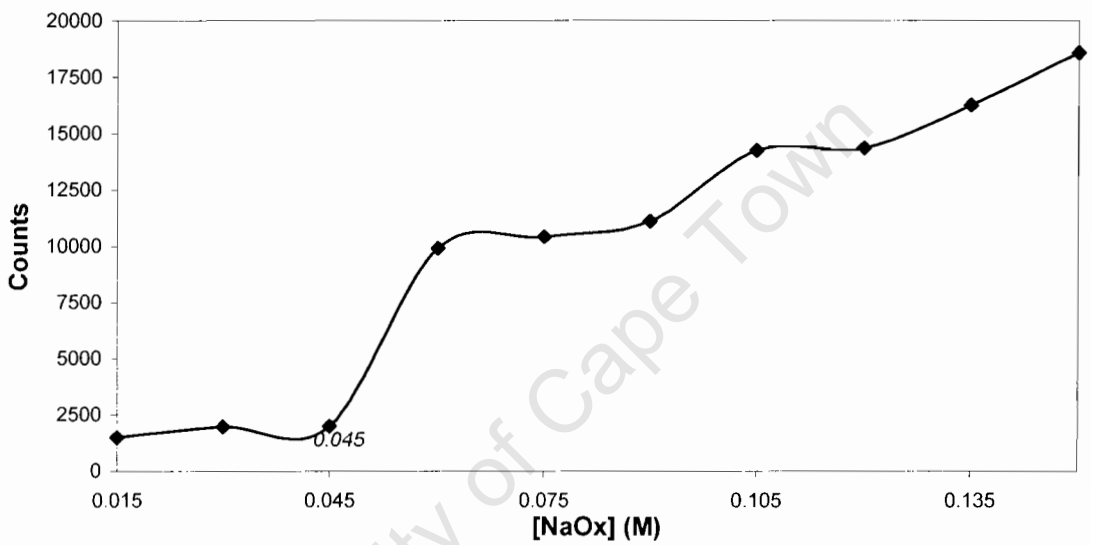

Figure 65. Determination of MSL of urine using Coulter Counter

MSL of five samples of urine were determined in the presence of imprinted and unimprinted polymers. The COM imprinted polymer brought about a decrease in the MSL of four of these, while the unimprinted polymer had no effect. An example is shown in figure 66. A Turbidimeter was used for this determination because the polymer particles are large enough to block the aperture of the Coulter Counter. The turbidimeter was calibrated against the Coulter Counter and counts were multiplied by the calibration factor.

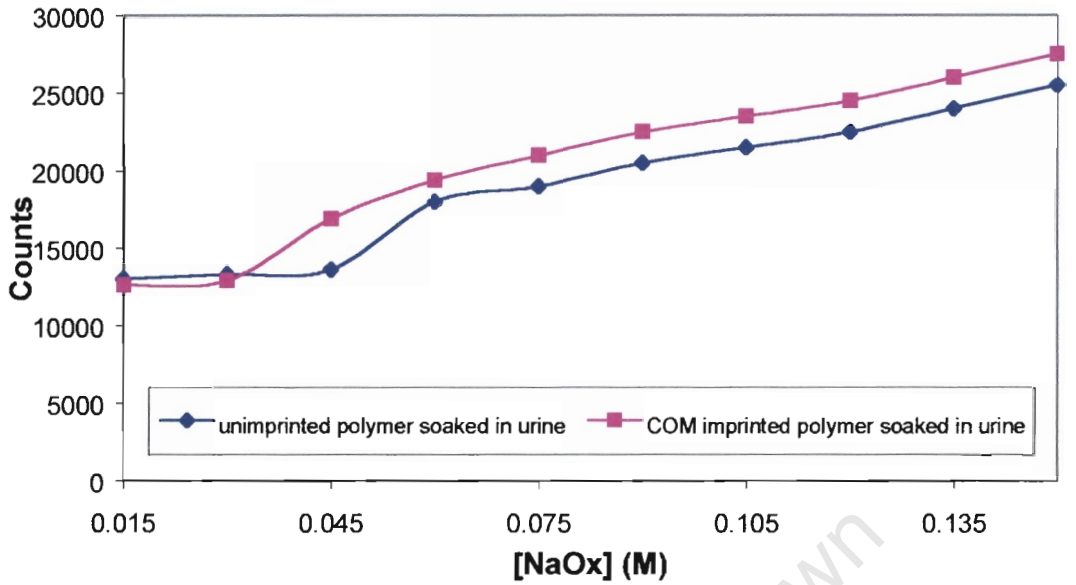

Figure 66. Effect of COM imprinted polymer on MSL

5.4.5. Precipitation from CaOx solution on COD imprinted polymer surface

In contrast to the COM imprinted polymer, the COD imprinted polymer did not direct nucleation of pure COD crystals. Crystallization did not occur when the washed COD imprinted polymer was soaked in 0.003 M CaOx solution (XRD spectrum: figure 67). However, COM with small amounts of COD precipitated from 0.005 M CaOx solution (XRD spectrum: figure 68). Pure COD crystals with traces of COT precipitated only when a solution with a 4:1 calcium-to-oxalate ratio was used (XRD spectrum: figure 69). The AA analysis in table 5.7 shows that the COD imprinted polymer, like the COM imprinted one facilitated the precipitation of CaOx crystals but it did not specifically direct nucleation of pure COD crystals.

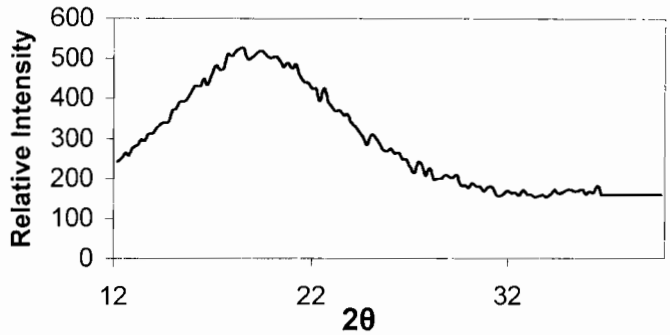

Figure 67. XRD pattern of washed COD imprinted polymer soaked in 0.003 M CaOx solution (i.e., solution I)

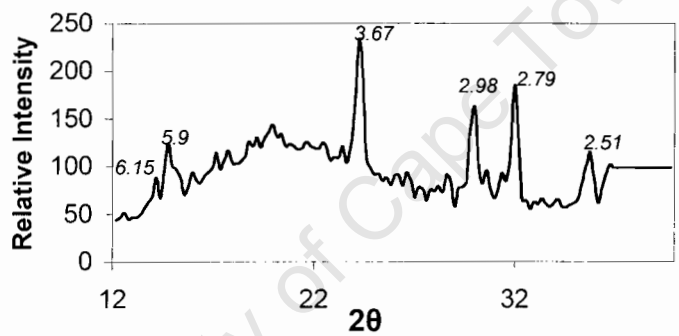

Figure 68. XRD pattern of a mixture of COM and COD precipitated on washed COD imprinted polymer after soaking in 0.005 M CaOx solution (i.e., solution II)

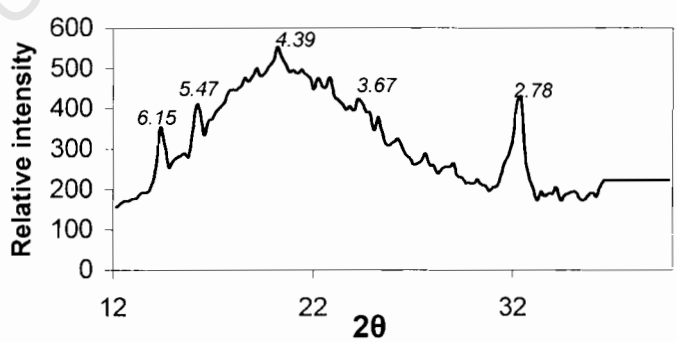

Figure 69. XRD pattern of COD and traces of COT precipitated on washed COD imprinted polymer after soaking in a solution with 4:1 calcium-to-oxalate ratio (i.e., solution III).

Table 5.7. Percentage of calcium precipitatedfrom 0.020 l of 0.003 M CaOx solution on unimprinted and washed COD imprinted polymers.

% Ca precipitated on COM imprinted polymer	% Ca precipitated on unimprinted polymer
52.3± 0.4	0.44 ± 0.05

5.4.6. Precipitation from artificial and real urines on COD imprinted polymer surface

In most of the cases where the washed COD imprinted polymer was soaked in artificial urine, brushite precipitated with traces of COD. There were many cases where all the three hydrates of calcium oxalate precipitated out (XRD spectrum: figure 70). When magnesium was made absent from the artificial urine (solution V), COD with traces of HAP and aragonite, $CaCO_3$, (ARAG) precipitated on the surface of washed COD imprinted polymer (XRD spectrum: figure 71). HAP and traces of all the three hydrates of CaOx precipitated from artificial urine prepared without citrate (solution VI) (XRD spectrum: figure 72). And when the concentrations of magnesium and citrate were reduced to quarter of those in solution IV (i.e., solution VII), brushite precipitated with traces of COD (XRD spectrum: figure 73). Brushite was precipitated almost exclusively when washed COD imprinted polymer was soaked in real urine (XRD spectrum: figure 74).

Unlike the COM imprinted polymer, the COD imprinted polymer did not direct specific nucleation of COD crystals from both artificial and real urines.

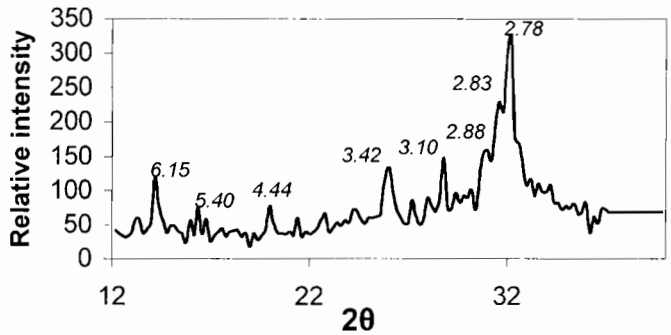

Figure 70. XRD pattern of solid precipitated on washed COD imprinted polymer after soaking in synthetic urine (i.e., solution IV)

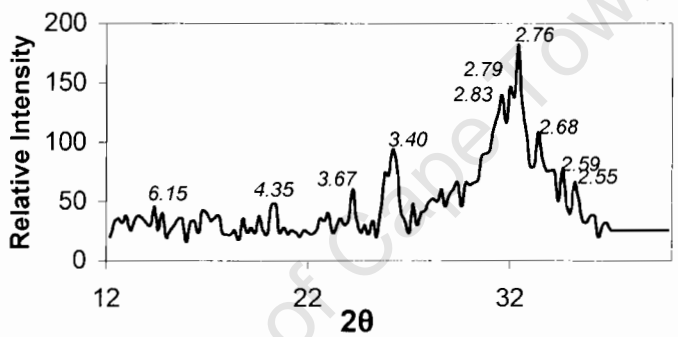

Figure 71. XRD pattern of solid precipitated on washed COD imprinted polymer after soaking in artificial urine without magnesium (i.e., solution V).

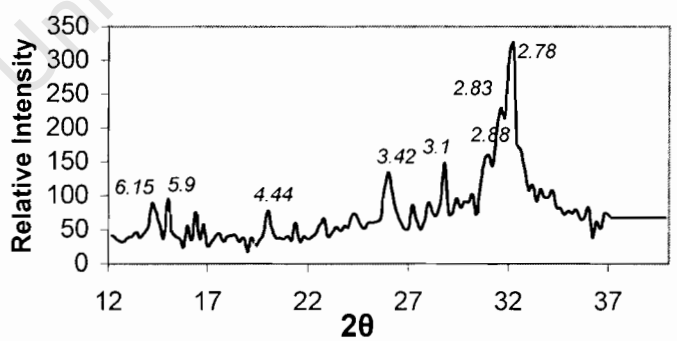

Figure 72. XRD patter of solid precipitated on COD imprinted polymer after soaking in artificial urine without citrate (i.e., solution VI).

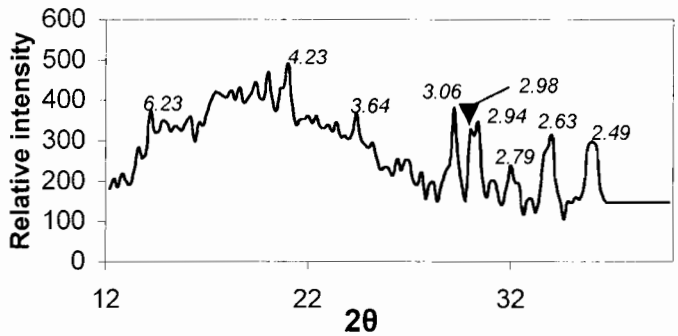

Figure 73. XRD pattern of solid precipitated on washed COD imprinted polymer after soaking in synthetic urine with magnesium and citrate concentrations reduced to 25% of those in solution IV (i.e., solution VII).

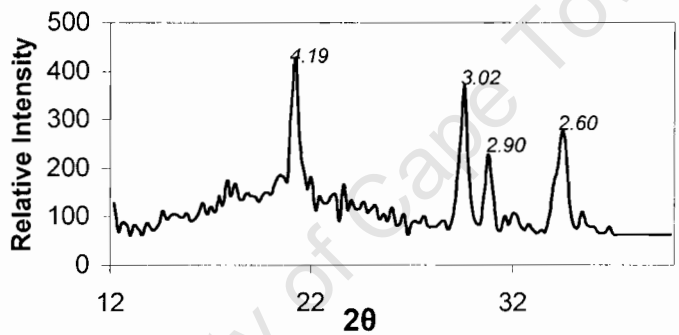

Figure 74. XRD pattern of brushite precipitated on washed COD imprinted polymer after soaking in real urine (i.e., solution VIII).

CHAPTER SIX- DISCUSSION

Molecular recognition by molecularly imprinted polymers usually involves a careful balance between rigidity and flexibility of the polymer. If it is too flexible, the recognition site does not survive removal of the template molecule, while if it is too rigid the entropy cost of binding a guest molecule at the recognition site is too high (Wulff, 1995). For this reason, relatively small quantities of cross-linking agents are normally used (Wulff, 1995). The discovery by D'Souza *et al.* (1999) that the highly rigid maaha/dvb co-polymer can specifically nucleate calcite crystal formation has opened a way to study biomineralization processes using such rigid molecularly imprinted polymers. The present study has shown that the same polymer is also capable of nucleating both COM and COD crystallization from aqueous, supersaturated solution of CaOx. This suggests that the co-polymer may also be useful for nucleating the crystallization of other calcium salts, and rigid polymers may thus be of quite general utility in the formation of solids.

It is essential that studies of molecularly imprinted polymers demonstrate adequately that the activity of the polymer is a result of the imprinting process. Thus multiple analytical techniques (XRD, FTIR, SEM and AAS) were employed in the present study and several control experiments were included to demonstrate that nucleation of CaOx crystallization is specific to the imprinted polymer.

Firstly, XRD and FTIR clearly showed that neither COM nor COD precipitation occurs spontaneously in any of the solutions investigated under the experimental conditions used.

Secondly, neither COM nor COD crystallization was induced from supersaturated CaOx solutions, artificial urine or real urine in the presence of the unimprinted polymer. Formation of COM and COD on the imprinted polymer is thus certainly not spontaneously brought about by the polymer itself. It could be argued that COM or COD crystals trapped in the polymer are responsible for nucleating the formation of these solids. However, this seems unlikely since no crystalline material was detected in the washed polymers using XRD and no CaOx was discernible in the washed polymer by FTIR. Moreover, AAS indicated that more than 99.8% of the calcium originally present in the unwashed, imprinted polymer had been removed in the washing process.

The conclusion that the molecular imprints on the surface of the cavities in the polymer produced in the imprinting process are responsible for nucleating COM crystallization is supported by SEM, which indicates that these cavities become filled with COM crystals. Similar to calcium carbonate, the present method was more effective for one crystal form than for another. In the case of calcium carbonate, D'Souza *et al.* (1999) showed that calcite, but not aragonite crystallization can be nucleated on the suitably imprinted polymer surface. In the present case of CaOx, both COM and COD crystallization can be induced on the appropriately imprinted surface, but only the COM imprinted surface nucleates formation of pure material. These results show that the COD imprinted surface appears to have induced both COD and COM crystallization, with the former being present in only trace amounts. It is possible that COD crystals were initially nucleated but then involved in a rapid transformation to the thermodynamically more stable COM. This hypothesis agrees with the findings of Gardner (1976) who suggested that COT undergoes a solid-

state transformation to COD and COM. Indeed, the presence of COT was detected in one of the SEM micrographs (figure 21) and FTIR (figure 20). The COT disappeared after the polymerization reaction (figure 26). Conversely, Brecevic *et al.* (1986) suggested that the transformation is a solution-mediated process. The appearance of COT when a washed COD imprinted polymer was soaked in a solution mixture of 0.012 M $CaCl_2$ and 0.003 M NaOx is in agreement with the latter proposal.

The pH dependent precipitation of brushite is well known and the critical range is reported to be above 5.5 (Ackerman, 1987). In the present study, the pH of the artificial urine was 6.5 while the pH of the real urines varied from 4.83 to 6.71. Thus, the formation of brushite can be attributed to the relatively high pH of the solutions, rather than to the imprinted polymer. However, it is noteworthy that despite the strong influence of pH in directing brushite formation, COM was nevertheless nucleated on the COM-imprinted polymer.

As mentioned in chapter one of this thesis, heterogeneous nucleation is the most likely mechanism by which crystals form in the urinary tract (Finlayson, 1978). In this process nucleation is induced on a foreign surface present in the crystallization medium. Human urine contains several such surfaces, cellular debris and sloughed-off epithelial membranes (Hess and Kok, 1996), while the walls of the urinary tract itself might provide a site (generally the papillae) for crystal formation (Grases *et al.*, 1994). The present study raises the interesting possibility that CaOx crystals may leave a lesion on the surface of the kidney as the cells around the retained crystals grow or as some of the protective lining

cells are damaged due to infection. After the retained crystal is removed by either excretion (before it grows to form a stone) or medical treatment, the remaining cavity may act as a catalytically active center and may reduce the activation energy for the precipitation of further crystals. But this is less likely to happen because of the continuous turning over of the epithelial cells. Several workers have recognized the importance of studying the early stages of CaOx crystallization using models that try to reproduce *in vivo* conditions. Substrates include renal epithelial cells (Lieske and Toback, 1993), rat renal papillary tip collecting duct cells (Mandel and Riese, 1991) and renal tubular brush border membrane rat vesicles (Khan *et al.*, 1993). In addition, some investigators have used a foreign surface immersed in urine-like systems to characterize CaOx crystallization processes. Amongst these surfaces have been self-assembled monolayers containing derivatized organic functional groups (Campbell, 1993), molten wax (Grases *et al.*, 1994) and the urothelium of pig urinary bladder (Grases *et al.*,1996). Thus, the use of an imprinted polymer in the present study provides yet another model for such investigations.

It is of some interest that a study by Geider *et al.* (1996) demonstrated that calcium carbonate (calcite) nucleated the epitaxial crystallization of CaOx. As such, it is perhaps not surprising that the co-polymer used in the present study was able to successfully nucleate CaOx, as it had previously been used for the nucleation of calcium carbonate (D'Souza *et al.*, 1999).

The present study has demonstrated that the mere presence of a suitable surface can induce crystallization of COM and COD, even from highly complex solutions such as urine.

Indeed, COM crystallization occurred from the urine of a healthy subject without modification of the urine itself having been made. While one cannot draw any definite conclusions about the physiological precipitation of CaOx from this observation, it does demonstrate that it is feasible for a substrate surface to crystallize CaOx from normal urine. This seems to lend some support to the hypothesis that CaOx stone formation is brought about by abnormalities in the epithelium or by the presence of suitable nucleating proteins. This appears possible even in the absence of any changes in urine composition.

The metastable limit of the urine samples from healthy white South African male subjects was observed to be 0.45 mM. Introducing COM and COD imprinted polymers reduced this value to 0.30 mM, whereas the control polymer did not change the MSL. This suggests that the imprinted polymers provided preformed surfaces and acted as heterogeneous nucleators.

The protocol described in this study may provide an additional diagnostic tool for stone researchers to determine the "stone forming risk" of a particular urine and it could thus be added to the existing array of protocols. It is suggested that it may be superior because urine composition is not altered in the work-up for the test. Determination of the CaOx metastable limit (Ryall *et al.*, 1985) or the Bonn-risk index (Laube *et al.*, 2000) requires chemical manipulation of the urine under investigation, whereas the imprint test utilizes urine in its natural voided state. It will thus be of considerable interest to determine whether the urine of stone formers is more susceptible to CaOx crystallization than that of healthy controls using the molecularly imprinted polymer model described in this study.

In conclusion, the present study has demonstrated that a maaha/dvb co-polymer imprinted with either COM or COD is capable of nucleating the formation of either of these solids from various CaOx solutions, including urine. This provides an interesting model system for further investigation of CaOx biomineralization.

CHAPTER SEVEN – CONCLUSION AND FUTURE WORK

The present study strongly suggests that heterogeneous nucleation is the decisively important mechanism in the process of kidney stone formation. The crystallization of CaOx from (i) metastable CaOx solutions of different concentrations (solutions I through III, table 4.1 *p* 50), (ii) artificial urine with varying concentrations of magnesium and citrate (solutions IV through VII, table 4.2 *p* 50) and (iii) real human urine on the surface of a molecularly imprinted polymer (maaha) is in agreement with the above hypothesis. XRD, FTIR, SEM and AA experiments demonstrated that maaha imprinted with COM and COD crystals directs nucleation of specific crystals from aqueous supersaturated CaOx solutions of different concentrations at metastability. This probably happened because the imprints in the polymer reduce the metastable limit of the solutions with respect to CaOx by providing preformed surfaces for crystal nucleation and growth.

When the polymers imprinted with COM and COD crystals were immersed in artificial urine in which the magnesium and citrate concentrations were varied, only the COM imprinted polymer directed nucleation of COM crystals and brushite without formation of COD, whereas the COD imprinted polymer led to precipitation of a mixture of many crystals containing mainly COM, COD and brushite. From this observation it can be suggested that magnesium and citrate inhibit the formation of CaOx crystals and that their effect seems to be additive. Furthermore; magnesium seems to inhibit better in the presence of citrate. The reason that only the COM imprinted polymer has directed nucleation of pure COM crystals could possibly be because of the greater thermal stability

of COM crystals, as a result of which the COD crystals might have been transformed to COM during the course of the reaction, or formed directly from the solution. It could also be because of the more negative surface charge of the COM crystals compared to COD crystals.

Both the COM and COD imprinted polymers lowered the metastable limit of human urine whereas the control polymer did not change it at all. When it comes to nucleation, only COM imprinted polymer (in some cases) led to the nucleation of pure COM crystals (although in most cases COM and brushite was formed). The COD imprinted polymer and the control polymer precipitated almost exclusively brushite.

This study concludes that heterogeneous nucleation is the process that plays determining role in the process of stone formation and that the imprinted polymer model may be used as a diagnostic tool in stone-risk assessment in urine.

The results of this thesis show the fulfillment of the objectives of the study. However, future studies should address the following. Firstly, additional concentrations of metastable solutions of CaOx must be considered in order to determine the smallest concentration that leads to nucleation of pure CaOx crystals on the surface of the imprinted polymers. Secondly, more combinations of varying concentrations of magnesium and citrate need to be studied in order to study how they affect each other and to investigate the ability of various ions to inhibit or promote CaOx crystal nucleation on the imprinted polymer surface. Thirdly, urine samples from stone-formers should be included in future studies,

since the present study comprised only non stone-formers. It would be of interest to investigate differences between the two groups with respect to CaOx nucleation. However, in the present study, only aqueous solutions reproducibly led to nucleation of pure CaOx crystals but not human urine. It may thus be necessary to find ways to inhibit brushite formation in order to study CaOx crystallization in urine using this system. The effect of urinary macromolecules and other ions present in urine on the crystallization of CaOx crystals on the surface of molecularly imprinted polymers could also be investigated. Lastly, an effort could be made to develop standardized assay for determining stone formation risk in urine samples using molecularly imprinted polymers.

REFERENCES

Abdulhadi, M. H., P. M. Hall and S. B. Streem (1993). Can citrate therapy prevent nephrolithiasis? *Urol.* **41**: 221-224.

Ackermann, D. and J. Baumann (1987). Chemical factors governing the state of saturation towards brushite and whewellite in urine of calcium stone formers. *Urol. Res.* **15**: 63-65.

Allie, S. and A. Rodgers (2003). Effects of calcium carbonate, magnesium oxide and sodium citrate bicarbonate health supplements on the urinary risk factors for kidney stone formation. *Clin. Chem. Lab. Med.* **1**: 39-45.

Bateson, E. M. (1973). Ranal tract calculi and climate. *Med. J. Aust.* **2**: 111-113.

Baumann, J. M. (1998). Stone prevention: why so little progress? *Urol. Res.* **26**: 77-81.

Beach, J. V. and K. J. Shea (1994). Designed catalysis: a synthetic network polymer that catalyzes the dehydrofluorination of 4-fluoro-4-(*p*-nitrophenyl)butan-2-one. *J. Am. Chem. Soc.* **116**: 379-380.

Bellanato, J., L. Delatte, A. Hidalgo and M. Santos (1973). Application of infrared spectroscopy to the study of renal stones. Urinary Calculi Int. Symp. Renal Stone Res., Madrid: 237-246.

Berg, C., L. Larsson and H. G. Tiselius (1990). Effects of different doses of alkaline citrate on urine composition and crystallization of calcium oxalate. *Urol. Res.* **18**: 13-16.

Berg, W., C. Brother, W. Pirlick and V. Janitzky (1986). Influence of magnesium on the absorption and excretion of calcium and oxalate ions. *Eur. Urol.* **12**: 274-282.

Beshensky, A. M., J.A. Wesson, E. M. Worcester, C. Snyder and J. G. Kleinman (2000). Urinary protein effects on heterogeneous nucleation of calcium oxalate on hydroxyapatite 9th International Symposium on Urolithiasis, South Africa, Cape Town: 116-118.

Beukes, G. J., H. D. Bruiyn and W. H. Vermaak (1987). Effect of changes in epidemiological factors on the composition and racial distribution of renal calculi. *Br. J. Urol.* **60**: 387-392.

Bilobrov, V. M., A. V. Chugaj and V. I. Bessarabov (1990). Urinaty pH variation dynamics in healthy individuals and stone formers. *Urol. Int.* **45**: 326-331.

Blacklock, N. J. (1982). 35. Epidemiology of urolithiasis. Scientific Foundations of Urology. I. David and D. Geoffrey. London, William Heinemann Medical Books Ltd. **I:** 235-243.

Blomen, L. J., E. J. Will, O. L. Bijvoet and H. V. Linden (1983). Growth kinetics of calcium oxalate monohydrate: II. The variation of seed concentration. *J. Cryst. Growth* **64**: 306-315.

Borghi, L., T. Meschi, A. Guerra, E. Bergamaschi, A. Mutti and A. Novarini (1995). Effect of urinary macromolecules on the nucleation of calcium oxalate in idiopatic stone formers and healthy controls. *Clin. Chim. Acta* **239**: 1-11.

Borghi, L., T. Meschi, T. Scianchi, A. Briganti, A. Guerra, J. Allegri and A. Novarini (1999). Urine volume: stone risk factor and preventive measure. *Nephron* **81**: 31-37.

Bosch, T., T. Wendler and H. Maschke (2003). Modified DALI LDL-apheresis using trisodium citrate anticoagulation plus bicarbonate or lactate-buffered hemofiltration substitution fluids as primers. *Artif. Organs* **27**: 555-564.

Boyce, W. and H. Strawcutter (1956). Incidence of urinary calculi among patients in general hospitals. *J. Am. Med. Assoc.* **161**: 1437-1442.

Brecevic, L., D. Skrtic and J. Garside (1986). Transformation of calcium oxalate hydrates. *J. Cryst. Growth* **74**: 399-408.

Brown, P., D. Ackermann and B. Finlayson (1989). Calcium oxalate dihydrate (weddellite) precipitation. *J. Cryst. Growth* **98**: 285-292.

Bullock, N., G. Sibley and R. Whitaker (1998). Essential urology. London, Churchill Livingstone.269.

Byrne, M. E., K. Park and N. A. Peppas (2002). Molecular imprinting within hydrogels. *Adv. Drug Del. Rev.* **54**: 149-161.

Campbell, A. A., E. F. Glen, G. L. Graff, P. C. Rieke and B. J. Tarasevich (1993). The nucleation and growth of calcium oxalate monohydrate on self-assembled monolayers (SAMS). *Scan. Microsc.* **7**: 423-429.

Cerini, C., S. Geider, B. Dussol, C. Hennequin, M. Daudon, S. Veesler, S. Nitsche, R. Boistelle, P. Berthezene, P. Dupuy, A. Vazi, Y. Berland, J.-C. Dagorn and J.-M. Verdier (1999). Nucleation of calcium oxalate crystals by albumin: involvement in the prevention of stone formation. *Kidney Int.* **55**: 1776-1786.

Christmas, K. G., L. B. Gower, S. R. Khan and H. El-Shall (2002). Aggregation and dispersion characteristics of calcium oxalate monohydratre: effect of urinary species. *J. Colloid Interface Sci.* **256**: 168-174.

Coe, L., G. Derg, E. Boeve, W. deBruijin, R. deWater, C. Verkoelen, J. Romijn and F. Schroder (1996). Zeta potential measurement and particle size analysis for a better understanding of calcium oxalate crystallization. *Scan. Microsc.*: 401-414.

Conte, A., P. Roca, C. Genester and F. Grases (1989). The relationship between orthophosphate and pyrophosphate in normal subjects and in patients with urolithiasis. *Urol. Res.* **17**: 173-175.

Craig, T. A., A. L. Rodgers and W. Brandt (2001). Inhibition of calcium oxalate crystallization by Tamm-Horsfall mucoprotein from two different population groups. 9th European Symposium on Urolithiasis, Netherlands, Shaker Publishing:59-60.

Curhan, G. C. (1997). Dietay calcium, dietary protein, and kidney stone formation. *Miner. Electrol. Metab.* **23**: 261-264.

Curhan, G. C., W. C. Willet, E. B. Rimm, D. Spiegelman and M. J. Stampfer (1996). Prospective study of beverage use and the risk of kidney stones. *Am. J. Epidemiol.* **143**: 240-247.

Curhan, G. C., W. C. Willet, E. B. Rimm and M. J. Stampter (1993). A prospective study of dietary calcium and other nutrients and the risk of symptomatic kidney stones. *N. Engl. J. Med.* **328**: 833-838.

Curhan, G. C., W. C. Willett, F. E. Speizer and M. J. Stampfer (2001). Twenty-four-hour urine chemistries and the risk of kidney stones among women and men. *Kidney Int.* **59**: 2290-2298.

Daudon, M., C. Bader and P. Jungers (1993). Urinary calculi: review of classification methods and correlations with etiology. *Scan. Microsc.* 7: 1081-1106.

Deganello, S., A. R. Kampf and P. B. Moore (1981). The crystal structure of calcium oxalate trihydrate: $Ca(H_2O)_3C_2O_4$. *Am. Mineral.* **66**: 859-865.

Doyle, I. R., V. R. Marshall, C. J. Dawson and R. L. Ryall (1995). Calcium oxalate crystal matrix extract: the most potent macromolecular inhibitor of crystal growth and aggregation yet tested in undiluted human urine *in vitro*. *Urol. Res.* **23**: 53-62.

D'Souza, S. M., C. Alexander, S. W. Carr, A. M. Wallers, M. J. Whitcombe and E. N. Vulfson (1999). Directed nucleation of calcite at a crystal-imprinted polymer surface. *Nature* **398**: 312-316.

Dussol, B. and Y. Berland (1998). Urinary kidney stone inhibitors. What is the news? *Urol. Int.* **60**: 69-73.

Edyvane, K. A., C. M. Hibberd, R. M. Harnett, V. R. Marshall and R. L. Ryall (1987). Macromolecules inhibit calcium oxalate crystal growth and aggregation in whole human urine. *Clin. Chim. Acta* **167**: 329-338.

Fan, J., P. S. Chandhoke and S. A. Grampas (1999). Role of sex hormones in experimental calcium oxalate nephrolithiasis. *J. Am. Soc. Nephrol.* **10**: S376-S380.

Farias, M. G., J. M. Soucie, W. McClellan and W. E. Mitch (1994). Race and the risk of peritonitis: an analysis of factors associated with the initial episode. *Kidney Int.* **46**: 1392-1396.

Finch, A. M., G. P. Kasidas and G. A. Rose (1981). Urine composition in normal subjects after oral ingestion of oxalate-rich foods. *Clin. Sci.* **60**: 411-418.

Finlayson, B. (1977). Calcium stones: some physical and clinical aspects. Calcium Metabilism in Renal Failur and Nephrolithiasis. D. David. New York, John Wiley & Sons. **Chapter 10:** 337-382.

Finlayson, B. (1978). Physicochemical aspects of urolithisis. *Kidney Int.* **13**: 344-360.

Finlayson, B., S. R. Khan and R. L. Hackett (1984). Mechanisms of stone formation - an overview. *Scan. Electron Microsc.* **3**: 1419-1425.

Gardner, G. L. (1976). Kinetics of the dehydration of calcium oxalate trihydrate crystals in aqueous solution. *J. Colloid Interface Sci.* **54**: 298-310.

Gardner, G. L. (1978). Effect of pyrophosphate and phosphate anions on the crystal growth kinetics of calcium oxalate hydrates. *J. Phys. Chem.* **82**: 864-870.

Garilevich, B. and I. Avdeichuk (1995). The characteristics of urolithiasis in flight personnel and the treatment results using a method of extracorporeal shockwave lithotripsy on the Russian lithotripter urat-P2. *Aviakosm Ekolog. Med.* **29**: 46-47.

Geider, S., B. Dussol, S. Nitsch, S. Veesler, P. Berthezene, P. Dupuy, J. Astier, R. Boistelle, Y. Berland, J. Dagorn and J. Verdier (1996). Calcium carbonate crystals promote calcium oxalate crystallization by heterogeneous or epitaxial nucleation: possible involvement in the control of urinary lithogenesis. *Calcified Tissue Int.* **59**: 33-37.

Giannini, S., M. Nobile, L. Sartori, L. Carbonare, M. Ciuffreda, P. Corro, A. D'Angelo, L. Calo and G. Crepaldi (1999). Acute effects of moderate dietary protein restriction in patients with idiopathic hypercalciuria and calcium nephrolithiasis. *Am. J. Clin. Nutr.* **69**: 267-271

Gohel, M. D., D. K. Shum and W. W. Wong (2000). Excretion of hyaluronan in urine samples of normals and stone-formers. 9th International Symposium on Urolithiasis, South Africa, University of Cape Town: 135-137.

Goldfarb, S. (1994). Diet and nephrolithiasis. *Annu. Rev. Med.* **45**: 235-243.

Goodman, H. O., R. P. Holmes and D. G. Assimos (1995). Genetic factors in calcium oxalate stone disease. *J. Urol.* **153**: 301-307.

Grases, F., A. Costa-Bauza and L. Garcia-Ferragut (1998). Biopathological crystallization: a general view about the mechanisms of renal stone formation. *Adv. Colloid Interface Sci.* **74**: 169-194.

Grases, F., A. Costa-Bauza and J. March (1994). Artificial simulation of the early stages of renal stone formation. *Br. J. Urol.* **74**: 298-301.

Grases, F., A. Costa-Bauza, J. March and L. Masarova (1991). Glycosaminoglycans, uric acid and calcium oxalate urolithiasis. *Urol. Res.* **19**: 375-380.

Grases, F., L. Garcia-Ferragut and A. Costa-Bauza (1996). Study of the early stages of renal stone formation: experimental model using urothelium of pig urinary bladder. *Urol. Res.* **24**: 305-311.

Grases, F., C. Genestar, A. Conte, P. March and A. Costa-Bauza (1989b). Inhibitory effect of pyrophosphate, citrate, magnesium and chondroitin sulphate in calcium oxalate urolithiasis. *Br. J. Urol.* **64**: 235-237.

Grases, F., J. Gil and A. Conte (1989a). Urolithiasis inhibitors and calculus nucleation. *Urol. Res.* **17**: 163-166.

Grases, F., A. Millan and A. Conte (1990). Production of calcium oxalate monohydrate, dihydrate or trihydrate: a comparative study. *Urol. Res.* **18**: 17-20.

Grover, P. K., R. L. Moritz, R. J. Simpson and R. L. Ryall (1998). Inhibition of growth and aggregation of calcium oxalate crystals *in vitro*. *Eur. J. Biochem.* **153**: 637-644.

Grover, P. K. and R. L. Ryall (1995). Urate and calcium oxalate stones: a new look at an old controversy. Calcium Oxalate in Bilogical Systems. S. Khan. New York, CRC press**:** 305-321.

Hallson, P., G. Rose and S. Sulaiman (1982). Magnesium reduces calcium oxalate crystal formation in human whole urine. *Clin. Sci.* **62**: 17-19.

Hallson, P. C. and G. A. Rose (1977). Seasonal variations in urinary crystals. *Br. J. Urol.* **49**: 277-284.

Hentze, H.-P. and M. Antonietti (2001). Template synthesis of porous organic polymers. *Curr. Opin. Solid State Mater. Sci.* **5**: 343-353.

Hermann, U., P. Schwille, A. Schmiedl, J. Fan and M. Manoharan (1999). Acute effects of calcium sodium citrate supplementation of a test meal on mineral homeostasis, oxalate, and calcium oxalate crystallization in the urine of healthy humans--preliminary results in patients with idiopathic calcium urolithiasis. *Biomed. Pharmacother.* **53**: 264-273.

Hess, B. (1994). Tamm-Horsfall glycoprotein and calcium nephrolithiasis. *Min. Electrol. Metab.* **20**: 393-398.

Hess, B. (1996). Low calcium diet in hypercalciuric calcium nephrolithiasis: first do no harm. *Scan. Microsc.* **10**: 547-556.

Hess, B. (2002). Nutritional aspects of stone disease. *Endocrinol. Metab. Clin. N. Am.* **31**: 1017-1030.

Hess, B., C. Jost, L. Zipperle, R. Takkinen and P. Jaeger (1998). High-calcium intake abolishes hyperoxaluria and reduces urinary crystallization during a 20-fold normal oxalate load in humans. *Nephrol. Dial. Transpl.* **13**: 2241-2247.

Hess, B. and D. Kok (1996). Nucleation, growth, and aggregation of stone-forming crystals. Kidney Stones. F. L. Coe, M. J. Favus, C. Y. Pak, J. H. Parks and G. M. Preminger. Philadelphia, Lippincott-Raven Publishers**:** 3-31.

Hess, B., H. Mauron, D. Ackermann and P. Jaeger (1999). Effects of a 'common sense diet' on urinary composition and supersaturation in patients with idiopathic calcium urolithiasis. *Eur. Urol.* **36**: 136-143.

Hess, B., Y. Nakagawa and F. Coe (1989). Inhibition of calcium oxalate monohydrate crystal aggregation by urine proteins. *Am. J. Physiol.* **257**: F99-F106.

Hess, B., R. L. Ryall, J. P. Kavanagh, S. R. Khan, D. J. Kok, A. L. Rodgers and H.-G. Tiselius (2001). Methods for measuring crystallization in urolirhiasis research: why, how and when? *Eur. Urol.* **40**: 220-230.

Hesse, A., R. Siener, H. Heynck and A. Jahnen (1993). The influence of dietary factors on the risk of urinary stone formation. *Scan. Microsc.* 7: 1119-1128.

Hesse, A., H. Wuzel and W. Vahlensieck (1986). The excretion of glycoglycans in the urine of calcium-oxalate-stone patients and healthy persons. *Urol. Int.* **41**: 81-87.

Hiratani, H. and C. Alvarez-Lorenzo (2002). Timolol uptake release by imprinted soft contact lenses made of N,N-diethyalacrylamide and methacrylic acid. *J. Control. Release* **83**: 223-230.

Hirvonen, T., P. Pietinen, M. Virtanen, D. Albanes and J. Virtamo (1999). Nutrient intake and use of beverages and the risk of kidney stones among male smokers. *Am. J. Epidemiol.* **150**: 187-194.

Holmes, R. P. and D. G. Assimos (1999). Dietary oxalate and its influence on urinary oxalate excretion. Eur. Urol., Cosenza, Editoriale Bios: 495-497.

Iguchi, M., T. Takamura, T. Umekawa, T. Kurita and K. Kohri (1999). Inhibitory effects of female sex hormones on urinary stone formation in rats. *Kidney Int.* **56**: 479-485.

Iwata, H., S. Nishio and M. Takeuchi (1994). The inhibitory effect of urinary heparan sulphate and chondroitin sulphate on calcium oxalate crystal growth. Urolithisis 2, New York, Plenum Press: 205-207.

Kavanagh, J. P. (1992). Methods for the study of calcium oxalate crystallization and their application to urolithiasis research. *Scan. Microsc.* **6**: 685-705.

Kavanagh, J. P., L. Jones and P. N. Rao (1999). Calcium oxalate crystalization kinetics at different concentrations of human and artificial urine, with a constant calcium to oxalate ratio. *Urol. Res.* **27**: 231-237.

Khan, S. R. (1995). Calcium oxalate in biological systems. New York, CRC press 400.

Khan, S. R., P. N. Shevock and H. R. L (1990). Membrane-associated crystallization of calcium oxalate *in vitro*. *Calcified Tissue Int.* **46**: 116-120.

Khan, S. R., P. O. Whalen and P. A. Glenton (1993). Heterogeneous nucleation of calcium oxalate crystals in the presence of membrane vesicles. *J. Cryst. Growth* **134**: 211-218.

Kim, K. M. (1982). The stones. *Scan. Microsc.* **4**: 1635-1660.

Kitamura, T. and C. Y. Pak (1982). Tamm and horsfall grycoprotein does not promote spontaneous precipitation and crystal growth of calcium oxalate *in vitro*. *J. Urol.* **127**: 1024-1026.

Kohri, K., J. Garside and N. J. Blacklock (1988). The role of magnesium in calcium oxalate urolithiasis. *Br. J. Urol.* **61**: 107-115.

Kok, D. J. (1997). Intratubular crystallization events. *World J. Urol.* **15**: 219-228.

Kok, D. J. and S. R. Khan (1994). Calcium oxalate nephrolithiasis, a free or fixed particle disease. *Kidney Int.* **46**: 847-854.

Konya, E., T. Umekawa, M. Iguchi and T. Kurita (2003). The role of osteopontin on calcium oxalate crystal formation. *Eur. Urol.* **43**: 564-571.

kriz, D., O. Ramstrom and K. Mosbach (1997). Molecular imprinting-based biomimetic sensors could provide an alternative to often unstable biosensors for industry, medicine and environmental analysis. Anal. Chem. Lund, Lund University. **69:** 345A-349A.

Kunitake, T. and Y. Okahata (1976). Multifactorial hydrolytic catalyses. 7. Cooperative catalysis of the hydrolysis of phenyl esters by a copolymer of N-methyl acrylohydroxamic acid and 4-vinylimidazole. *J. Am. Chem. Soc.* **98**: 7793-7799.

Laube, N., A. Schneider and A. Hesse (2000). A new approach to calculate the rise of calcium oxalate crystallization from unprepared native urines. *Urol. Res.* **28**: 274-280.

Lele, B. S., M. G. Kulkrani and R. A. Mashelkar (1999). Molecularly imprinted polymer mimics of chymotripsin. *React. Funct. Polym.* **40**: 215-229.

Levine, B. S., J. S. Rodman, S. Wiernman, R. S. Bockman and J. M. Lane (1994). Effect of calcium citrate supplementation on urinary calcium oxalate saturation in female stone formers. *Am. J. Clin. Nutr.* **60**: 592-596.

Levison, D., P. Crocker and S. Banim (1982). Silica stones in the urinary bladder. *Lancet* **1**: 704-705.

Lewandowski, S., A. Rodgers and I. Schloss (2001). The influence of a high-oxalate/low-calcium diet on calcium oxalate renal stone risk factors in non-stone-forming black and white South African subjects. *Br. J. Urol. Int.* **87**: 1-5.

Li, M. K., N. J. Blacklock and J. Garside (1985). Effect of magnesium on calcium oxalate crystallization. *J. Urol.* **133**: 123-125.

Lieske, J. C. and F. G. Toback (1993). Regulation of renal epithalial cell endocytosis of calcium oxalate monohydrate crystals. *Am. J. Physiol.* **264**: F800-F807.

Lingeman, J., R. Kahnoski, H. Mardis, D. Goldfarb, M. Grasso, S. Lacy, S. J. Scheinman, J. R. Asplin and F. L. Coe (1999). Divergence between stone composition and urine supersaturation: clinical and laboratory implications. *J. Urol.* **161**: 1077-1081.

Mandel, N. and R. Riese (1991). Crystal cell interactions: crystal binding to rat renal papillary tip collecting duct cells in culture. *Am. J. Kidney Dis.* **17**: 402-405.

Mann, F. G., B. C. Saunders (1967). Practical Organic Chemistry. London, Longmans. Part II: 241-252.

Massey, L. K., H. Roman-Smith and R. A. Sutton (1993). Effect of dietary oxalate and calcium on urinary oxalate and risk of formation of calcium oxalate kidney stones. *J. Am. Diet Assoc.* **93**: 901-906.

Mathew-Krotz, J. and K. J. Shea (1996). Imprinted polymer membranes for the selective transport of target neutral melecules. *J. Am. Chem. Soc.* **118**: 8154-8155.

Mensah, P., A. L. Rodgers and E. D. Sturrock (2003). Inhibitory effect of urinary albumin from black and white South Africans on calcium oxalate monohydrate crystal aggregation. *Urol. Res.* **31**: 91.

Mercier, A., H. Deleuze and O. Mondain-Monval (2000). Preparation and functionalization of (vinyl) polystyrene polyHOPE. Short routes to binding functional groups through a dimethylene spacer. *React. Funct. Polym.* **46**: 67-79.

Modlin, M. (1967). Urinary ionized calcium and renal stone. An inter-ratial study. *J. Urol.* **97**: 567-572.

Modlin, M. and P. J. Davies (1981). The composition of renal stones analysed by infrared spectroscopy. *S. Afr. Med. J.* **59**: 337-341.

Mosbach, K. and O. Ramstrom (1996). The emerging technique of molecular imprinting and its future impact on biotechnology. *Bio-Technol.* **14**: 163-170.

Moyad, M. A. (2003). Calcium oxalate kidney stones: another reason to encourage moderate calcium intakes and other dietary changes. *Urol. Nurs.* **23**: 310-313.

Nancollas, G. H. and G. L. Gardner (1974). Kinetics of crystal growth of calcium oxalate monohydrate. *J. Cryst. Growth* **21**: 267-276.

Nancollas, G. H., S. A. Smesko, A. A. Campbell, C. F. Richardson, M. Johnsson, R. A. Iadiccico, J. P. Binette and M. Binette (1991). Physical chemical studies of calcium oxalate crystallization. *Am. J. Kidney Dis.* **17**: 392-395.

Nishio, S., M. Hatanaka, H. Takeda, K. Aoki, T. Iseda, H. Iwata and M. Yokoyama (2001). Calcium phosphate crystal-associated proteins: α–2–HS-glycoprotein, prothrombin 1 and osteopontin. *Int. J. Urol.* **8**: S58-S62.

Nishio, S., M. Hatanaka, H. Takeda, T. Iseda, H. Iwata and M. Yokoyama (1999). Analysis of urinary concentrations of calcium phosphate crystal-associated proteins: α–2-HS-glycoprotein, prothrombin F1, and osteopontin. *J. Am. Soc. Nephrol.* **10**: S394-S396.

Pak, C., K. Koenig, R. Khan, S. Haynes and P. Padalino (1992). Physicochemical action of potassium-magnesium citrate in nephrolithiasis. *J. Bone Nimer. Res.* 7: 281-285.

Pak, C., M. Ohata and K. Holt (1975). Effect of diphosphodnate on crystallization of calcium oxalate *in vitro*. *Kidney Int.* 7: 154-160.

Pak, C. Y. (1998). Kidney stones. *Lancet* **130**: 1115-1118.

Pak, C. Y. (1999). Madical prevention of renal stone disease. *Nephron* **81**: 60-65.

Pak, C. Y. and C. Fuller (1986). Idiopathic hypocitraturic calcium-oxalate nephrolithiasis successfully treated with potassium citrate. *Ann. Int. Med.* **104**: 33-37.

Pin, N., N. Ling and L. Siang (1992). Dehydration from outdoor work and urinary stones in a tropical environment. *Occup. Med.* **42**: 30-32.

Prien, E. L. (1971). The riddle of urinary stone disease. *J. Am. Med. Assoc.* **216**: 503-507.

Ramello, A., C. Vitale and M. Marangella (2000). Epidemiology of nephrolithiasis. *J. Nephrol.* **13**: S45-S50.

Ramstrom, O. (1996). Molecular imprinting technology: a way to make artificial locks for molecular keys. Lund, Lund University. **2003**.

Rachkov, A. and N. Minoura (2001). Towards molecularly imprinted polymers selective to peptides and proteins: the epitope approach. *Biochim. Biophys. Acta.* **1544**: 255-266.

Randall, A. (1940). Papillary pathology as a precursor of primary renal calculus. *J. Urol.* **44**: 580-589.

Reaser, E. G. (1935). Racial incidence of urolithiasis. *J. Urol.* **34**: 148-155.

Riese, R. J., N. S. Mandel, J. H. Wiessner, G. S. Mandel, C. G. Becker and J. G. Kleinman (1992). Cell polarity and calcium oxalate crystal adherence to cultured collecting duct cells. *Am. J. Physiol.* **262**: F177-F184.

Robertson, N. G. and M. Peacock (1980). The cause of adiopathic calcium disease: hypercalciuria or hyperoxaluria? *Nephron* **26**: 105.

Robertson, W. and M. Peacock (1983). Review of risk factors in calcium oxalate urolithiasis. *J. Urol.* **1**: 114-118.

Robertson, W. G. (1987). Diet and calcium stones. *Miner. Electrol. Metab.* **13**: 228-234.

Robertson, W. G. (1999). Mild hyperoxaluria: a criteria review and future outlook. Eur. Urol., Cosenza, Editoriale Bios: 33-42.

Robertson, W. G., J. C. Gallagher, D. H. Marshall, M. Peacock and B. E. Nordin (1974). Seasonal variations in urinary excretion of calcium. *Br. Med. J.* **4**: 436-437.

Robertson, W. G., P. J. Heyburn, M. Peacock, F. A. Hanes and R. Swaminathan (1979a). The effect of high animal protein intake on the risk of calcium stone-formation in the urinary tract. *Clin. Sci.* **57**: 285-288.

Robertson, W. G. and H. Hughes (1994). Epidemiology of urinary stone disease in Saudi Arabia. Urolithiasis 2, New York, Plenum Press: 453-455.

Robertson, W. G. and B. E. Nordin (1982). 37. Physico-chemical factors governing stone formation. Scientific Foundations of Urology**:** 254-267.

Robertson, W. G., M. Peacock, P. J. Heyborn, D. H. Marshall and P. G. Clark (1978). Risk factors in calcium stone disease of the urinary tract. *Br. J. urol.* **50**: 449-454.

Robertson, W. G., M. Peacock, P. J. Heyburn, F. A. Hanes, A. Rutherford, E. Clementson, R. Swaminathan and P. B. Clark (1979b). Should renal calcium oxalate stone formers become vegeterians? *Br. J. Urol.* **51**: 427-431.

Robertson, W. G., M. Peacock, R. W. Marshall, R. Speed and B. E. Nordin (1975). Seasonal varietions in the composition of urine in relation of urinary stone-formation. *Clin. Sci. Mol. Med.* **49**: 597-602.

Robertson, W. G., M. Peacock and B. E. Nordin (1968). Activity product in stone-forming and non-stone-forming urine. *Clin. Sci.* **34**: 579-594.

Robertson, W. J. and M. Peacock (1981). Epidemiological factors in the genesis of calcium-containing urinary stones. Metabolic, physiochemical, therapeutical aspects of urolithiasis. F. Linari, M. Bruno, B. Fruttero and M. Marangella. Milano, Wichtig Editore**:** 5-20.

Rodgers, A., D. Ball and W. Harper (1993). Urinary macromolecules are promotors of calcium oxalate nucleation in human urine: turbidimetric studies. *Clin. Chim. Acta* **220**: 125-134.

Rodgers, A. L. (1997). Effect of mineral water containing calcium and magnesium on calcium oxalate urolithiasis risk factors. *Urol. Int.* **58**: 93-99.

Rodgers, A. L. (1999). Effect of cola consumption on urinary biochemical and biophysical risk factors associated with calcium oxalate urolithiasis. *Urol. Res.* **27**: 77-81.

Rodgers, A. L. and S. Lewandowski (2002). Effects of 5 different diets on urinary risk factors for calcium oxalate kidney stone formation: evidence of different renal handling mechanisms in different race groups. *J. Urol.* **168**: 931-936.

Rodgers, A. L. and M. Spector (1981). Human stones. *Endeavour*. **5:** 119-126.

Rodgers, A. R. (1991). Urinary calculi: (I) Epidemiology. Human Stones. Cape Town, University of Cape Town**:** 18-31.

Rose, G. and S. Sulaiman (1982). Tamm-Horsfall mucoprotein promotes calcium oxalate crystal formation in urine: quantitative studies. *J. Urol.* **127**: 177-179.

Rose, G. A. and E. J. Westbury (1979). Seasonal and geographic variations in urinary composition in England, Scotland and Wales. *Urol. Res.* 7: 235-240.

Ryall, R. L. (1989). The formation and investigation of urinary calculi. *Clin. Biochem. Revs.* **10**: 149-157.

Ryall, R. L. (1996). Glycosaminoglycans, proteins, and stone formation: adult themes and child's play. *Pediatr. Nephrol.* **10**: 656-666.

Ryall, R. L. (1997). Urinary inhibitors of calcium oxalate crystallization and their potential role in stone formation. *World J. Urol.* **15**: 155-164.

Ryall, R. L., D. E. Fleming, I. R. Doyle, N. A. Evans, C. J. Dean and V. R. Marshal (2001). Intracrystalline proteins and the hidden ultrastructure of calcium oxalate urinary structures: implications for kidney stone formation. *J. Struct. Biol.* **134**: 5-14.

Ryall, R. L., R. M. Harnett, C. M. Hibberd, K. A. Edyavane and V. R. Marshall (1991). Effects of chondroitin sulphate, human serum albumin and Tamm-Horsfall mucoprotein on calcium oxalate crystallization in undiluted human urine. *Urol. Res.* **19**: 181-188.

Ryall, R. L., R. M. Harnett and V. R. Marshall (1981). The effect of urine, phosphate, citrate, magnesium and glycosaminoglycans on the growth and aggregation of calcium oxalate crystals *in vitro*. *Clin. Chim. Acta* **112**: 349-356

Ryall, R. L., C. M. Hibberd and V. R. Marshall (1985). A method for studying inhibitory activity in whole urine. *Urol. Res.* **13**: 285-289.

Ryall, R. L. and A. M. Stapleton (1995). Urinary macromolecules in calcium oxalate stone and crystal matrix: good, bad, or indifferent? Calcium Oxalate in Biological Systems. S. R. Khan. New York, CRC press: 265-290.

Sakhaee, K., S. Baker, J. Serwekh, J. Poindexter, P. Garcia-Hernandez and C. Pak (1994). Limited risk of kidney stone formation during long-term calcium citrate supplementation in nonstone forming subjects. *J. Urol.* **152**: 324-327.

Sakhaee, K., J. Harvey, P. Padalino, P. Whitson and Y. Pak (1993). The potential role of salt abuse on the risk for kidney stone formation. *J. Urol.* **150**: 310-312.

Sakhaee, K., M. Nicar, K. Hill and C. Pak (1983). Contrasting effects of potassium citrate and sodium citrate therapies on urinary chemistries and crystallization of stone-forming salts. *Kid. Int.* **24**: 348-352.

Sakhaee, K., S. Nigam, P. Snell, M. C. Hsu and C. Y. Pak (1987). Assesment of the pathogenetic role of physical exercise in renal stone formation. *J. Clin. Endocr. Metab.* **65**: 974-979.

Schwille, P., G. Rumenapf, R. Kohler and F. Sorgel (1987). Effects of acute oral sodium potassium citrate load in healthy males - outlook of treatment of patients with calcium-containing renal stones. *Urol. Int.* **42**: 81-88.

Schwille, P. O. and U. Hermann (1992). Environmental factors in the pathophysiology of recurrent idiopathic calcium urolithiasis (RCU), with emphasis on nutrition. *Urol. Res.* **20**: 72-83.

Schwille, P. O., A. Schmiedl, U. Herman, R. Schwille, E. Fink and M. Monoharan (1997). Acute oral calcium-sodium citrate load in healthy males. Effect on acid-base and mineral metabolism, oxalate and other risk factors of stone formation in urine. *Meth. Find. Exp. Clin. Pharmacol.* **19**: 417-427.

Scott, R. (1985). Epidemiology of stone disease. *Br. J. Urol.* **57**: 491-497.

Scurr, D. and W. G. Robertson (1986). Modifiers of calcium oxalate crystallisation II. Studies on their models of action in an artificial urine. *J. Urol.* **136**: 128-131.

Sellergren, B. (2000). Imprinted polymers with memory for small molecules, proteins, or crystals. *Angew. Chem. Int. Ed.* **39**: 1031-1037.

Sheng, X., M. D. Ward and J. A. Wesson (2003). Adhesion between molecules and calcium oxalate crystals: critical interactions in kidney stone formation. *J. Am. chem. Soc.* **125:** 2854-2855

Shi, H., W.-B. Tsai, M. D. Garrison, S. Ferrari and B. D. Ratner (1999). Template-imprinted nanostructured surfaces for protein recognition. *Nature* **398**: 593-597.

Shirane, Y. and S. Kagawa (1993). Scanning electron microscopy study of the effect of citrate and pyrophosphate on calcium oxalate crystal morphology. *J. Urol.* **150**: 1980-1983.

Shum, D. K. and M. D. Gohel (1993). Separate effects of urinary chondroitin sulphate and heparan sulphate on the crystallization of urinary calcium oxalate: difference between stone formers and normal control subjects. *Clin. Sci.* **85**: 33-39.

Siener, R. and A. Hesse (1995). Influence of a mixed and a vegetarian diet on urinary magnesium excretion and concentration. *Br. J. Nutr.* **73**: 783-790.

Sohnel, O. and F. Grases (1995). Calcium oxalate monohydrate renal calculi. Formation and development mechanism. *Adv. Colloid Inteface Sci.* **59**: 1-17.

Soucie, J. M., M. J. THun, R. J. Coates, W. McClellan and H. Austin (1994). Demographic and geographic variability of kidney stones in the United States. *Kidney Int.* **46:** 893-899

Spivac, D. and K. J. Shea (1999) Molecular imprinting of carboxylic acids employing novel functional macroporous polymers. *J. Org. Chem.* **64:** 4627-4634

Strikovsky, A., J. Hradil and G. Wulff (2003). Catalitically active, molecularly imprinted polymers in bead form. *React. Funct. Polym.* **54**: 49-61.

Sutor, D. J. and S. Scheidt (1968). Identification standards for human urinary calculus components, using crystallographic methods. *Br. J. Urol.* **XI**: 22-28.

Takasaki, E. (1986). Chronological variation in the chemical composition of upper urinary tract calculi. *J. Urol.* **136**: 5-9.

Thind, S. K., R. Nath, S. Farooqui and M. S. Murthy (1981). Therapeutic role of vitamine B_6 on oxalate metabolism in urolithiasis and its effect on hyperoxaluria induced in rats by ethylene glycol. Urolithiasis: Clinical Basic Res., Proc. Int. Symp.: 869-873.

Tietz, N. W. (1976). Analysis of calculi. Fundamentals of Clinical Chemistry. A. E. Fiereck. Philadelphia, Saunders, W B Company**:** 1015-1025.

Timio, F., S. M. Kerry, K. M. Anson, J. B. Eastwood and F. P. Cappuccio (2003). Calcium urolithiasis, blood pressure and salt intake. *Blood Pressure* **12**: 122-126.

Tiselius, H.-G. (1981). The effect of pH on the urinary inhibition of calcium oxalate crystal growth. *Br. J. Urol.* **53**: 470-474.

Tiselius, H.-G., C. Berg, A.-M. Fornander and M.-A. Nilsson (1993). Effects of citrate on the different phases of calcium oxalate crystallization. *Scan. Microsc.* 7: 381-390.

Toorisaka, E., K. Uezu, M. Goto and S. Furusaki (2003). A molecularly imprinted polymer that shows enzymatic activity. *Biochem. Engng. J.* **14**: 85-91.

Webber, D., A. Rodgers and E. Sturrock (2002). Synergism between urinary prothrombin fragment 1 and urine: a comparison of inhibitory activities in stone-prone and stone-free population groups. *Clin. Chem. Lab. Med.* **40**: 390-396.

Webber, D., A. Rodgers and E. Sturrock (2003). Selective inclusion of proteins into urinary calcium oxalate crystals: comparison between stone-prone and stone-free population groups. *J. Cryst. Growth* **259**: 179-189.

Werness, P. G., C. M. Brown, L. H. Smith and B. Finlayson (1985). EQUIL2: a basic computer program for the calculation of urinary saturation. *J. Urol.* **134**: 1242-1244.

Wesson, J. A., R. J. Richard, M. Mazzali, A.M. Beshensky, S. Stietz, C. Giachelli, L. Liaw, C. E. Alpers, W. G. couser, J. G. Kleinman and J. Hughes (2003). Osteopontin is a critical inhibitor of calcium oxalate crystal formation and retention in renal tubules. *J. Am. Soc. Nephrol.* **14:** 139-147.

Wesson, J. A., J. H. Weissner, N. S. Mandel and J. G. Kleinman (2000). Polymer chemical structures that control calcium oxalate polymorphism. 9th International Symposium on Urolithiasis, South Africa, Cape Town.

Whalley, N. A., M. C. Martins, R. C. Van Dyk and A. M. Meyers (1999). Lithogenic risk factors in normal black volunteers, and black and white recurrent stone formers. *Br. J. Urol.* **84**: 243-248.

Whalley, N. A., M. F. Moraes, T. G. Shar, S. S. Pretorius and A. M. Meyers (1998). Lithogenic risk factors in the urine of black and white subjects. *Br. J. Urol.* **82**: 785-790.

Wilson, D. M., L. H. Smith and S. B. Erickson (1989). Renal oxalate handling in normal subjects and patients with idiopathic renal lithiasis: primary and secondary hyperoxaluria. Urolithiasis, New York, Plenum.

Worcester, E. M. (1996). Inhibitors of stone formation. *Sem. Nephrol.* **16**: 474-486.

Wulff, G. (1995). Molecular imprinting in cross-linked materials with aid of molecular templates - a way towards artificial antibodies. *Angew. Chem. Int. Ed. Engl.* **34**: 1812-1832.

Yamate, T., K. Kohri, T. Umekawa, M. Iguchi and T. Kurita (1998). Osteopontin antisense oligonucleotide inhibits adhesion of calcium oxalate crystals in Madin-Darby canine kidney cell. *J. Urol.* **160**: 1506-1512.

Yamate, T., K. Kohri, T. Umekawa, E. Konya a, Y. Ishikawa, M. Iguchi and T. Kurita (1999). Interaction between osteopontin on Madin-Darby canine kidney cell membrane and calcium oxalate crystal. *Urol. Int.* **62**: 81-86.

Ye, L. and K. Mosbach (2001). Molecularly imprinted microspheres as antibody binding mimics. *React. Funct. Polym.* **48**: 149-157.

Zebrower, M. E., F. J. Kieras and W. T. Brown (1986). Analysis by high-performance liquid chromatography of hyaluronic acid and chondroitin sulphate. *Anal. Biochem.* **157**: 93-99.